2016

A Neural Circuit of Appetite Control in C. elegans

Kristen C. Davis
Virginia Commonwealth University

A NEURAL CIRCUIT OF APPETITE CONROL IN *C. ELEGANS*

A dissertation submitted in partial fulfillment of the requirements for the degree of Doctor of Philosophy at Virginia Commonwealth University.

by

KRISTEN C. DAVIS

Bachelors of Science, Longwood University, 2011

Director: Young-Jai You, Ph.D.

Department of Biochemistry and Molecular Biology

Virginia Commonwealth University

Richmond, Virginia

April 2016

Acknowledgement

I would like to acknowledge my mentor Dr. Young-Jai You for her guidance, enthusiasm, and training. She taught me what it means and what is to be a scientist. I would also like to acknowledge Dr. Andrew Larner for agreeing to be my advisor for the remaining months of my degree.

I would like to thank my committee members, past and present, Drs. Andrew Davies, Andrew Larner, Babette Fuss, Carmen Sato-Bigbee, Leon Avery, and Jessica Bell. You all challenged me to do my very best and would not settle for less, and for that I am incredibly grateful.

I am thankful for my family and friends who have supported me up to and through graduate school. A special thanks to my fiancé, Jason Amos, and my younger sisters, you always encouraged and believed in me when even I did not. I also have to thank Jason Amos for being so supportive and helping me come up with better word choices at all hours of the night while writing this document.

Table of Contents

List of Figures

Page

List of Abbreviations

cGMP	cyclic Guanosine Monophosphate
GFP	Green Fluorescent Protein
RFP	Red Fluorescent Protein
IPTG	Isopropyl β-D-1-thiogalactopyranoside
NaCl	Sodium Chloride
NGM	Nematode Growth Medium
TGFβ	Transforming Growth Factor beta
EMS	Ethyl methanesulfonate
GCaMP	GFP, Calmodulin, & M13 peptide
NST	Nucleus of the Solitary Tract
OFC	Orbitofrontal Cortex
ASI	Amphid Sensory neuron pair I
ASH	Amphid Sensory neuron pair H
AIA	Amphid Interneuron pair A
RIC	Interneuron pair in the neural Ring C
NPY	Neuropeptide Y
AgRP	Agouti-related Peptide
POMC	Preopiomelanocortin
CCK	Cholecystokinin

ATR	All trans-retinal
NLP	Neuropeptide-like Protein
NPR	Neuropeptide Receptor
DTT	Dithiothreitol
LB	Luria Broth
NHR	Nuclear Hormone Receptor
TMC	Transmembrane-like Channel

Abstract

A Neural Circuit of Appetite Control in *C. elegans*

By Kristen C. Davis

A Dissertation submitted in partial fulfillment of the requirements for the degree of Doctor of Philosophy at Virginia Commonwealth University.

Virginia Commonwealth University, 2016

Major Director: Young-Jai You, Ph.D.

Assistant Professor, Department of Biochemistry and Molecular Biology

Feeding behavior and its associated neural circuitry is complex and intricate in mammalian systems, however, a simple model organism, such as *C. elegans* provides a more basic approach to understand factors and molecules involved. The fruit-dwelling nematode provides a unique set of resources; it only consists of 959 cells, 302 of which are neurons. In addition, each neuron's connectivity and position within the worm is known and consistent between animals. Conservation of neurotransmitters and biochemical processes add to this impressive list. These resources provide an excellent background to address feeding behavior and the neural structures governing it.

Feeding behavior in worms mimics feeding behavior in more complex organisms. They decide when to eat based on recent feeding behavior, current nutritional status, availability of food, and familiarity with the food available. Following starvation and refeeding worms enter a behavioral state similar to post-prandial sleep. The worms will stop eating and stop moving, in a state referred to as satiety quiescence. The ability to enter this state and maintain it is dependent on a pair of neurons in the head of *C. elegans* called ASI. Using calcium imaging and an automated satiety quiescence assay, our lab has found that this neuron pair is important for entering satiety quiescence and senses food. Feeding behavior, such as satiety quiescence, is regulated by numerous factors internal and external to the worm. Another pair of head neurons, ASH are capable of suppressing ASI's activity in the presence of noxious stimuli and the presence of nutrients (potentially acting via ASI) can suppress ASH's activation to noxious stimuli under starvation conditions.

The interaction between these two neuron pairs can be regulated by other signals from the rest of the worm. We identified an opioid signal that can modulate the response of

ASI to noxious stimulus signaling from ASH under starvation conditions. Other signals were identified to influence satiety behavior and this circuit including serotonin, octopamine, glutamate, and adenosine. In addition to these signals, a group of transcription factors were identified that may play a role in conveying the status of fat storage within the worm to its nervous system. Nuclear hormone receptors were found to increase their expression during starvation then decrease their expression upon refeeding. Upon completion of this work, we have a reached a greater understanding of the internal and external conditions governing feeding and avoidance behaviors.

Clarification of Contributions

The experiments which generated the data for all figures in this document were conducted by Kristen Davis with the assistance of an undergraduate, Young-In Choi. Experiments were designed by Kristen Davis and Dr. Young-Jai You. Microfluidic devices were initially provided by Manuel Zimmer until the protocol was established in the lab by Kristen Davis. Locomotion tracking experiments done on the multi-camera platform (frame built by former Avery lab member Dr. Boris Shtonda and equipped with cameras by Dr. Thomas Gallagher) were analyzed using software written by Dr. Thomas Gallagher. The Hidden Markov model analysis software was written by Dr. Leon Avery. Worm strains were kindly provided by Drs. Alkema, Ferkey, L'Etoile, Sengupta, Bargmann, Ilino, Ishihara, Hirotsu, Schaeffer as well as the Caenorhabditis Genetics Center. This work was supported by the Virginia Commonwealth University Department of Biochemistry and Molecular Biology as well as National Institutes of Health and American Heart Association grants to Dr. Young-Jai You and Dr. Leon Avery.

A Neural Circuit of Appetite Control in *C. elegans*

*Portions of this work are published in Scientific Reports

1. Background

1.1 Behavioral Choices

Making the correct behavioral choices is essential for any animal's survival. To make the correct choices, an animal integrates its sensory input to evaluate whether the condition is beneficial or harmful. In nature, however, an animal often faces conflicting cues and the choice could, in turn, decide the animal's survival. As an example, upon the discovery of a potentially harmful yet nutritious source, an animal must sense its current nutritional status to determine whether to eat it against the harm from consuming it. The more the animal is starved, the more risk the animal is willing to take.

Feeding behavior is determined by an animal's current nutritional status, recent feeding history, and the presence of different stimuli. Avoidance behaviors are governed by the same set of criteria, the difference being which end of the balance the criteria favor. If the conditions favor feeding, that is the choice made and if the conditions favor avoidance, the animal will flee. In addition to the stimulus itself, the animal's previous experience with the stimulus is important as well. Associations made between certain food sources and otherwise unrelated conditions can also influence the decision making process. For instance, when the nematode *C. elegans* are raised at a set temperature on highly nutritious food, it will show a preference for that temperature in the future because of that previous association (Mori & Ohshima, 1995).

Determining how these conditions weigh against each other, which neural structures make these calculations, and where the threshold is set for each behavior is a challenging task. In order to address these questions, it requires breaking down each

component while controlling others to tease apart conditions necessary and sufficient to induce the behaviors in question.

1.2 Nutrient Sensation

For humans to physically sense the nutrients present in a food item, it first encounters the taste buds of the mouth and the olfactory receptors in the nose. For taste, the chorda tympani and glossopharyngeal nerves transmit their signals through the nucleus of the solitary tract (NST). From there, it goes to the thalamus, which then sends the signal to the insula, the frontal operculum cortex, and the orbitofrontal cortex (OFC). The smell of foods is another aspect of the taste; food does not taste the same when eaten with nostrils obstructed versus when they are unobstructed. This aspect of olfaction is sensed in the olfactory mucosa of the nose, located high in the nasal cavity. The olfactory muscosa is a dime-sized region that holds the olfactory receptors and located such that air flows past during normal breathing. The air contains the odorants that subsequently interact with olfactory receptors. There are 350 known olfactory receptors and they all respond to a narrow range of odorants. Different odorants activate different odorant receptors; therefore the pattern of glomeruli activation will vary with the odorants present in the nasal cavity. The olfactory sensory information passes from the olfactory to the piriform cortex and the amygdala. It then travels from these two locations to the OFC (Garrett, 2009; Goldstein, 2010).

Upon consumption, food enters the gastrointestinal (GI) tract where food comes into contact with the mucosal layer. The mucosal layer of the GI tract consist of small

transverse folds called plicae circulares and on these folds are small finger-like projections called villi. The villus is where enteroendocrine cells (EEC) are located. These cells are responsible for sensing the nutrient contents of meals and signaling to other areas of the body by releasing gut peptides to the vagus nerve/spinal cord and directly into the bloodstream (Cummings & Overduin, 2007; Johnson, 2011; Kohan, Yoder, & Tso, 2011). There are numerous signals released to provide information concerning the value of the consumed food to the nervous system which helps the organism decide whether they need to consume more of that food, find a new nutrient source, or stop eating entirely. The overall nutritional status of the organism is also conveyed from their adipose tissue via leptin. Leptin is a signal released from adipocytes and the concentration of leptin in the blood stream is an indicator of an animal's amount of body fat. This signal readily crosses the blood brain barrier (BBB) and interacts with neurons in multiple brain areas to influence feeding behavior (Banks, DiPalma, & Farrell, 1999). Dysfunction in leptin signaling can result in excessive weight gain, diabetes, and health problems associated with those two issues.

1.3 Neural Circuit of Appetite Control

For years the hypothalamus has been studied as an important structure for appetite control in mammalian systems. There are many signals released to and from this brain region. Two well-studied populations of neurons in the arcuate nucleus of the hypothalamus are the agouti-related protein (AgRP) releasing neurons and the pro-opiomelanocortin (POMC) releasing neurons.(Adan, Nijenhuis, & Kas, 2003; Balthasar et

al., 2004; Elmquist, Elias, & Saper, 1999; Meister, 2007; Wang et al., 2014) The AgRP neurons promote food-seeking behavior and the POMC neurons suppress food-seeking behavior.(Chen, Lin, Kuo, & Knight, 2015) AgRP and POMC act on melanocortin-4-receptor (MC4R) as either an inverse agonist or agonist, respectively.(Adan et al., 2003; Balthasar et al., 2005; Qi, Kraft, Hunter, & Hu, 2008) Under fasting or ghrelin-treatment (a hunger signal in mammals), the AgRP neurons are normally activated and POMC neurons are inhibited. A recent study demonstrated that the presentation of food to fasted or ghrelin-treated mice suppresses the AgRP neurons and activates the POMC neurons in the arcuate nucleus. In fact, the smell alone was sufficient to suppress the AgRP neurons and activate the POMC neurons, however, upon removal of the food without consumption, the circuit resets to the fasting state (Figure 1)(Chen et al., 2015). This suggests that homeostatic signals from the body can reset the circuit if sufficient nutrients were not consumed. Many components of this circuit remain to be determined, including exactly how the olfactory signal of the food is communicated to the hypothalamus. Connections between the olfactory bulb and the hypothalamus exist but the nature of the connection and the signals used are unknown (Garrett, 2009; Schwartz, Woods, & Porte, 2000). In addition, how is this circuit regulated and by which structure in the event of a "bad" food discovery? Is there an interaction between these components and a currently unknown location that suppresses feeding in the presence of contaminated food or some other threat to the organism's survival (Figure1)?

Figure 1

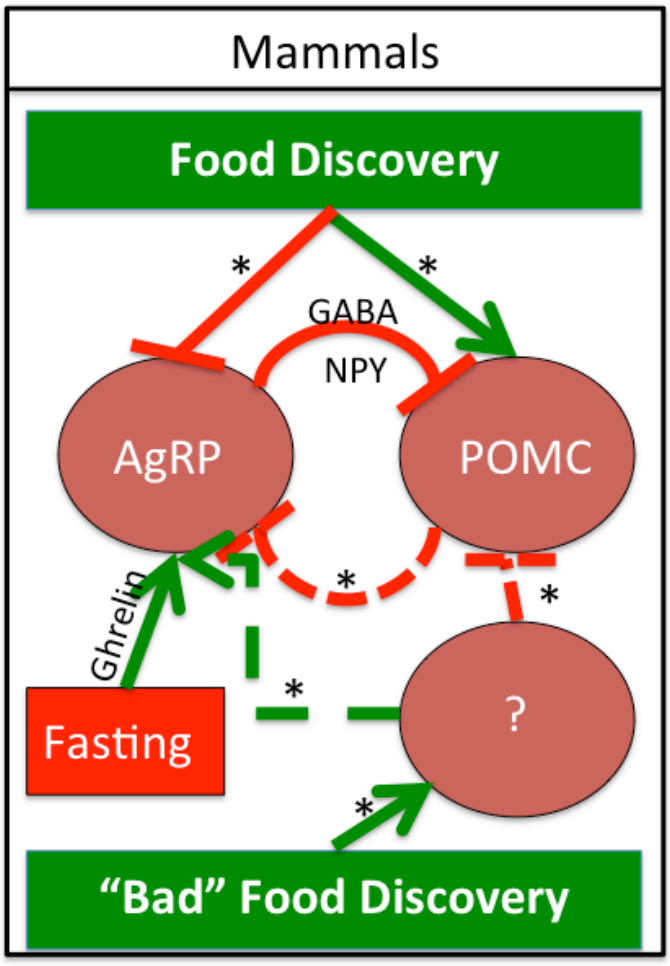
Mammals
Food Discovery
GABA
NPY
AgRP
POMC
Ghrelin
Fasting
?
"Bad" Food Discovery

Figure 1. Known and unknown connections in mammalian feeding circuitry Based on evidence currently available in the literature **(Balthasar et al., 2004; Chen et al., 2015; Elmquist et al., 1999; Meister, 2007)**. GABA – Gamma-amino-butyric acid, NPY – Neuropeptide Y, POMC – Preopiomelanocotrin, AgrP – Agouti-related Protein

1.4 *Caenorhabditis elegans* as a model organism

C. elegans have a very simple nervous system, consisting of 302 neurons with known connectivity based on a reconstruction of electron micrographs.(Chalfie & White, 1988) Using this incredibly helpful resource, we wish to use these known connections to identify the neuron pairs and their connections, which regulate appetite. In addition to a simple nervous system, *C. elegans* is transparent which allows the easy use of optogenetic tools such as GCaMP and channel rhodopsin.

Amphid neurons are sensory neurons in the nose of the worm that detect various stimuli in the external environment. There are 12 pairs of these neurons and they begin in development in nose of the worm and extend dendrites into the amphid channel.(Chalfie & White, 1988) The amphid channel is exposed to the external environment and its formation requires sheath glial cells. Amphid neurons sense the environment through this channel and without it, amphid neurons do not respond to chemicals known to cause activation under normal conditions.(Bacaj, Tevlin, Lu, & Shaham, 2008) We have identified one pair of amphid neurons, ASI, which activate to nutrient-rich stimuli. ASI is also important for the behavioral state referred to as satiety quiescence. Satiety quiescence in *C. elegans* is similar to post-prandial sleep in mammals. It is defined as a lack of feeding and motion, there are two other behavioral states based on locomotion that our lab measures in relation to feeding, dwelling and roaming. Roaming is searching for a food source while dwelling is browsing the current food source. Without ASI, worms have difficulty transitioning into satiety quiescence and spend more time in dwelling. This behavioral triad provides a tool

to determine the appetite of an individual worm and how different conditions and mutations can influence these behavioral states.

1.5 Obesity

Obesity is defined by the Centers for Disease Control (CDC) as a body mass index (BMI) above 30. Obesity among modern Americans is a huge problem affecting approximately one third of all adults, while approximately two thirds of all adults are considered overweight. The underlying cause of this trend does not have a single culprit in all cases; there are a variety of factors that can culminate in an individual being overweight/obese (Levi, Segal, Laurant, & Rayburn, 2013; Ogden, Carroll, Kit, & Flegal, 2012).

One recently discovered cause of obesity is leptin resistance or insensitivity. This can occur through a few mechanisms. Some individuals are born with mutations in the leptin or leptin receptor gene; this would prevent the activation of anorexigenic (decrease feeding) neuronal populations and allow the continuation of orexigenic (increase feeding) signaling in others. These individuals are very similar in phenotype to the mice with the same problems (Halaas, Gajiwala, Maffei, & Cohen, 1995; R. B. Harris, 1999; C. Li, 1998; Pelleymounter et al., 1995). Leptin insensitivity is caused by long-term consumption of a high fat diet in animal models. Westernized diets and lifestyles consist of fatty foods and limited physical activity that cause excess fat storage and as a result higher leptin signaling. However, long-term fat consumption not only increases fat storage but also decreases leptin receptor expression in the arcuate nucleus and reduces leptin sensitivity

throughout the body (He, Lam, Obici, & Rossetti, 2006; Lin & Huang, 1999; Lin, Storlien, & Huang, 2000). A decrease in leptin sensitivity causes improper regulation of homeostatic feeding. Without leptin sensitivity, the NPY/AgRP neurons are not inhibited sufficiently and can produce high levels of hunger despite satiation (Cowley et al., 2001). Obese individuals do have higher levels of NPY and leptin when compared to normal and anorexic patients (Figure 2). This also prevents proper activation of the POMC neurons to decrease feeding behaviors (Cowley et al., 2001).

In addition to this imbalance, obese patients also have a reduced release of CCK in response to a meal compared to normal and anorexic patients (Figure 2). This reduction will also prevent the normal decrease in feeding upon satiation. This may be caused by faster gastric emptying which reduces the amount of time consumed food is in contact with the mucosal layer of the GI tract (Higham, Vaillant, Yegen, Thompson, & Dockray, 1997). Also, obese patients have much higher levels of galanin when compared to normal and anorexic patients. High galanin levels will increase eating high fat foods, which will only make the signaling problems worse (Adams, Clapham, Wynick, & Speakman, 2008). Obese individuals release significantly lower levels of postprandial bile acids when compared to normal weight individuals (Glicksman et al., 2010; Katsuma, Hirasawa, & Tsujimoto, 2005; Steinert et al., 2013). This makes sense in conjunction with the lower levels of CCK found in obese patients.

Also, Bauer et al., discovered several gene variants which cause an increase in food consumption. *SH2B1, KCTD15,* and *NEGR1* variants (single nucleotide polymorphisms) cause an increase in total fat intake and *MTCH2* and *KCTD15* cause an increase in

carbohydrate intake (Bauer et al., 2009). The role of these genes in nutrition signaling is not fully understood; *SH2B1* enhances leptin signaling, *NEGR1* is involved in neurite outgrowth, *MTCH2* is part of a complex associated with cellular apoptosis, and the function of *KCTD15* is unknown (Bauer et al., 2009; Grinberg, Schwarz, & Zaltsman, 2005; Z. Li, Zhou, Carter-Su, Myers, & Rui, 2007; Schäfer, Bräuer, Savaskan, Rathjen, & Brümmendorf, 2005). Another study also found variants of *MC4R* to cause an increase in total energy and fat. *MC4R* is the gene encoding the MC4R, which when bound by α-MSH decreases feeding but when antagonized by AgRP increases feeding (Qi et al., 2008). More work is needed to determine the roles of these genes in feeding behavior.

2. Results and Conclusions

2.1 Amphid neuron pair, ASI, senses nutrients

All animals must sense nutrients to maintain a nutritional status that ensures their survival. Previous work in our lab demonstrated that an amphid neuron pair, ASI, was important for regulating feeding behavior and activates (measured via calcium imaging) when presented with a nutrient-rich stimulus (Figure 2A). The nutrient-rich stimulus we used is Luria Broth, LB. ASI responds reliably to the presentation of this stimulus so I decided to break down which component in LB was responsible for this activation. LB is composed of NaCl, yeast extract, and tryptone. Upon testing the concentrations of these components in our system, I found that yeast extract and tryptone could activate ASI whereas NaCl did not (Figure 2B & C). Yeast extract is a very complex reagent with many components so I did not attempt to further explore this substance for what was activating ASI. Tryptone is much simpler, it is a trypsin digest of peptone, which makes it a combination of single amino acids and di- or tri- peptides. To determine if the activation is caused by amino acids, I tested an enzymatic casein hydrolysate, which is similar to tryptone but digested more and has fewer peptides. The casein hydrolysate activated similarly to the tryptone (Figure 2C).

All of these experiments led us to believe the important factor was an amino acid or a combination of amino acids that activate ASI. Initially, I tried the combination and concentration of amino acids found in casein, however this did not activate ASI even when increased to five times the levels seen in casein. Casein includes 17 of the 20 standard

amino acids so to fully test the possibility of amino acids, I added the remaining three (glutamine, cysteine, and asparagine) to the mixture of 17 (Table 1). This combination activated ASI similar to the magnitude seen in tryptone and casein. Next, I tested these three separate from the other 17 but did not see activation. In addition, I tested each of them individually and did not see activation. From this, I concluded that one of the three is interacting with one of the other 17 amino acids found in casein. So I mixed each individually with casein with the thought that it would hopefully enhance the activation typically seen to casein because more of the activating component is present. Adding aspartate or glutamine did not enhance the casein activation in ASI (Figure 2F & G), however, the addition of cysteine enhanced the activation of casein to a magnitude similar to LB (Figure 2H).

From these data, I hypothesized that cysteine might form disulfide bonds with certain amino acids in casein while it is in the autoclave; all of the components for calcium imaging are autoclaved prior to use in the calcium imaging system. To test this idea, I decided to search for what was potentially made in the autoclave using mass spectrometry. I prepared two samples, one of casein alone and another with casein and cysteine. Dr. Kristina Nelson (VCU, Chemistry) ran my samples. The results did not show any difference in mass sizes between the two samples, nor did it show an increase in a particular mass size (Figure 3A & B). There are differences in the peak intensity but not in the mass. There was no guarantee that the mass spectrometer could find the difference between the two samples and identify the structure of the activation enhancer. The lack of

an answer from the mass spectrometer does not mean a structure is not being formed; it simply could not measure it against the background.

To test my hypothesis regarding formation of disulfide bonds, I used dithiothreitol (DTT) to interfere with any disulfide bonds formed in the casein and cysteine mixture. DTT reduces disulfide bonds via thiol-disulfide exchange reactions when used in solutions with a pH above 7. The activation of ASI to casein and cysteine was significantly reduced by DTT ($p < 0.0001$), as was the activation to casein alone (Figure 4A, B, & C). This suggests that the enhancement of casein's activation in ASI when cysteine is added may results from a disulfide bond. This is not sufficient to identify which, if any, other amino acid (s) is (are) involved in this enhancement.

The potential combinations of the 17 amino acids with cysteine to determine where the interaction is happening are 131054. Due to this technical difficulty, we decided to pursue the project another time and instead to focus on identifying neural circuit of appetite control.

Figure 2

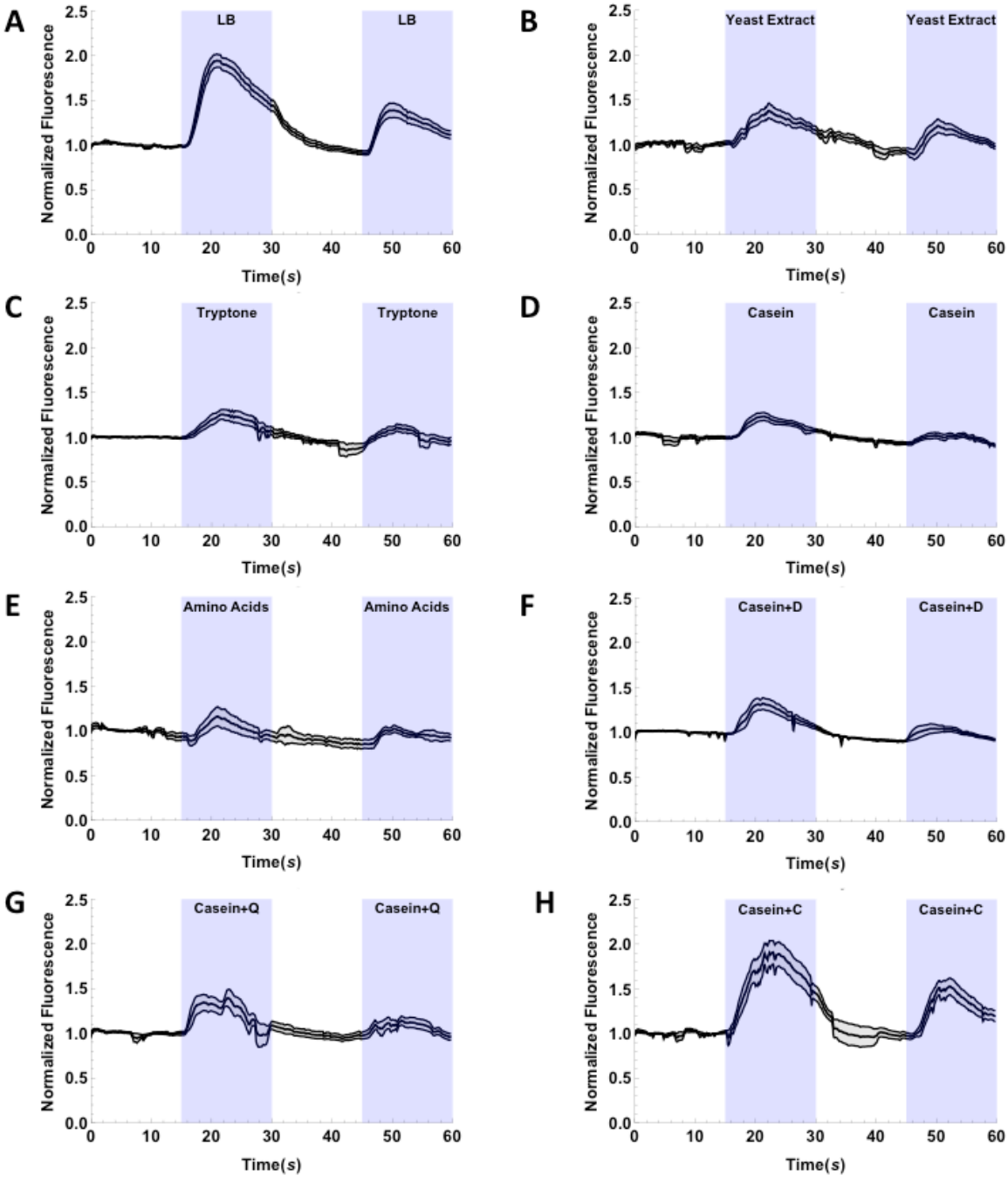
A
LB
LB
B
Yeast Extract
Yeast Extract
C
Tryptone
Tryptone
D
Casein
Casein
E
Amino Acids
Amino Acids
F
Casein+D
Casein+D
G
Casein+Q
Casein+Q
H
Casein+C
Casein+C
Normalized Fluorescence
Time(s)

Figure 2. ASI activates to nutrients, especially amino acids.

A. ASI activating to LB. *n=17*

B. ASI activating to yeast extract. *n=10*

C. ASI activating to tryptone. *n=9*

D. ASI activating to enzymatic hydrolysate of casein. *n=9*

E. ASI activating to 20 amino acids. *n=5*

F. ASI activating to casein with asparagine added. *n=6*

G. ASI activating to casein with glutamine added. *n=6*

H. ASI activating to casein with cysteine added. *n=7*

All graphs are the result of calcium imaging and are normalized to the initial 15 second of the recording during which the worms' noses are washed with S buffer. The dark central trace is the average and the lighter lines above and below are standard error of the mean. The blue segments indicate when the worms are receiving the stimulus.

Table 1

Amino Acid	Molar	mg/50 mL
Alanine	0.0038	16.8
Arginine	0.0034	30.2
Aspartic Acid	0.0013	8.7
Cysteine	0.0046	28
Glutamic Acid	0.006	38.6
Glycine	0.00118	4.4
Histidine	0.00172	13.3
Isoleucine	0.011	71.9
Leucine	0.011	71.9
Lysine	0.006	61.1
Methionine	0.003	22.7
Phenylalanine	0.00398	33
Proline	0.00128	7.4
Serine	0.0054	28.7
Threonine	0.0036	21.5
Tryptophan	0.00084	8.6
Tyrosine	0.00154	14
Valine	0.0062	36.4

Table 1. Contents of amino acids mixture

The amount of each amino acid used in the experiments. This is 5× the amount of each amino acid listed in the product details for a casein hydrolysate from MP Biomedicals (http://www.mpbio.com/).

Figure 3

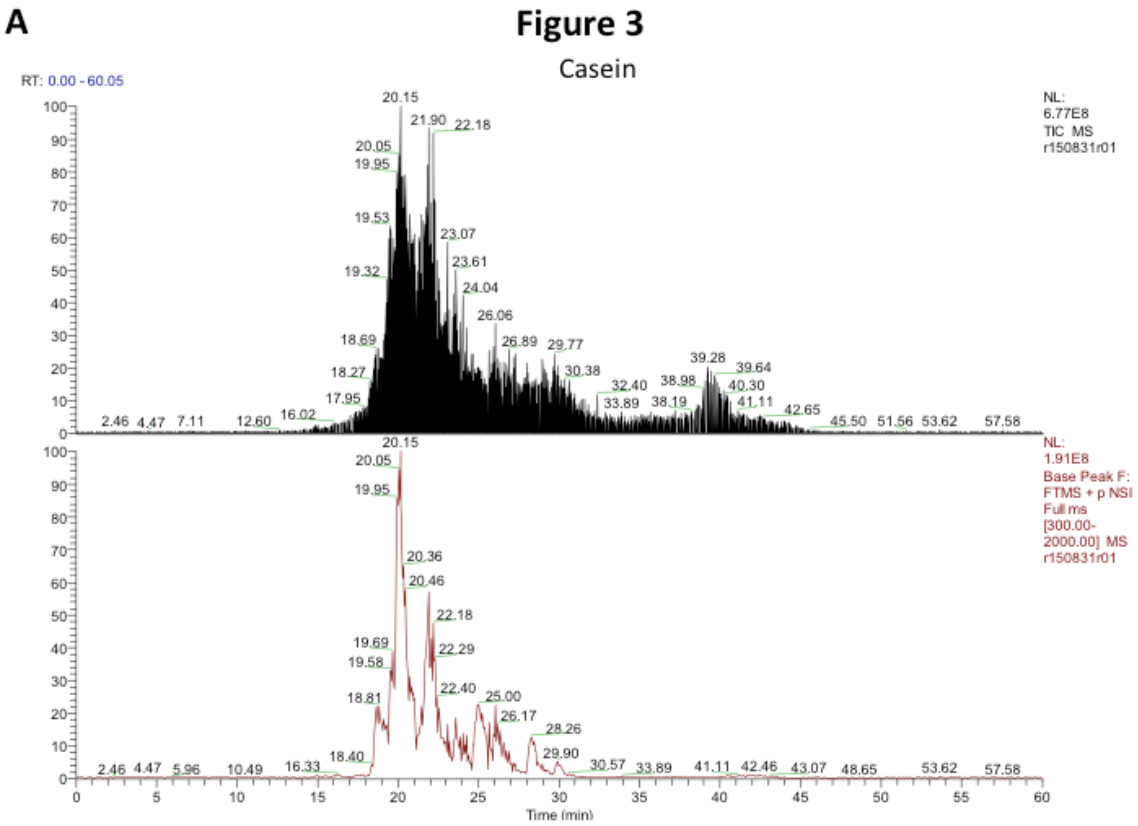
A
Casein
RT: 0.00 - 60.05
NL:
6.77E8
TIC MS
r150831r01
NL:
1.91E8
Base Peak F:
FTMS + p NSI
Full ms
[300.00-
2000.00] MS
r150831r01
Time (min)

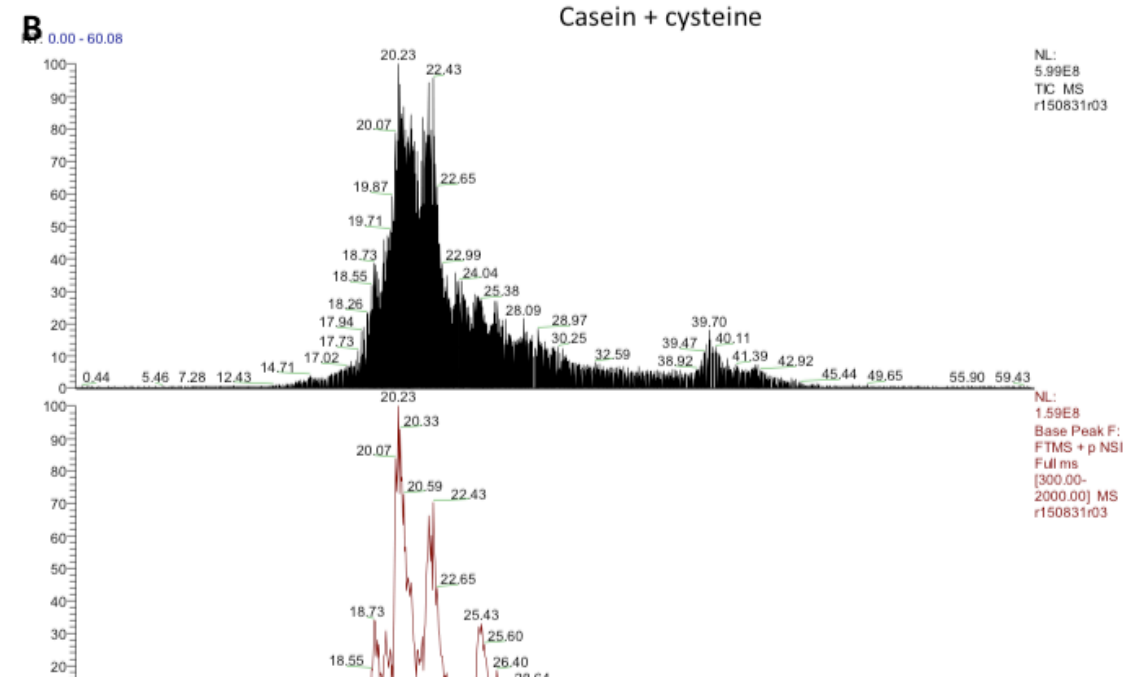
B
Casein + cysteine
RT: 0.00 - 60.08
NL:
5.99E8
TIC MS
r150831r03
NL:
1.59E8
Base Peak F:
FTMS + p NSI
Full ms
[300.00-
2000.00] MS
r150831r03

Figure 3. Mass Spectrometry results for casein and casein with cysteine.

A. Casein.

B. Casein with cysteine.

Figure 4

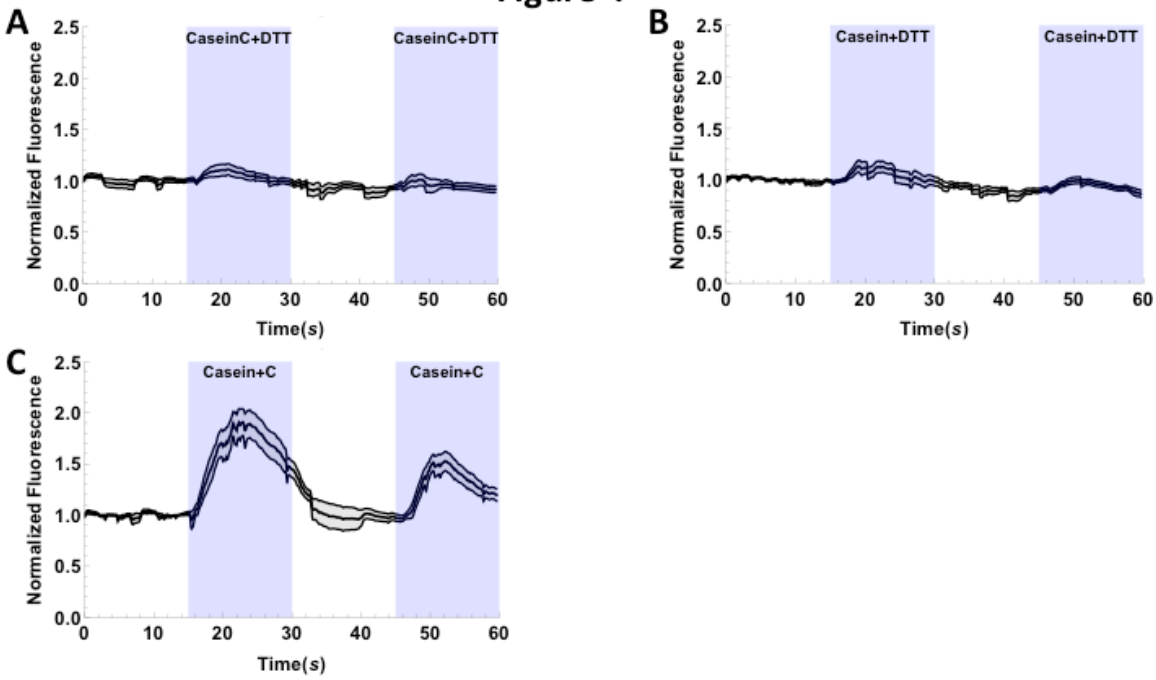
A
CaseinC+DTT
CaseinC+DTT
Normalized Fluorescence
Time(s)
B
Casein+DTT
Casein+DTT
Normalized Fluorescence
Time(s)
C
Casein+C
Casein+C
Normalized Fluorescence
Time(s)

Figure 4. Disulfide bonds may be involved in the casein signal enhancement by cysteine

A. ASI activating to casein with cysteine and DTT. *n=10*

B. ASI activating to casein and DTT. *n=15*

C. ASI activating to casein with cysteine added. *n=7*

All graphs are the result of calcium imaging and are normalized to the initial 15 second of the recording during which the worms' noses are washed with S buffer. The dark central trace is the average and the lighter lines above and below are standard error of the mean. The blue segments indicate when the worms are receiving the stimulus.

Starving elicits a stronger response to food when compared to the response an animal has when well-fed. To determine if starvation and nutrient concentration change the activation I see in ASI, I fasted worms for six hours and tested ASI activation to three concentrations of LB. After six hours of starvation, worms show a similar but larger response to 100% LB when compared to well-fed worms (Figure 5A & B). LB is such a strong stimulus there is a ceiling effect and the activation can not be enhanced. The same holds true for 50% LB, the activation is similar to that seen in well-fed worms tested with 50% LB (Figure 5C & D). The biggest difference is with 10% LB, the six hours starved worms activate to a greater extent than the well-fed worms. The peak differences between well-fed and 6 hours fasted are all significantly different ($p < .05$) with the exception of the 50% LB condition. The area under the curve was significantly different ($p = .003$) between fasted and well-fed for all conditions but 100% and 10% LB. Starvation seems to sensitize and enhance the activation of ASI to nutrients. While the exact mechanism of this sensitivity is unknown, a similar effect has been observed in POMC releasing neurons in mice (Chen et al., 2015). There are many signals in mammals that inform the nervous system of nutrient depletion of the body, this signal has not been found and confirmed in *C. elegans* (Malik, McGlone, Bedrossian, & Dagher, 2008; Nagase, Nakajima, Sekihara, York, & Bray, 2002). There is probably more than one signal to relay this information to the nervous system of worms as well.

Figure 5

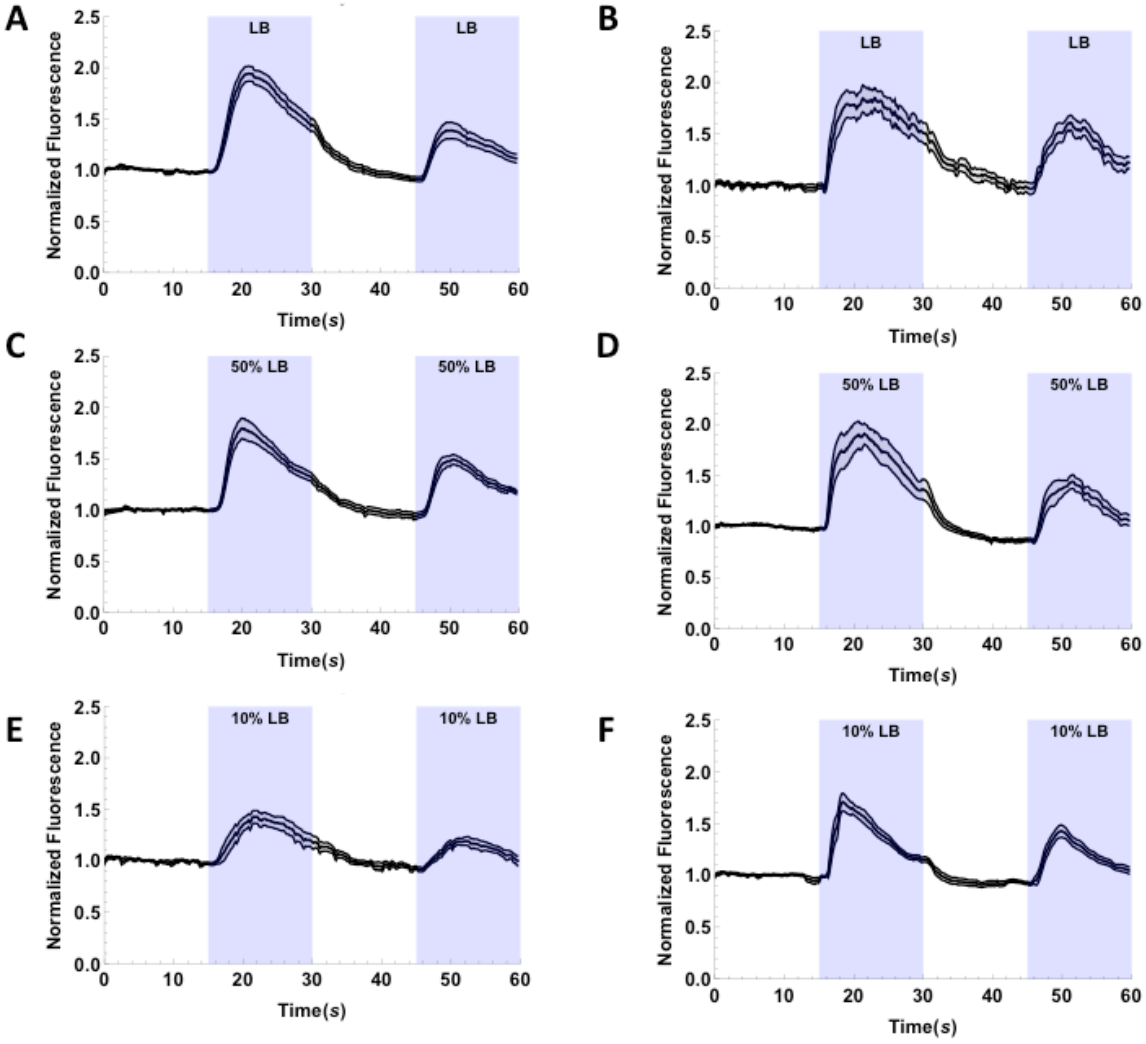
A
LB
LB
B
LB
LB
C
50% LB
50% LB
D
50% LB
50% LB
E
10% LB
10% LB
F
10% LB
10% LB
Normalized Fluorescence
Time(s)
0.0
0.5
1.0
1.5
2.0
2.5
0
10
20
30
40
50
60

Figure 5. Nutrient concentration and feeding history influence ASI activation

A. ASI activating to 100% LB. *n=17*

B. Six hour starved ASI activating to 100% LB. *n=12*

C. ASI activating to 50% LB. *n=10*

D. Six hour starved ASI activating to 50% LB. *n=10*

E. ASI activating to 10% LB. *n=10*

F. Six hour starved ASI activating to 10% LB. *n=13*

All graphs are normalized to the initial 15 second of the recording during which the worms' noses are washed with S buffer. The dark central trace is the average and the lighter lines above and below are standard error of the mean. The blue segments indicate when the worms are receiving the stimulus.

2.2 How ASI activates to nutrients

The activation of neurons in *C. elegans* is by calcium transients, they did not use Na+/K+ based action potentials because their size does not require it (R. A. Kerr, 2006). Graded calcium potentials are sufficient so measuring calcium fluxes in the cell body are a direct way to read the neuron's activation (R. Kerr, 2006). It was shown previously that cyclic nucleotide gated channels are important for the feeding behavior satiety quiescence (You, Kim, Raizen, & Avery, 2008). The specific channel identified in that study is composed of the subunits TAX-2 and TAX-4. Without the TAX-4 subunit, this channel is nonfunctional so a mutant in this subunit alone should be sufficient to prevent the use of the TAX-2 subunit. For worms to enter satiety quiescence, a sequence of events must occur. First, a membrane bound guanylyl cyclase, *daf-11*, is activated and this produces cGMP. It is thought that this cGMP can then activate a cyclic nucleotide gated channel to cause an influx of calcium into the neuron. It has been shown that all of these components need to be present in ASI for worms to transition to satiety quiescence. To test if the cyclic nucleotide gated channel composed of TAX-2/ TAX-4 is responsible for ASI's activation to nutrients, I crossed the ASI transgenic GCaMP line with *tax-4* mutants. However, the mutants show normal activation to LB (Figure 6A & B). There are other cyclic nucleotide gated channels which could lead to the calcium transient I observe in the neuron and there is an inositol triphosphate channel, *itr-1*, that can cause a calcium release from intracellular stores into the cytosol.

Another component of the satiety process is a cGMP dependent kinase (PKG), *egl-4*. *egl-4* has been implicated in many processes but for the intents and purposes of this study, I tested a gain of function mutant to determine if its activity can influence ASI's activation of LB. Previous work in the lab has demonstrated that an *egl-4* loss of function mutant does not enter satiety quiescence as much or long as wild type and a gain of function mutant spends a large amount of time in satiety quiescence (Gallagher, Bjorness, Greene, You, & Avery, 2013; Gallagher, Kim, Oldenbroek, Kerr, & You, 2013). It is thought that activation of *egl-4* over time signals to increase satiety quiescence. I anticipated the gain of function in *egl-4* would increase some dimension of the activation seen in ASI (the peak height or the area under the curve for example). The response in the *egl-4* gain of function background is wider but is a lower magnitude than wild type (Figure 6C & 6A). After analysis, the area under the curve is significantly greater in wild type than in the mutant ($p < 0.0001$), as is the peak of the first curve ($p < 0.0001$). I currently do not have the means to measure the width of a response; area under the curve is the closest measure to that. Further exploration of this change by *egl-4* gain of function may explain this difference.

Finally, I tested the internal levels of cGMP in ASI during LB presentation using a cGMP sensor, WincG2 (a gift from the Ferkey lab at the University of California San Francisco). I looked in the cell body as well as in the neural processes but I did not see a change in fluorescence in either location (only cell body data is included in Figure 6D). Previous work in our lab indicates that cGMP is sufficient to activate ASI in calcium imaging but this sensor indicates cGMP may not be the driving force behind ASI

Figure 6

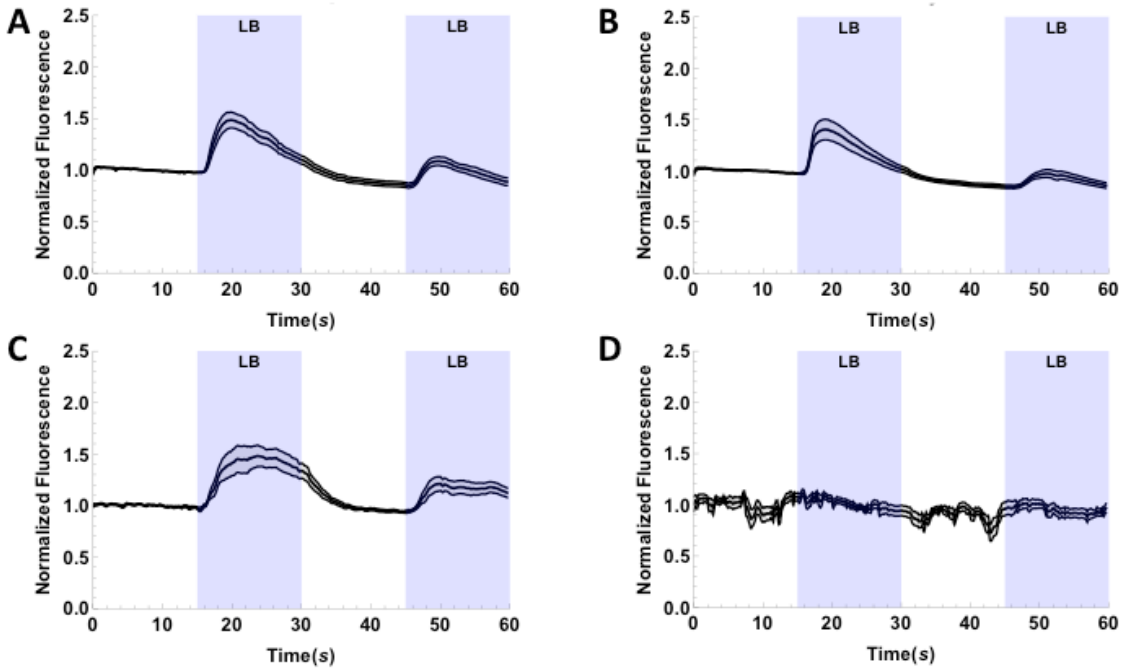
A
B
C
D
LB
LB
Normalized Fluorescence
Time(s)
0.0
0.5
1.0
1.5
2.0
2.5
0
10
20
30
40
50
60

Figure 6. Potential mechanism of ASI's activation

A. ASI activation to LB (extra-chromosomal array of GCaMP). *n=20*

B. ASI activation to LB in *tax-4* mutants (extra-chromosomal array of GCaMP). *n=15*

C. ASI activation to LB in *egl-4* gain of function mutants. *n=11*

D. cGMP imaging with WincG2 in ASI to LB. *n=10*

All graphs are normalized to the initial 15 second of the recording during which the worms' noses are washed with S buffer. The dark central trace is the average and the lighter lines above and below are standard error of the mean. The blue segments indicate when the worms are receiving the stimulus.

activation to LB. There could be an increase in cGMP that is too small to measure using this sensor; a FRET-based sensor would give a more sensitive measurement of cGMP changes following LB presentation. ASI's activation to cGMP is not reliable and only occurs approximately for half of the worms tested. Behaviorally, cGMP is important for satiety behavior and preventing dauer entry, perhaps cGMP levels need to increase over time to effect behavior and it is not involved in the immediate response seen in ASI to LB(Gallagher, Kim, et al., 2013; You et al., 2008).

2.3 Can aversive cues suppress ASI's activation to nutrients?

Our lab serendipitously found that the addition of certain substances can suppress ASI's activation to LB. Specifically, the addition of food coloring to the LB results in decreased activation in ASI. I attempted to replicate this with minimal success (Figure 7A) and attempted to study different colors of food coloring in satiety quiescence (Figure 7B) but abandoned this attempt for a several of reasons. Food coloring lacked a biological significance for our system; food coloring is not something typically present in a worm's natural food source. In addition, the manufacturer of the food coloring would not disclose the specific ingredients in their food coloring due to proprietary reasons. When the food coloring was added to the bacteria on plate and during imaging, it began to diffuse throughout the plate. The food coloring in the bacteria as well as throughout the plate interfered with the worm tracking software. The software would lose the worm very easily because the worm would become indistinguishable from the background. Based on these

Figure 7

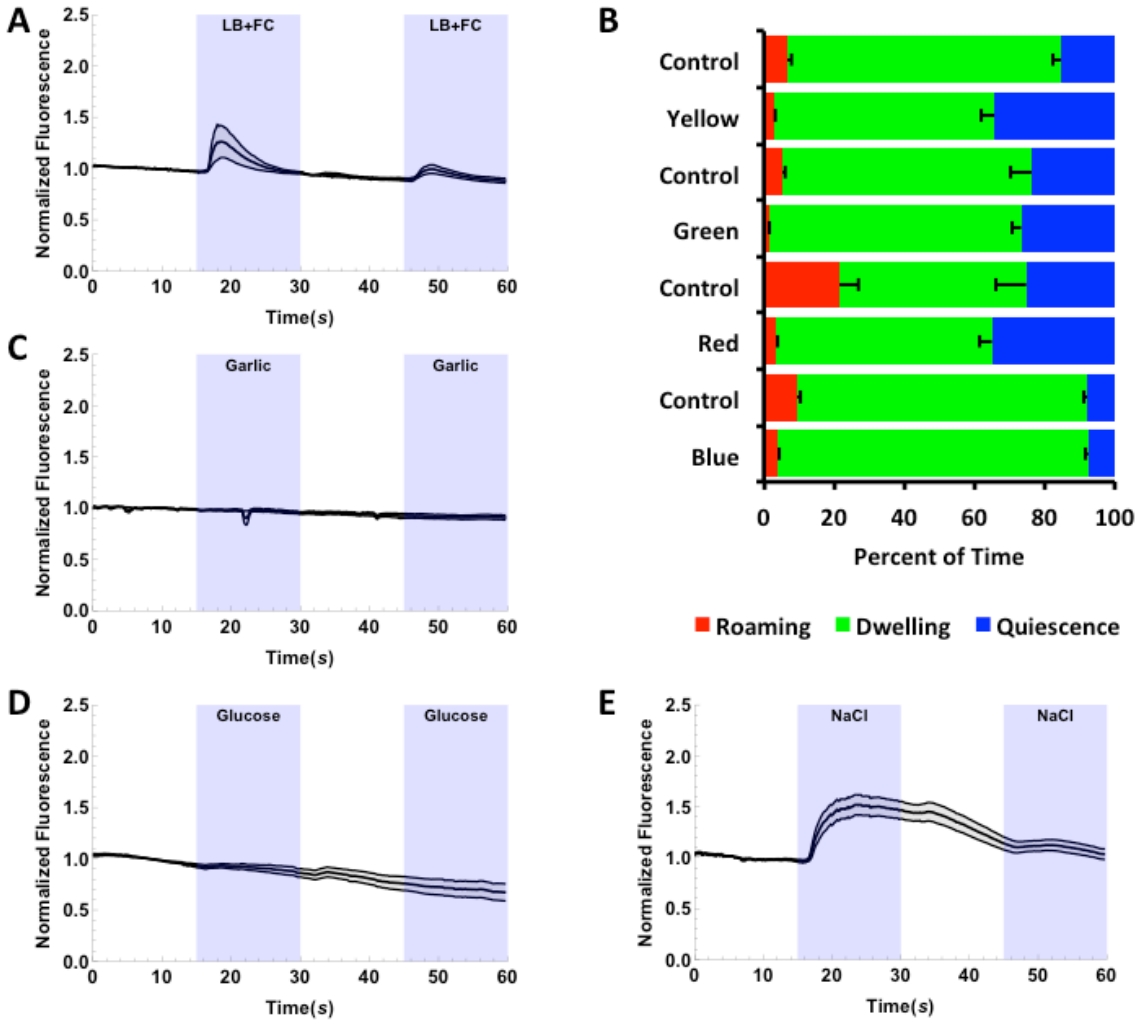
A
LB+FC
LB+FC
Normalized Fluorescence
Time(s)
B
Control
Yellow
Control
Green
Control
Red
Control
Blue
Percent of Time
Roaming
Dwelling
Quiescence
C
Garlic
Garlic
D
Glucose
Glucose
E
NaCl
NaCl

Figure 7. Searching for a stimulus to activate ASH

A. ASI activation to food coloring mixed with LB (extra-chromosomal array of GCaMP). *n=3*

B. Automated satiety quiescence assay with N2 worms on bacteria mixed with food dye colors

C. ASH activity to powdered garlic (extra-chromosomal array of GCaMP). *n=6*

D. ASH activity to 2 M glucose (extra-chromosomal array of GCaMP). *n=6*

E. ASH activation to 4 M NaCl (extra-chromosomal arrar of GCaMP). *n=14*

All graphs are normalized to the initial 15 second of the recording during which the worms' noses are washed with S buffer. The dark central trace is the average and the lighter lines above and below are standard error of the mean. The blue segments indicate when the worms are receiving the stimulus.

reasons, I sought to find another stimulus that could possibly suppress ASI. To do this, we identified another amphid neuron pair that can sense noxious stimuli. The rationale being that this neuron pair could sense this noxious stimulus and sensing noxious stimulus in turn suppress the activation of ASI. ASH is the neuron pair best known in *C. elegans* as a noxious stimulus sensor. I tried a few stimuli that are sensed by ASH (Bargmann, Thomas, & Horvitz, 1990; Chatzigeorgiou, Bang, Hwang, & Schafer, 2013; Culotti & Russell, 1978; Hilliard et al., 2005; Hilliard, Bergamasco, Arbucci, Plasterk, & Bazzicalupo, 2004). These included garlic powder, glucose, and high concentrations of NaCl (Figure 7C, D, & E). Garlic powder and glucose did not activate ASH in this setup, which could be due to a few factors such as the sensitivity of GCaMP in comparison a FRET-based calcium indicator or the ability of powdered garlic to activate in comparison to fresh garlic.

2.4 ASH activates to noxious stimuli and suppresses ASI activation

After testing these different chemicals for activation of ASH, I decided to work with a high concentration of NaCl. ASH activates to NaCl consistently via the TMC-1 channel (Chatzigeorgiou et al., 2013) and the flow of NaCl through the microfluidic device was easy to control. I modified the way by which I used the microfluidic device; in the place of continuous buffer flow I gave the worms NaCl. To ensure ASH had time to fully activate in the experiments, I allowed the worm's nose to be exposed for 4 minutes. After this time had passed, I presented the worms with LB and measured the activation of ASI. I tested 1, 2, 3, and 4M NaCl to determine if the magnitude of suppression changed based on the concentration, the higher the concentration of NaCl, the greater the suppression of ASI's activation to LB (Figure 8A, C, E, & G). All of these concentrations significantly

Figure 8

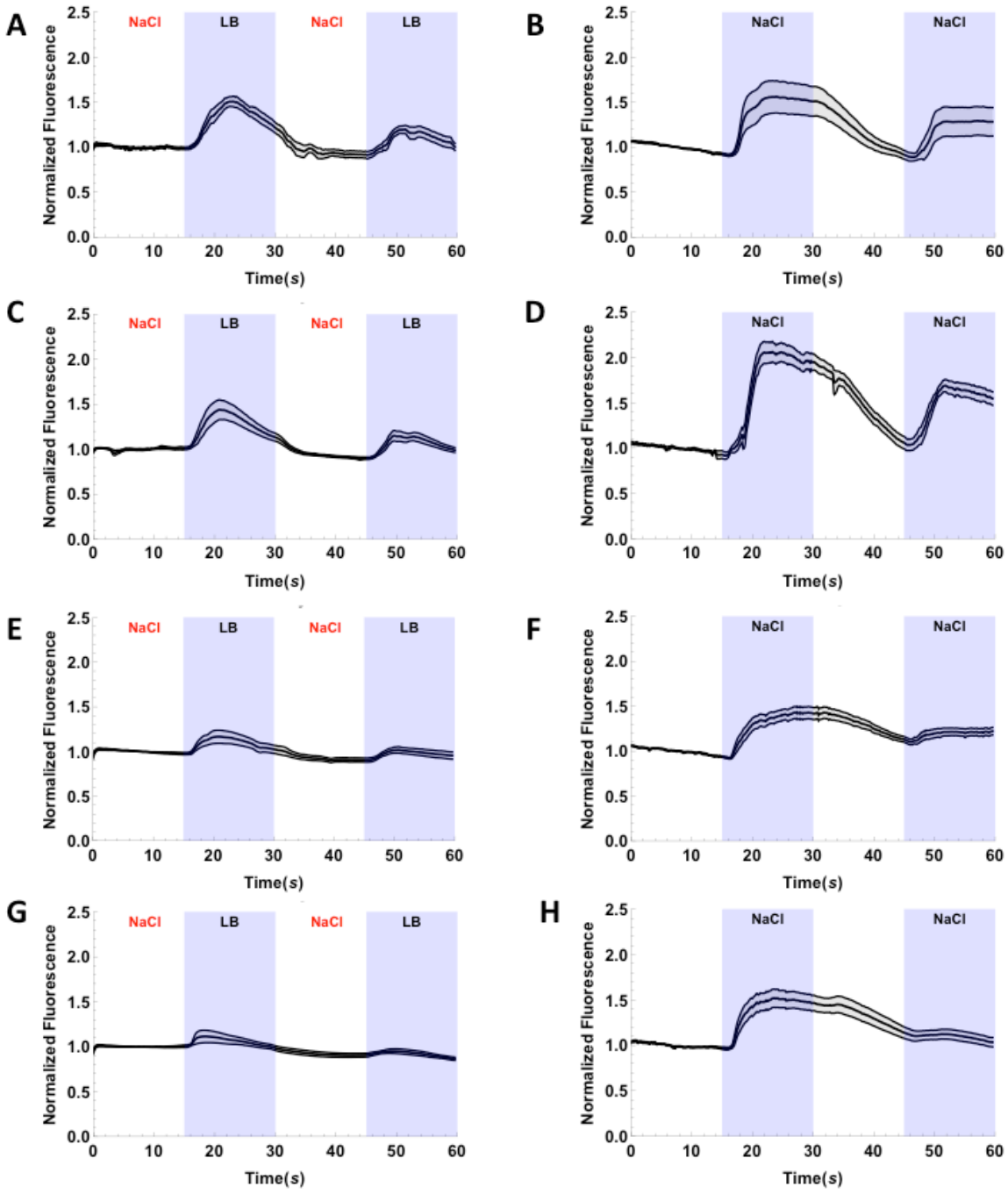
A
B
C
D
E
F
G
H
NaCl
LB
NaCl
LB
Normalized Fluorescence
Time(s)
0.0
0.5
1.0
1.5
2.0
2.5
0
10
20
30
40
50
60

Figure 8. ASH's activation to NaCl is dose dependent, as is ASH's suppression of ASI

A. ASI activation to LB after exposure to 1 M NaCl (5 min.). *n=12*

B. ASH activation to 1 M NaCl (extra-chromosomal array of GCaMP). *n=13*

C. ASI activation to LB after exposure to 2 M NaCl (4 min.). *n=10*

D. ASH activation to 2 M NaCl (extra-chromosomal array of GCaMP). *n=12*

E. ASI activation to LB after exposure to 3 M NaCl (4 min.). *n=10*

F. ASH activation to 3 M NaCl (extra-chromosomal array of GCaMP). *n=13*

G. ASI activation to LB after exposure to 4 M NaCl (4 min.). *n=12*

H. ASH activation to 4 M NaCl (extra-chromosomal array of GCaMP). *n=14*

All graphs are normalized to the initial 15 second of the recording during which the worms' noses are washed with S buffer or NaCl (presence of which is indicated at the top of the graph). The dark central trace is the average and the lighter lines above and below are standard error of the mean. The blue segments indicate when the worms are receiving the stimulus.

Figure 9

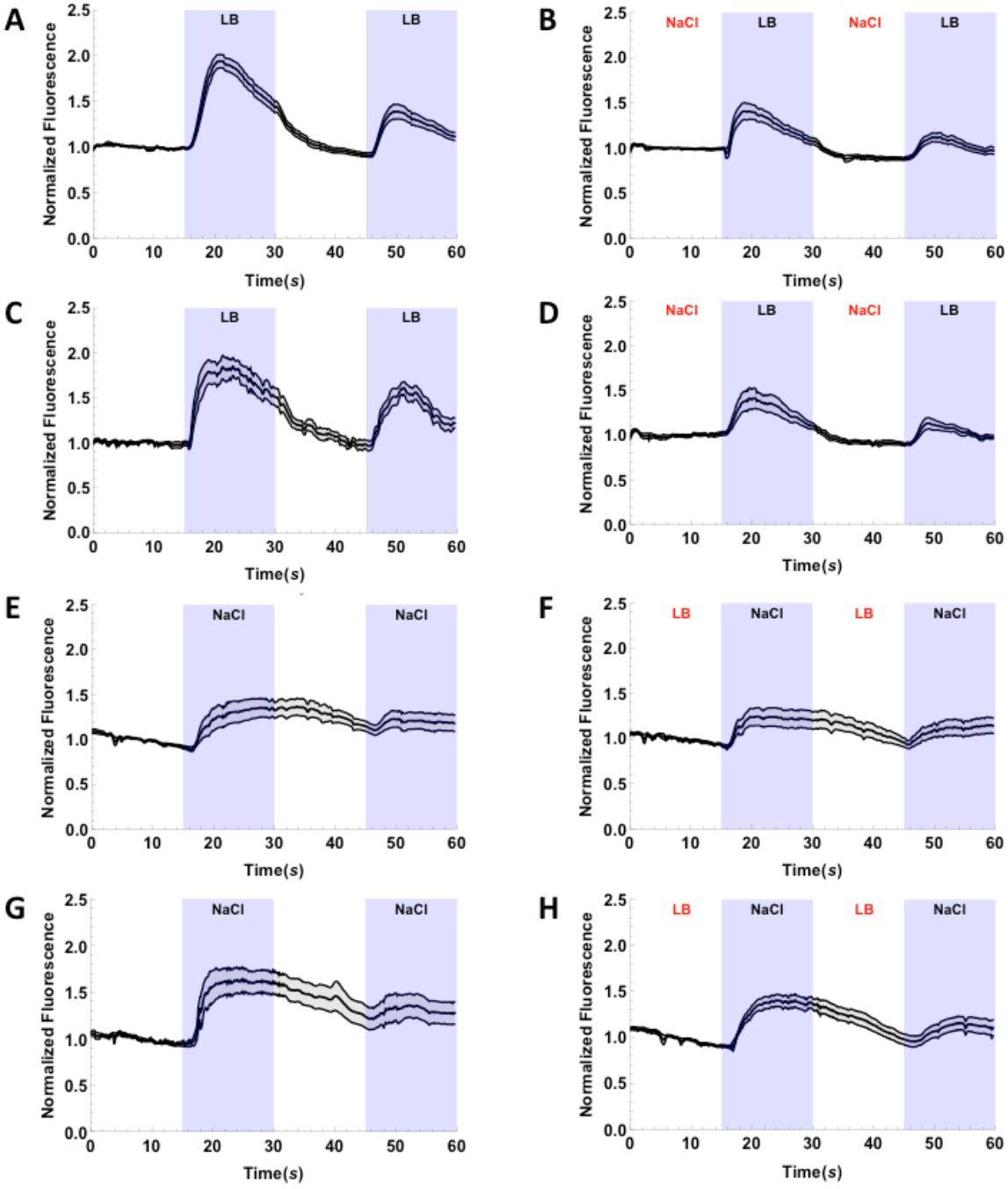
A
LB
LB
B
NaCl
LB
NaCl
LB
C
LB
LB
D
NaCl
LB
NaCl
LB
E
NaCl
NaCl
F
LB
NaCl
LB
NaCl
G
NaCl
NaCl
H
LB
NaCl
LB
NaCl
Normalized Fluorescence
Time(s)

Figure 9. Modulation of ASI and ASH's activation by feeding status and other signals

A. ASI activation to LB. *n=17*

B. ASI activation to LB after exposure to 0.5 M NaCl. *n=10*

C. ASI activation to LB after 6 hours of starvation. *n=12*

D. ASI activation to LB after 6 hours of starvation and exposure to 0.5 M NaCl. *n=11*

E. ASH activation to 2 M NaCl (extra-chromosomal array of GCaMP). *n=10*

F. ASH activation to 2 M NaCl after exposure to LB (4 min.) (extra-chromosomal array of GCaMP). *n=11*

G. ASH activation to 2 M NaCl after 6 hours of starvation (extra-chromosomal array of GCaMP). *n=7*

H. ASH activation to 2 M NaCl after 6 hours of starvation and exposure to LB (4 mins.) (extra-chromosomal array of GCaMP). *n=10*

All graphs are normalized to the initial 15 second of the recording during which the worms' noses are washed with S buffer, LB, or NaCl (presence of which is indicated at the top of the graph). The dark central trace is the average and the lighter lines above and below are standard error of the mean. The blue segments indicate when the worms are receiving the stimulus.

suppression ASI's activation ($p < 0.005$) Of those four concentrations of NaCl, 2M maximally activates ASH (Figure 8B, D, F, & H).

I have already shown that ASI's activation is influenced by the worm's recent feeding history; I tested the suppression of NaCl on ASI's activation to LB to determine if ASI can overcome this suppression when the worms are starved. Using 0.5 M NaCl, I did not see a difference in activation to LB in well-fed worms or 6 hour fasted worms (Figure 9A-D). It is possible that even 0.5 M NaCl is still too strong for ASI to overcome its suppression through ASH after 6 hours of starvation. Also it is possible that after a longer starvation (12 hours), ASI could overcome this suppression. However worms become very fragile after a longer starvation period and the fragility of these worms prevents proper loading in the microfluidic device, they burst before they can be positioned properly.
To fully explore the possibility of a longer starvation period overcoming this suppression, I would need a microfluidic device in which I could starve the worms individually then test them or a different for method loading the worms that would not put as much pressure on them. Another possibility is ASH regulates ASI sensitivity after starvation. In fact, others have found that not only can ASH suppress ASI, but ASI can also suppress ASH (Guo et al., 2015). I tested the activation of ASH to 2 M NaCl following 4 minutes exposure to LB in the well-fed condition and the worms did not show any difference between those that received only 2 M NaCl or those that received LB followed by 2M NaCl (Figure 9E & F). Following 6 hours of starvation, there is a difference in the activation of ASH when comparing 2M NaCl alone and LB prior to 2M NaCl (Figure 9G & H). It appears that under well-fed conditions, the activation of ASI does not influence the activity of ASH but

during starvation, ASI's activity may suppress ASH's activation to NaCl. This suppression is not statistically significant but it is trending on significance (p=0.0981). This may be a means to increase food intake under more desperate circumstances when worms are nutritionally depleted and are will to risk the presence of noxious stimuli to consume the necessary nutrients.

To see if this relationship between ASI and ASH affects food related behaviors, I tested genetic ablations of ASI and ASH (ASI- and ASH-) in the automated satiety quiescence assay. The ASI genetic ablation was previously tested in the lab by Dr. Thomas Gallagher, I included his data for reference to make comparisons between conditions easier (Gallagher, Kim, et al., 2013). In the fasted and well-fed condition, ASI- worms show increased dwelling and reduce roaming and quiescence when compared to the concurrent wild type (Figure 8A). ASI is important for transitioning between these behavioral states into quiescence, which our lab has previously reported(Gallagher, Kim, et al., 2013). In the fasted and well-fed conditions, ASH- worms show increased quiescence behavior compared to the concurrent wild type (Figure 10A). This suggests that the absence of ASH removes an inhibitory signal on ASI to increase the amount of time spent in quiescence. To determine which neuron is downstream of the other, I tested a double genetic ablation of ASI and ASH. In the fasted and well-fed conditions, ASI-/ASH- worms show a phenotype most similar to ASI- worms with increased dwelling and reduced quiescence and roaming compared to the concurrent wild type ($p < 0.00001$, Figure 10A). Based on the calcium imaging data, ASH- should be the phenotype seen in the fasted condition when testing ASI-/ASH-, giving increased quiescence compared to the concurrent wild type. However,

the satiety quiescence assay allows 3 hours of refeeding for worms to replenish their fat stores. Without this refeeding period worms are too pale to accurately track on the bacterial lawn under the cameras. The replenishing of fat stores could reset any starvation signaling originating in the intestine. If a starvation signal from the intestine is stopped by the return of fat stores, it could allow the ASI/ASH circuit to rebalance back to the well-fed state. I tested the food intake of these genetic ablations compared to wild type worms in the well-fed condition to determine if this circuit also influences the amount bacteria consumed in addition to satiety. I could not accurately quantify the ASH- and ASI-/ASH- worms because the ASH ablation is marked by an RFP protein and the way I measured food intake was to image the level of red fluorescent bacteria present in each worm's intestine. This extra RFP signal in the coelomocytes of the worms interferes with the quantification of the overall fluorescence. However, I have included sample photos to demonstrate that wild type worms (Figure 10B) consume more food (show greater fluorescence) than ASH- or ASI-/ASH- worms (Figure 10C & D). This further supports the satiety behavior, without ASH these worms eat less because they spend more time in quiescence. Dr. Gallagher had previously tested ASI ablated worms in this food intake assay and found that without ASI, worms eat more because of the increased time spent in dwelling (Gallagher, Kim, et al., 2013). The food intake assay more closely mimics the ASH- phenotype in this assay when testing ASI-/ASH- worms.

Next I conducted two experiments to ensure the suppression of ASI in these experiments was via ASH activation. To more directly and cleanly activate ASH, I created strain in which channel rhodopsin is expressed in ASH and GCaMP is expressed in ASI.

Figure 10

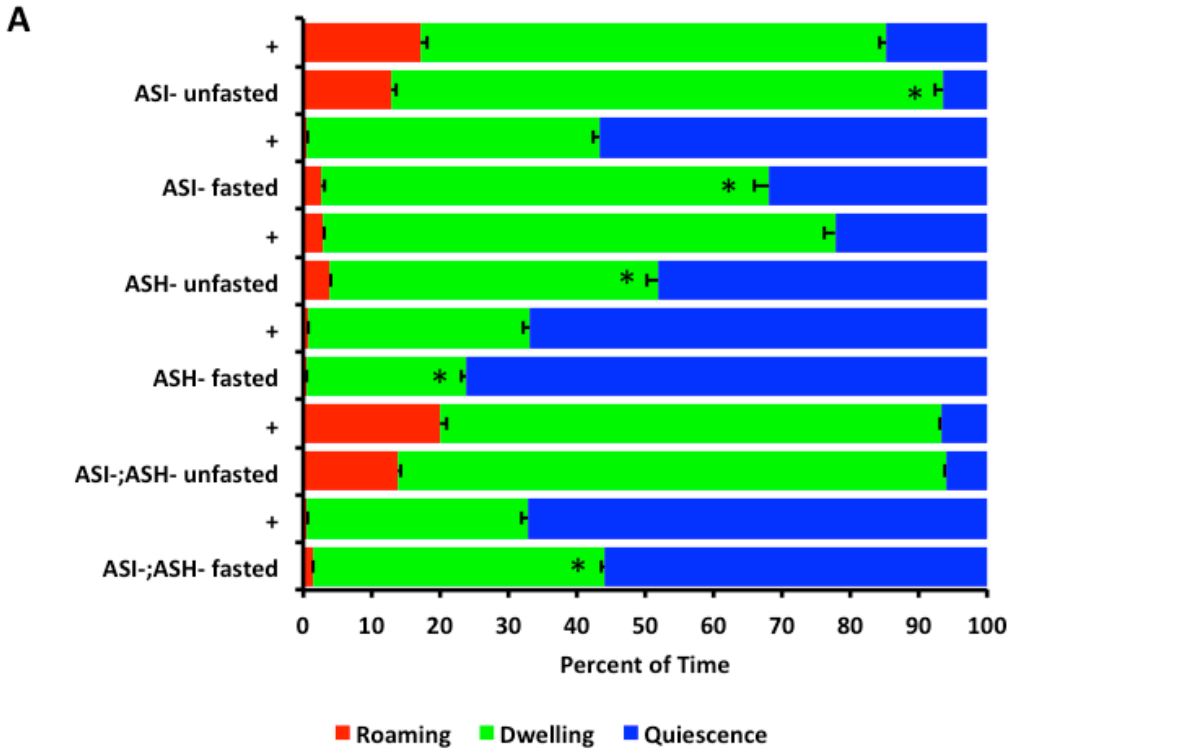
A
+
ASI- unfasted
+
ASI- fasted
+
ASH- unfasted
+
ASH- fasted
+
ASI-;ASH- unfasted
+
ASI-;ASH- fasted
0
10
20
30
40
50
60
70
80
90
100
Percent of Time
Roaming
Dwelling
Quiescence

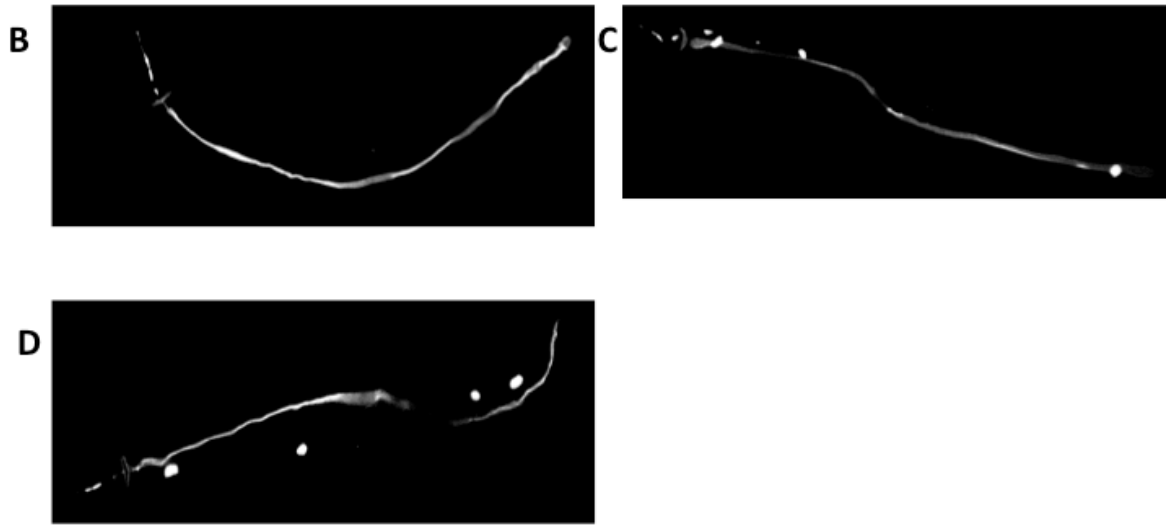
B
C
D

Figure 10. ASI and ASH genetic ablation behavior

A. Concurrent wild type (+), ASI genetic ablation (ASI-) (Gallagher, Kim, et al., 2013), ASH genetic ablation (ASH-), and ASI/ASH genetic ablation (ASI-;ASH-) tested in the automated satiety quiescence assay. ASI- unfasted *n=11, + n=20;* ASI- fasted *n=7, + n=16;* ASH- unfasted *n=24, + n=15;* ASH- fasted *n=27, + n=13;* ASI-;ASH- unfasted *n=28, + n=15;* ASI-;ASH- fasted *n=27, + n=14* * = statistically significant

B. Example image of N2 intestine in food intake assay.

C. Example image of ASH genetic ablation intestine in food intake assay.

D. Example image of ASI/ASH genetic ablation intestine in food intake assay.

Figure 11

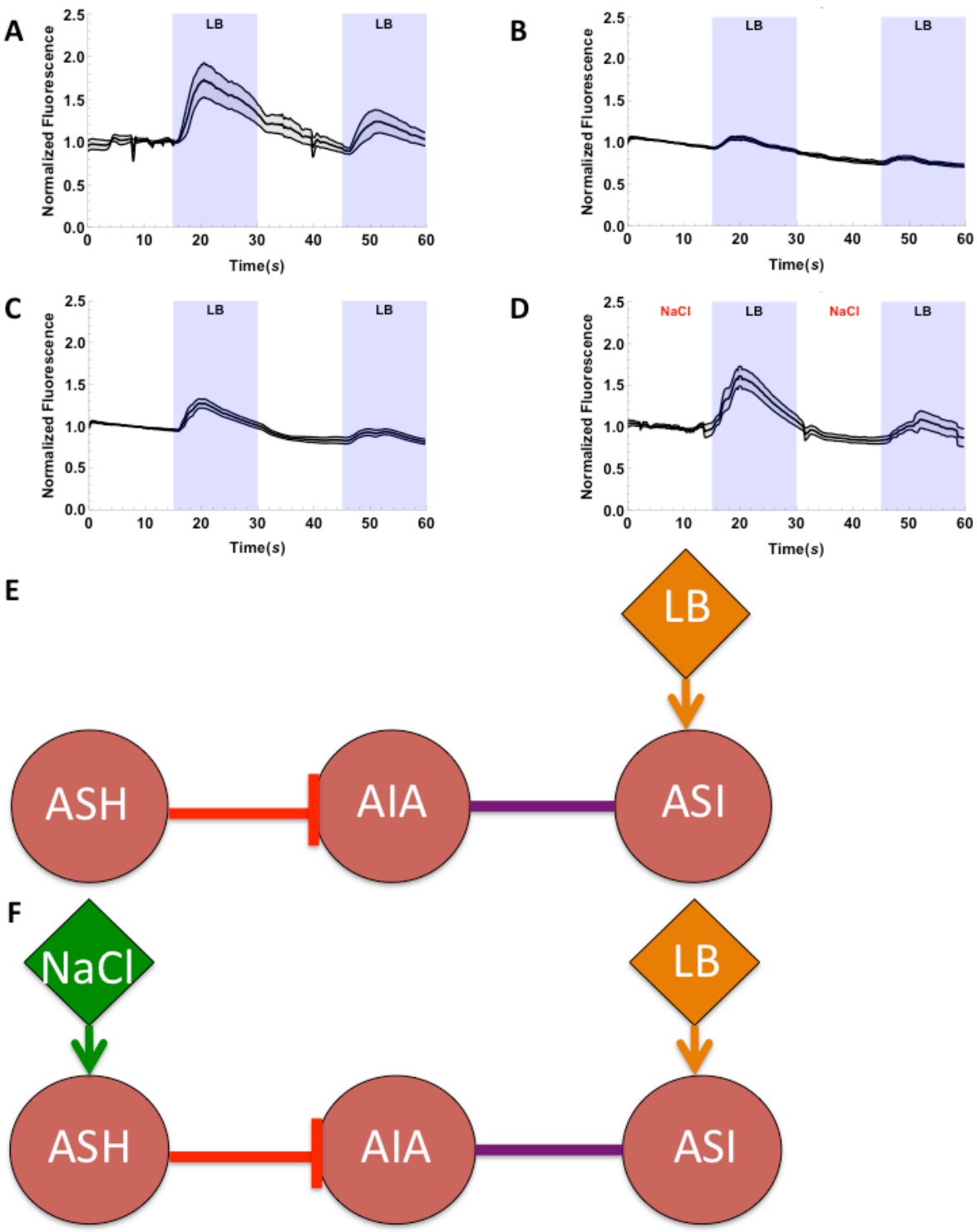

Figure 11. Verifying ASH is responsible for ASI's suppression to noxious stimuli

A. ASI activation to LB in worms grown on ethanol *n=5*

B. ASI activation to LB in worms grown on ATR and ChR activation in ASH *n=10*

C. ASI activation to LB in ASH genetic ablation background (transgenic GCaMP). *n=12*

D. ASI activation to LB in ASH genetic ablation background after exposure to 4 M NaCl (1 min.) *n=10*

E. Proposed circuit between ASI and ASH in the absence of noxious stimuli based on known connectivity data (Bhatla, 2014)

F. Proposed circuit between ASI and ASH in the presence of noxious stimuli based on known connectivity data (Bhatla, 2014)

All graphs are normalized to the initial 15 second of the recording during which the worms' noses are washed with S buffer or NaCl (presence of which is indicated at the top of the graph). The dark central trace is the average and the lighter lines above and below are standard error of the mean. The blue segments indicate when the worms are receiving the stimulus.

To use channel rhodopsin in worms, the worms must be grown on all-trans retinal (ATR) from hatching until they are tested. The ATR is necessary for channel rhodopsin to work and worms do not naturally produce ATR or any other similar cofactor that channel rhodopsin could use. Channel rhodopsin is activated by blue light; the lab's calcium imaging setup uses blue light (470 nm) to image GCaMP. Worms expressing channel rhodopsin in ASH grown on ATR plates show a much smaller activation to LB in ASI than the same worms grown on the vehicle (ethanol) (Figure 11A & B). This gives a clean, definitive activation of ASH and shows suppression in ASI. The inverse experiment is the removal of ASH, which I did using the ASH genetic ablation in the strain expressing GCaMP as a transgene in ASI. ASI continues to show LB activation to comparable levels regardless of the presence of 4M NaCl (figure 11C & D). These two experiments verify that the suppression of ASI by high concentrations of NaCl is acting via ASH.

These experiments led me to test a possible circuit in *C. elegans* based on known connectivity data. I hypothesized that ASH could influence ASI via an interneuron pair, AIA, when a noxious stimulus was present (Figure 11E-F).

2.5 AIA, an interneuron acting on ASI and ASH

Knowing the location and identity of every neuron in *C. elegans* is a tremendous resource that allows the development of potential circuits and the framework with which to test them. Based on this known connectivity data, I identified AIA as a possible mediator and integrator of information between ASI and ASH. AIA is an interneuron pair located in

the head of the worm. It shares a gap junction with ASI as well as a chemical synapse in which ASI is presynaptic. AIA is presynaptic and postsynaptic to ASH via two chemical synapses they share. Interneurons work to integrate multiple information sources and determine an appropriate behavioral output. AIA is well placed to integrate the sensory information from ASI and ASH to decide what behavior output is appropriate for its received input. To determine if AIA may play role in the circuit and its behavioral output, I tested worms with an AIA genetic ablation in the satiety quiescence assay. The genetic ablation was accomplished by over expressing *mec-4* in AIA as a transgene. *mec-4* is a sodium channel and ectopic expression of this channel overexcites the neurons and kills them. Worms lacking AIA show increased satiety quiescence when compared to their transgenic siblings and to concurrent wild type ($p < 0.0001$, Figure 12A). This supports my argument that AIA is mediating the suppression of ASI because the removal of AIA results in an increased ASI-mediated behavior.

To determine if signals from ASH and ASI activate AIA, I acquired a strain expressing GCaMP in AIA. Calcium imaging for interneurons is different than in a sensory neuron such as ASI. There is a lot of noise and the activations are frequently seen in only the processes instead of the processes and cell body. I tested AIA in the fed-well condition first and saw some activation to the presentation of LB (Figure 12B & C). I also saw some slight activation to NaCl in the well-fed condition in a few worms (Figure 12D & E)). To determine if AIA may respond to starvations similarly to ASI or ASH, I starved them for six hours prior to calcium imaging. I did not see any difference between average AIA activation to LB and NaCl in the starved or well-fed conditions (Figure 12F, G & 13A, B).

Figure 12

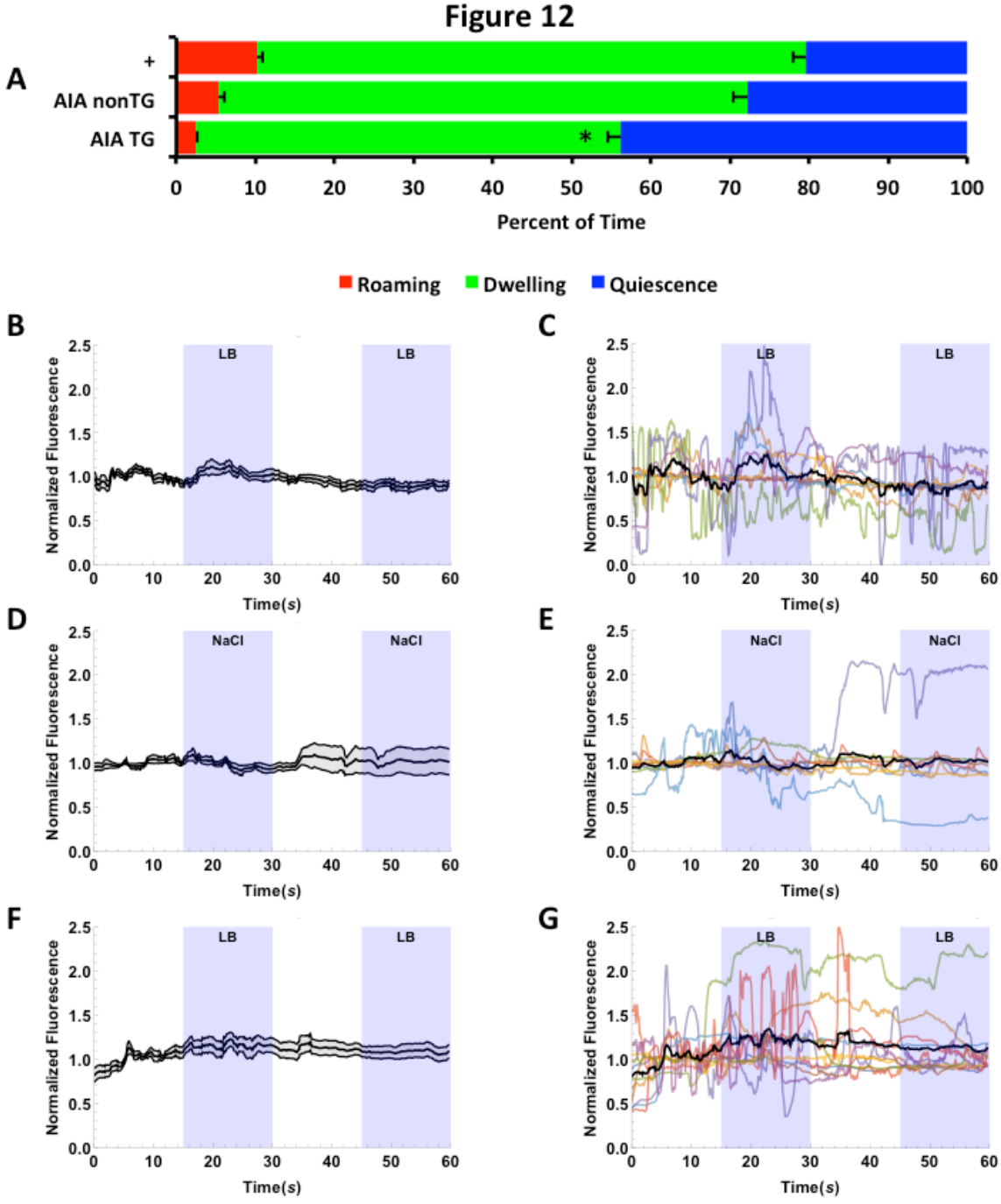
A
+
AIA nonTG
AIA TG
*
0 10 20 30 40 50 60 70 80 90 100
Percent of Time
Roaming
Dwelling
Quiescence
B
C
D
E
F
G
Normalized Fluorescence
LB
NaCl
Time(s)

Figure 12. AIA potentially integrates the signal between ASI and ASH part I

A. Concurrent wild type (+) and AIA genetic ablation (AIA TG) with non-transgenic siblings (AIA nonTG) tested in the automated satiety quiescence assay. AIA TG *n=18,* AIA nonTG *n=17, + n=17* *= statistically significant

B. AIA activity to LB well-fed average graph (transgenic GCaMP) *n=9*

C. AIA activity to LB well-fed individual traces (transgenic GCaMP) *n=9*

D. AIA activity to 4 M NaCl well-fed average graph (transgenic GCaMP) *n=8*

E. AIA activity to 4 M NaCl well-fed individual traces (transgenic GCaMP) *n=8*

F. AIA activity to LB 6 hours fasted average graph (transgenic GCaMP) *n=11*

G. AIA activity to LB 6 hours fasted individual traces (transgenic GCaMP) *n=11*

All graphs are normalized to the initial 15 second of the recording during which the worms' noses are washed with S buffer. The dark central trace is the average and the lighter lines above and below are standard error of the mean. Individual traces are denoted by different colors and the average line is black. The blue segments indicate when the worms are receiving the stimulus.

Figure 13

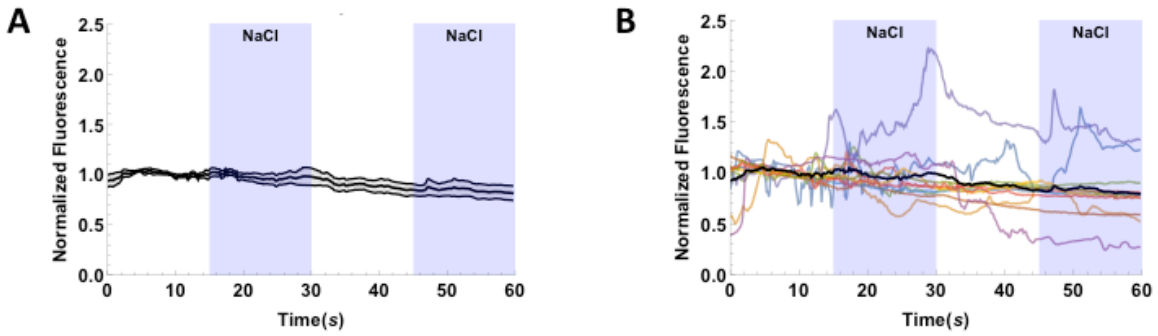
A
NaCl
NaCl
Normalized Fluorescence
Time(s)
B
NaCl
NaCl
Normalized Fluorescence
Time(s)

Figure 13. AIA potentially integrates the signal between ASI and ASH part II

A. AIA activity to 4 M NaCl 6 hours fasted average graph (transgenic GCaMP) *n=11*

B. AIA activity to 4 M NaCl 6 hours fasted individual traces (transgenic GCaMP) *n=11*

All graphs are normalized to the initial 15 second of the recording during which the worms' noses are washed with S buffer. The dark central trace is the average and the lighter lines above and below are standard error of the mean. Individual traces are denoted by different colors and the average line is black. The blue segments indicate when the worms are receiving the stimulus.

However, AIA showed more activity in the individual traces at a higher magnitude when tested with LB when compared to experiments with NaCl (12C, G & 12E, 13B). Activity from ASH may suppress AIA's general activity, previous work from others demonstrated an inhibitory connection between ASH and AIA (Shinkai et al., 2011). There are technical challenges with imaging interneuron processes because slight movements can change how much of the process is in focus and moves the location of the process which at times brings more background fluorescence into the region of interest. These two factors can create issues in the analysis.

2.6 Signals that influence this circuit: glutamate, opioids, serotonin, and octopamine

C. elegans possess the same neurotransmitters that more complex animals also use. To determine which neurotransmitters are capable of regulating the ASI and ASH interaction I tested a variety of them in several ways. The main neurotransmitter released from ASH is glutamate. To determine if this is how ASH conveys its suppression to ASI, I tested mutants deficient in glutamate signaling in the automated satiety quiescence assay. I tested a triple mutant, which lacks *avr-14*, *avr-15*, and *glc-1*. All three of these genes encode inhibitory glutamate receptors, so if ASH is suppressing ASI via one of these the behavior should mimic the ASH ablation in this assay. The triple mutant showed an increase in roaming and an increase in quiescence in the well-fed condition when compared to the concurrent wild-type control ($p < 0.0001$, Figure 14A) but not the increase observed in the ASH ablation when well fed (Figure 10A). However, there are other

inhibitory glutamate receptors so I tested *eat-4* mutants. EAT-4 is an ortholog of the mammalian vesicular glutamate transporter (Lee, Sawin, Chalfie, Horvitz, & Avery, 1999). This mutant showed no significant difference from the concurrent control when fasted but did show an increase in quiescence when well-fed ($p < 0.0001$, Figure 14A). I crossed the ASI expressed GCaMP integration line into the *eat-4* background and tested this mutant in calcium imaging. These mutants show a normal response to 2 M NaCl followed by LB (Figure 14B) and they show a normal response to LB when well fed (Figure 14C). I did not test these worms fasted in calcium imaging because their behavior in the fasted condition did not look different from the control (Figure 14A). This change in quiescence could be affecting another neuron pair that then acts on ASI. In addition, the difference seen in *eat-4* mutants in satiety behavior could be a long-term effect that I am not able to measure in the short-term conditions of calcium imaging. Long-term calcium imaging combined with behavioral recordings could potentially pick apart what is truly going on to give these behavioral results.

The next step in characterizing this circuit is to determine which neurotransmitters are released and act on each pair of neurons. Recent work identified an opioid signaling pair in *C. elegans*, neuropeptide receptor (*npr-17)* and neuropeptide-like protein (*nlp-24*).(Cheong, Artyukhin, You, & Avery, 2015) Cheong and colleagues found this signal to be important during starvation to regulate feeding via ASI. This signal is very appealing for a couple of reasons: 1) they already demonstrated this signal can regulate a feeding behavior in starvation 2) opioids are long term signals, during starvation a long term signal is necessary to properly regulate starvation related behaviors and 3) ASH responds to

noxious or painful stimuli and opioids are natural pain relievers in other animal systems, making *nlp-24* a good candidate to regulate this interaction. To ascertain that opioid signaling could influence satiety behavior, we tested an opioid blocking drug, naloxone. Worms tested on 5 mM naloxone show increased quiescence in the well-fed condition ($p < 0.0001$, Figure 15A). To determine if the previously identified signaling pair were involved, we tested *npr-17* and *nlp-24* mutants in our satiety quiescence assay. Worms lacking *npr-17* have increased quiescence in the well-fed condition ($p < 0.0001$) but no difference in the fasted condition when compared to the concurrent control (Figure 15A). This result mimics the naloxone result, indicating this receptor may be the site of action for naloxone in satiety behavior. Worms lacking *nlp-24* show no significant difference from the concurrent control in the well-fed condition and increased quiescence in the fasted condition ($p = 0.0041$, Figure 15A). To further characterize the influence of the opioid signaling on this circuit, I tested *nlp-24* mutants using calcium imaging. Worms lacking *nlp-24* do not show any difference in activation to LB well-fed (Figure 15B) and do not show any difference in activation to 10% LB after 6 hours of starvation (Figure 15C). I decided to test the response to NaCl and LB under well-fed and fasted conditions. Both conditions result in a suppressed but intact ASI response on average (Figure 15D & E). However, on an individual basis, the *nlp-24* mutants after 6 hours of starvation show more variations in their response. Out of 11 worms, 5 did not show any activation at all to LB following 2 M NaCl after 6 hours of starvation (Figure 16A). In the well-fed condition, all of the worms tested showed activation to LB following 2 M NaCl (Figure 16B). The well-fed peak was significantly greater ($p = .0038$) compared to fasted. From this I conclude

Figure 14

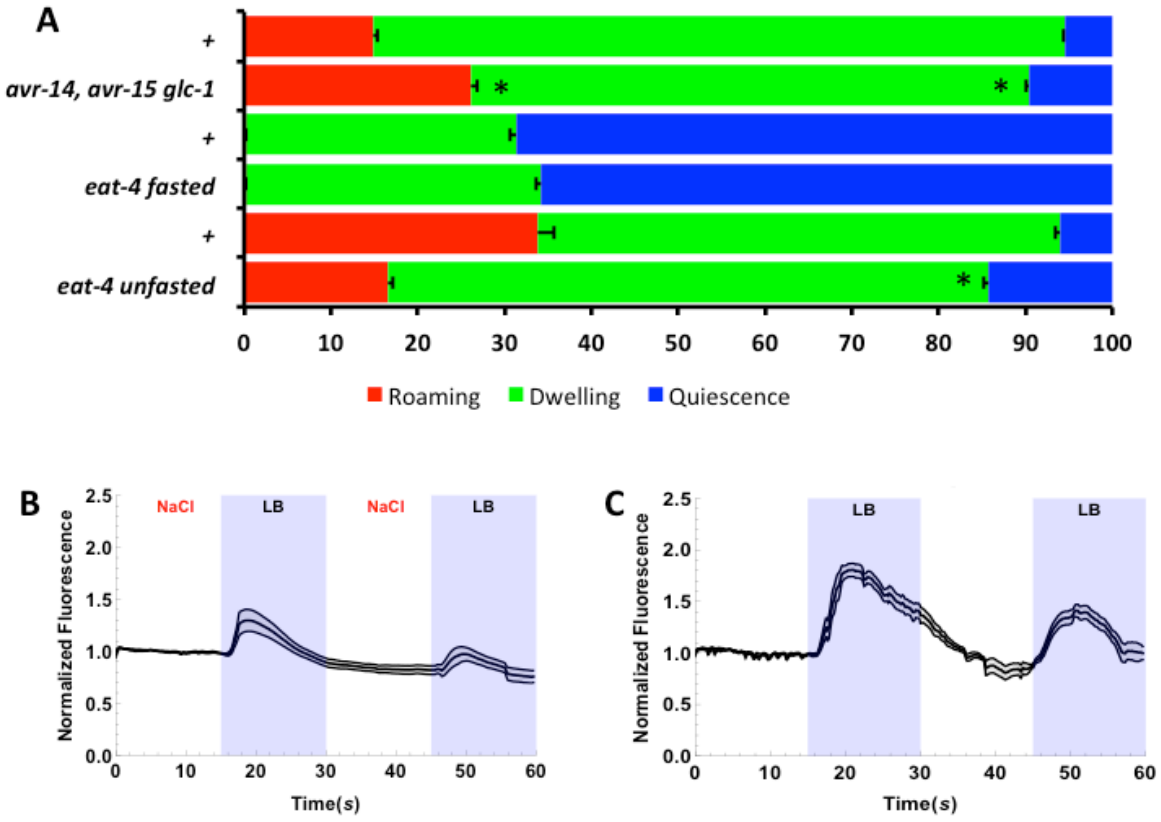
A
+
avr-14, avr-15 glc-1
+
eat-4 fasted
+
eat-4 unfasted
0
10
20
30
40
50
60
70
80
90
100
Roaming
Dwelling
Quiescence
B
NaCl
LB
NaCl
LB
Normalized Fluorescence
Time(s)
C
LB
LB
Normalized Fluorescence
Time(s)

Figure 14. Glutamate influences satiety behavior but not short term ASI activity

A. Concurrent wild type (+), *avr-14, avr-15 glc-1* mutants, and *eat-4* mutants tested in the automated satiety quiescence assay. *avr-14, avr-15 glc-1 n=26, + n=20; eat-4* fasted *n=26, + n=14; eat-4* unfasted *n=24, + n=12* ***=** statistically significant

B. ASI activation to LB after exposure to 2 M NaCl *n=10*

C. ASI activation to LB *n=10*

All graphs are normalized to the initial 15 second of the recording during which the worms' noses are washed with S buffer or NaCl (presence of which is indicated at the top of the graph). The dark central trace is the average and the lighter lines above and below are standard error of the mean. Individual traces are denoted by different colors and the average line is black. The blue segments indicate when the worms are receiving the stimulus.

that *nlp-24* regulates the ASI/ASH circuit in starved conditions, potentially as a pain-relieving signal to ASI.

Serotonin regulates various food related behaviors in both invertebrates and vertebrates. It increases pharyngeal pumping (means by which worms ingest food) and appears to signal the presence of food to the worm (Leon Avery & You, 2012). I tested *tph-1* mutants (tryptophan hydroxylase, an enzyme needed for serotonin production) and found a significant difference in satiety behavior ($p = 0.0023$, Figure 17A). However, when worms are tested on 10 mM serotonin, there is an enormous increase in well-fed satiety quiescence ($p < 0.0001$, Figure 17A). To determine if this increase in quiescence is to due an increase in food intake, I measured the worms' intake of fluorescent bacteria on control or 10 mM serotonin plates. There was a significant increase in food intake in worms tested on 10 mM serotonin (Figure 17B). Next, we tested the impact of serotonin on ASI activation to LB. Chronic exposure to 10 mM serotonin decreased the response of ASI to 10% LB (Figure 17C). Worms fasted for 6 hours on 10 mM serotonin also show a decrease in ASI's response to 10% LB (Figure 17D). The suppression of ASI by serotonin in both conditions is statistically significant ($p < 0.0001$). This suppression of ASI by serotonin is slightly puzzling at first glance, especially given the increase in quiescence in the automated assay. However, worms release serotonin when they first encounter a lawn of bacteria. This results in a slowing of the worm's locomotion and serotonin also increases the pumping rate of the pharynx. This combination of behaviors in response to food is serotonin dependent and is thought to be a means to increase the food intake of the animal

Figure 15

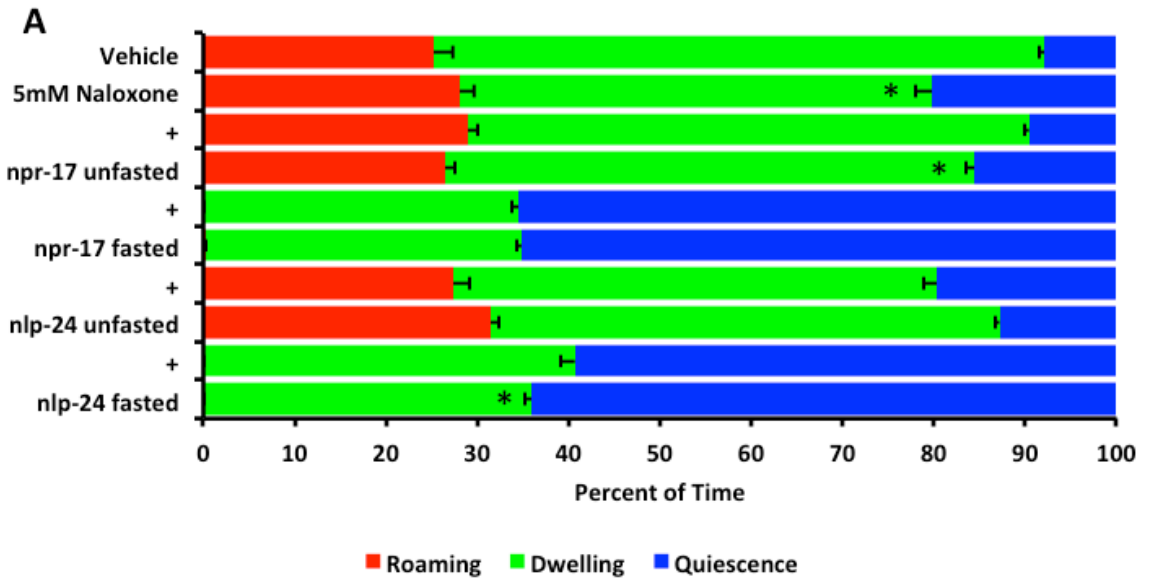
A
Vehicle
5mM Naloxone
+
npr-17 unfasted
+
npr-17 fasted
+
nlp-24 unfasted
+
nlp-24 fasted
0 10 20 30 40 50 60 70 80 90 100
Percent of Time
Roaming
Dwelling
Quiescence

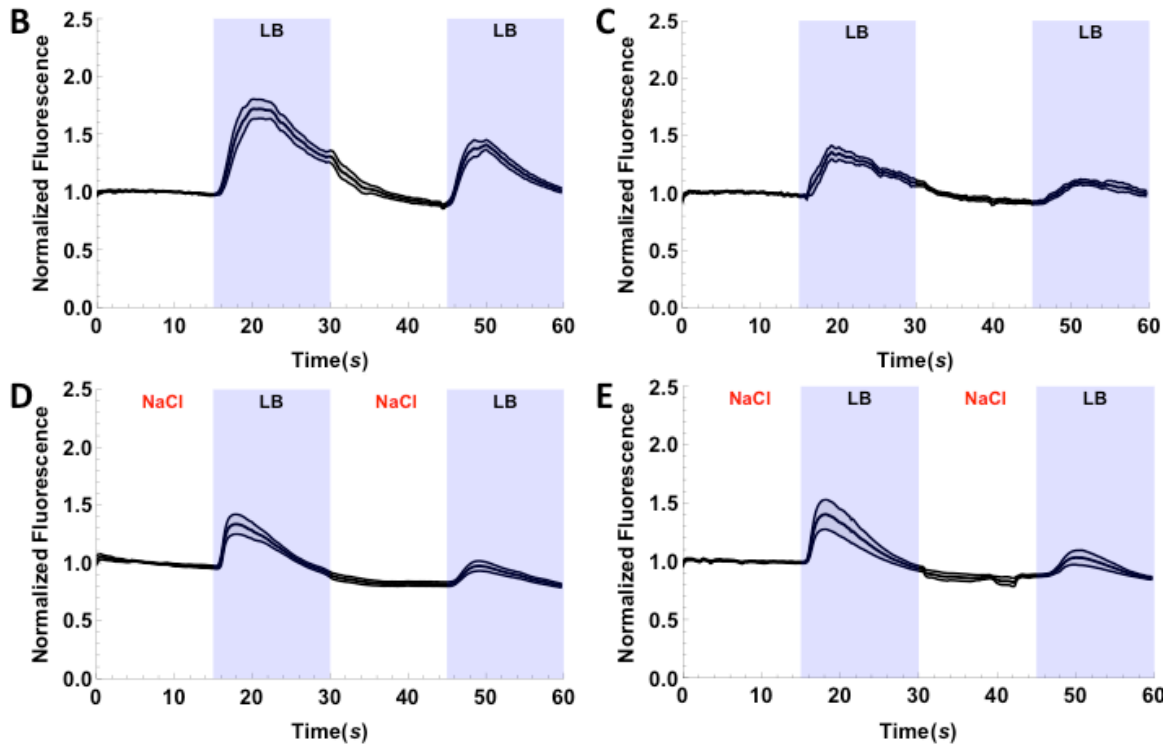
B
C
D
E
LB
NaCl
Normalized Fluorescence
Time(s)

Figure 15. Opioid signaling modulates the ASI and ASH interaction part I

A. Concurrent wild type (+)/vehicle, 5mM naloxone-treated, *npr-17* mutants, and *nlp-24* mutants tested in the automated satiety quiescence assay. 5 mM naloxone-treated *n=15,* vehicle *n=12; npr-17* fasted *n=26, + n=14; npr-17* unfasted *n=23, + n=18; nlp-24* fasted *n=25, + n=12; nlp-24* unfasted *n=31, + n=17*

B. ASI activation to LB in an *nlp-24* mutant background *n=10*

C. ASI activation to 10% LB in an *nlp-24* mutant background after 6 hours starvation *n=10*

D. ASI activation to LB in an *nlp-24* mutant background after exposure to 2 M NaCl average graph *n=12*

E. ASI activation to LB in an *nlp-24* mutant background after 6 hours starvation and exposure to 2 M NaCl average graph *n=11*

All graphs are normalized to the initial 15 second of the recording during which the worms' noses are washed with S buffer or NaCl (presence of which is indicated at the top of the graph). The dark central trace is the average and the lighter lines above and below are standard error of the mean. The blue segments indicate when the worms are receiving the stimulus.

Figure 16

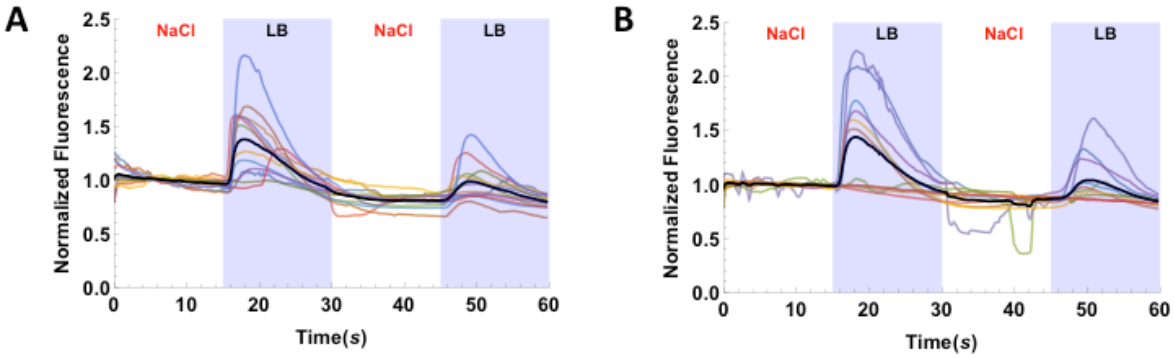
A
NaCl
LB
NaCl
LB
Normalized Fluorescence
Time(s)
B
NaCl
LB
NaCl
LB
Normalized Fluorescence
Time(s)

Figure 16. Opioid signaling modulates the ASI and ASH interaction part II

A. ASI activation to LB in an *nlp-24* mutant background after exposure to 2 M NaCl individual traces *n=12*

B. ASI activation to LB in an *nlp-24* mutant background after 6 hours starvation and exposure to 2 M NaCl individual traces *n=11*

All graphs are normalized to the initial 15 second of the recording during which the worms' noses are washed with S buffer or NaCl (presence of which is indicated at the top of the graph). The dark central trace is the average and the lighter lines above and below are standard error of the mean. Individual traces are denoted by different colors and the average line is black. The blue segments indicate when the worms are receiving the stimulus.

upon encountering food. I think the increase in quiescence seen in the automated assay may not be true satiety quiescence in that the worms' pharynges are still pumping. By definition, during satiety quiescence, the worms should not be pumping. The cameras in the automated assay did not reach the resolution required to discern pumping behavior. The serotonin is suppressing locomotive behavior and simultaneously increasing the pumping rate, this also explains the increase in food intake (Figure 15B) paired with the increase in quiescence, a combination that does not typically occur in the two assays.

Guo and colleagues found that ASI can cause the release of serotonin from ADF (another neuron pair located in the worm's head) and inhibit ASH's activation (Guo et al., 2015). To test if this was possible to induce by simply giving the worms serotonin during calcium imaging, I exposed the worms to 10mM serotonin across their nose for 4 minutes then presented them with 2M NaCl. These conditions elicited the smallest response from ASH to 2M NaCl I have observed across all experiments (Figure 15E) and this suppression is statistically significant ($p = .0087$). This suggests that serotonin could be the signal that ASI's activation to LB increases under fasted conditions to suppress ASH's response to 2M NaCl (Figure 10G). I did not pursue this line of questioning further because it is already published and would not add any significance to my work. I will discuss further what could be done to verify this in future directions.

Octopamine has been implicated as a hunger signal in worms (Gallagher, Kim, et al., 2013; Greer, Perez, Gilst, Lee, & Ashrafi, 2008; Suo, Culotti, & Van Tol, 2009). It is produced from tyrosine to tyramine by tyrosine decarboxylase (*tdc-1*) and tyramine is converted to octopamine by tyramine β-hydroxylase (*tbh-1*). Tyramine can also function as

Figure 17

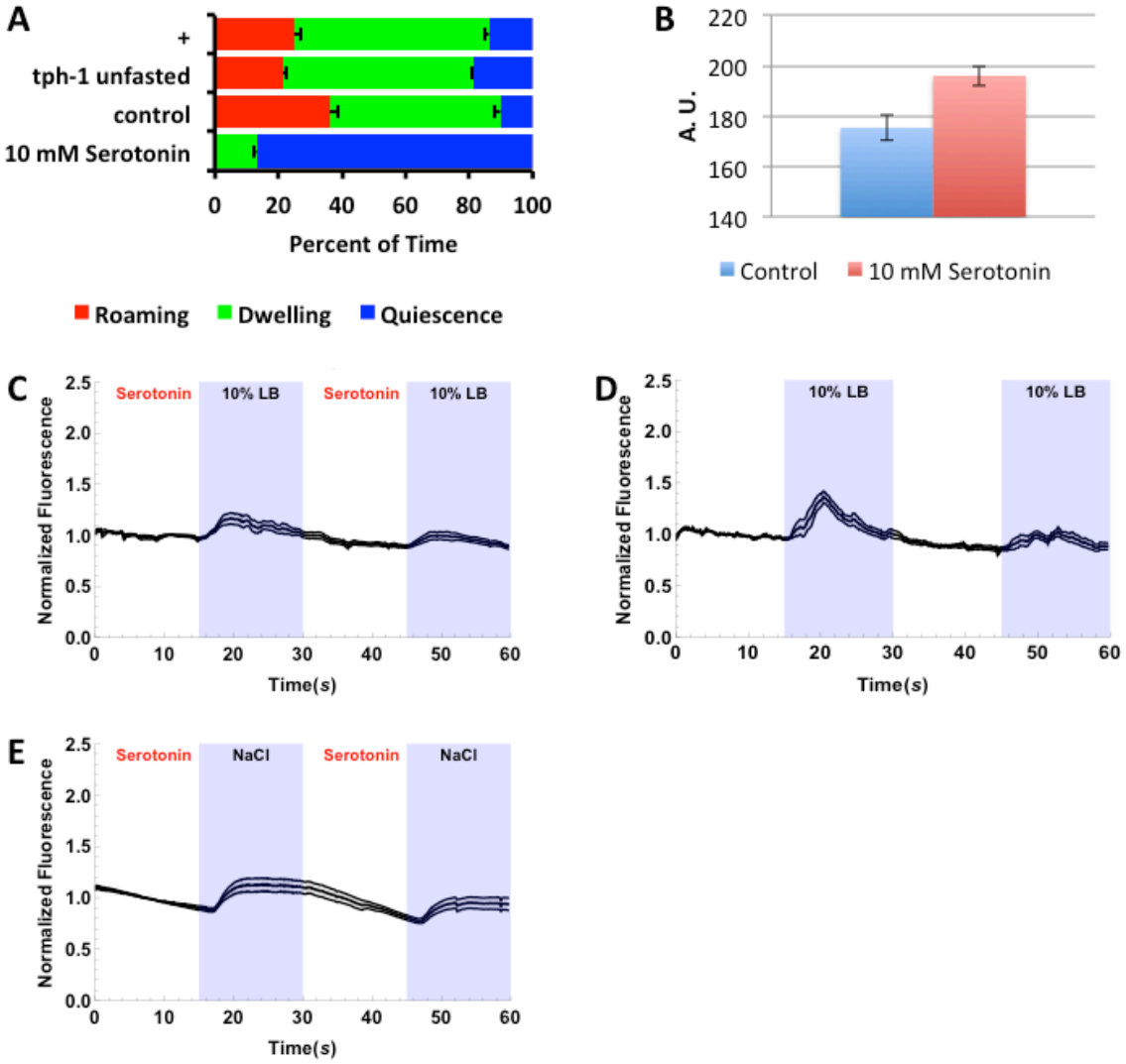
A
+
tph-1 unfasted
control
10 mM Serotonin
0
20
40
60
80
100
Percent of Time
Roaming
Dwelling
Quiescence
B
220
200
180
160
140
A. U.
Control
10 mM Serotonin
C
Serotonin
10% LB
Serotonin
10% LB
Normalized Fluorescence
Time(s)
D
10% LB
10% LB
Normalized Fluorescence
Time(s)
E
Serotonin
NaCl
Serotonin
NaCl
Normalized Fluorescence
Time(s)

Figure 17. Serotonin affects the activity of ASI and ASH as well as feeding behavior

A. Concurrent wild type (+)/vehicle, *tph-1* mutants, and 10 mM serotonin-treated tested in the automated satiety quiescence assay. *tph-1* fasted *n=29,* + *n=15;* 10 mM serotonin-treated *n=18,* vehicle *n=9*

B. Food intake assay of N2 on vehicle (*n=20*) or 10 mM serotonin-treated (*n=26*) plates (A. U. = arbitrary units of fluorescence).

C. ASI activation to 10% LB after exposure to 10 mM serotonin (4 min.) *n=10*

D. ASI activation to 10% LB after 6 hours starvation on 10 mM serotonin-treated plates *n=7*

E. ASI activation to LB in an *nlp-24* mutant background after exposure to 2 M NaCl average graph *n=12*

E. ASH activation to 2 M NaCl after exposure to 10 mM serotonin (4 min.) *n=10*

All graphs are normalized to the initial 15 second of the recording during which the worms' noses are washed with S buffer or serotonin (presence of which is indicated at the top of the graph). The dark central trace is the average and the lighter lines above and below are standard error of the mean. The blue segments indicate when the worms are receiving the stimulus.

a neurotransmitter independent of octopamine (Alkema, Hunter-Ensor, Ringstad, & Horvitz, 2005). TDC-1 is produced in two pairs of head neurons in *C. elegans*, RIC and RIM, while TBH-1 is only produced in RIC. It is important to note that TBH-1 and TDC-1 are also found in the gonadal sheath and TDC-1 is also found in the UV1 (neurosecretory cells involved in egg-laying)(Alkema et al., 2005; Lints & Hall, 2009). In the absence of food, RIC releases octopamine and previous work in our lab has demonstrated that silencing RIM/RIC with DAF-7 (signal from ASI) is necessary for satiety quiescence (Gallagher, Kim, et al., 2013; Greer et al., 2008; Suo et al., 2009). The conclusion was that octopamine was released from RIC and reduced satiety quiescence. To test the involvement of this signal, I tested several conditions.

The *tdc-1* mutants (lacking tyramine and octopamine) showed no change in satiety behavior compared to the concurrent wild type but did show increased roaming ($p < 0.0001$, Figure 18A). Next, *tbh-1* mutants showed increased satiety behavior and no change in roaming ($p < 0.0001$, Figure 18A). There seems to be some balance between tyramine and octopamine signaling, the absence of both does not change satiety but the absence of octopamine only increases satiety. To explore the role of octopamine with *daf-7*, I tested a double mutant lacking *daf-7* and *tbh-1*. To enter satiety quiescence, ASI needs to release *daf*-7 (a TGFβ in *C. elegans*). The *daf-7* mutants resemble ASI ablated worms because the *daf-7* needed for satiety quiescence comes primarily from ASI. Without *daf-7*, worms spend more time in dwelling and less time in roaming or quiescence. The idea behind this experiment is to determine if removal of the potential hunger signal, octopamine, can alleviate the defect in quiescence seen in *daf-7* mutants to resemble wild

type levels satiety behavior. The *daf-7;tbh-1* mutant worms did show more satiety quiescence than ASI ablated worms (Figure 11A) and *daf-7* mutants (Gallagher, Kim, et al., 2013) but they do not match the concurrent wild type controls (Figure 18A). This supports the notion that there is a balance between tyramine and octopamine signaling that is lost when *tbh-1* is no longer functioning.

To further test the involvement of octopamine and tyramine, I tested worms on plates treated with octopamine or tyramine. The octopamine treated plates showed the same level of satiety quiescence as the control and shows an increase in roaming (p = 0.0002, Figure 18A). This result fits with the *tbh-1* mutants lacking octopamine and showing an increase in quiescence. If octopamine is a hunger signal, it would make sense for extra octopamine to increase food-seeking behavior and a lack of octopamine to increase satiety. However, this does not explain *tdc-1* mutants not showing the same phenotype. To see what role tyramine may play, I tested worms on tyramine treated plates. These worms show an increase in roaming and decreased quiescence ($p < 0.0001$ & p = 0.002, Figure 18A), which does not match with the rest of the data at all. In the case of the *tbh-1* mutants, that is a similar condition to having extra tyramine because none of the tyramine made by *tdc-1* is converted to octopamine. However, this extra tyramine may remain inside of RIC/RIM and not influence other neurons at all. The discrepancy between these experiments could be the result of a lack of octopamine in other pathways that eventually influence satiety behavior in ways that have not been investigated.

In an attempt to rectify this confusing situation, I tested receptor mutants for octopamine and tyramine. The octopamine receptor *ser-3* has been implicated by others as

a suppressor of ASI activity (Guo et al., 2015). Worms lacking *ser-3* show decreased dwelling with an increase in roaming and very little change in satiety compared to wild type ($p < 0.0001$, Figure 18B). This is different from worms lacking ASI, which show decrease roaming and quiescence with an increase in dwelling, which is almost the opposite of *ser-3* mutants. This could indicate that without *ser-3* worms are capable of transitioning between these behavioral states easier because ASI is more active but that may not be the full picture because I would expect to see an increase in quiescence compared to wild type that is not there. Next, *tyra-3* (tyramine receptor) mutants showed increased quiescence ($p < 0.0001$, Figure 18B) which fits the data from the tyramine treated plates, but does not match with *tdc-1* or *tbh-1* mutants. Finally, I tested *octr-1* (octopamine receptor) mutants and found an increase in roaming and quiescence ($p < 0.0001$, Figure 18B), which is similar to the results I saw with *ser-3* mutants. It could be that a double mutant of *ser-3* and *octr-1* would give a clearer picture of octopamine's influence on satiety behavior. In the *octr-1* mutant background, *ser-3* could make up for the lack of *octr-1* to suppress ASI and the same could hold true for *octr-1* in the *ser-3* mutant background.

I decided to test octopamine in calcium imaging to determine if it could activate or suppress ASI. Due to the evidence that ASI signals satiety, I would expect a hunger signal to suppress ASI's activation. ASI did not respond to 4 mM octopamine (Figure 19A) and 4mM nor 8mM octopamine strongly suppressed ASI's activation to LB (Figure 19B & C). I finally tested worms exposed to 4 mM octopamine for 2 hours. If octopamine is a starvation or hunger signal, this longer exposure should give similar results when tested

Figure 18

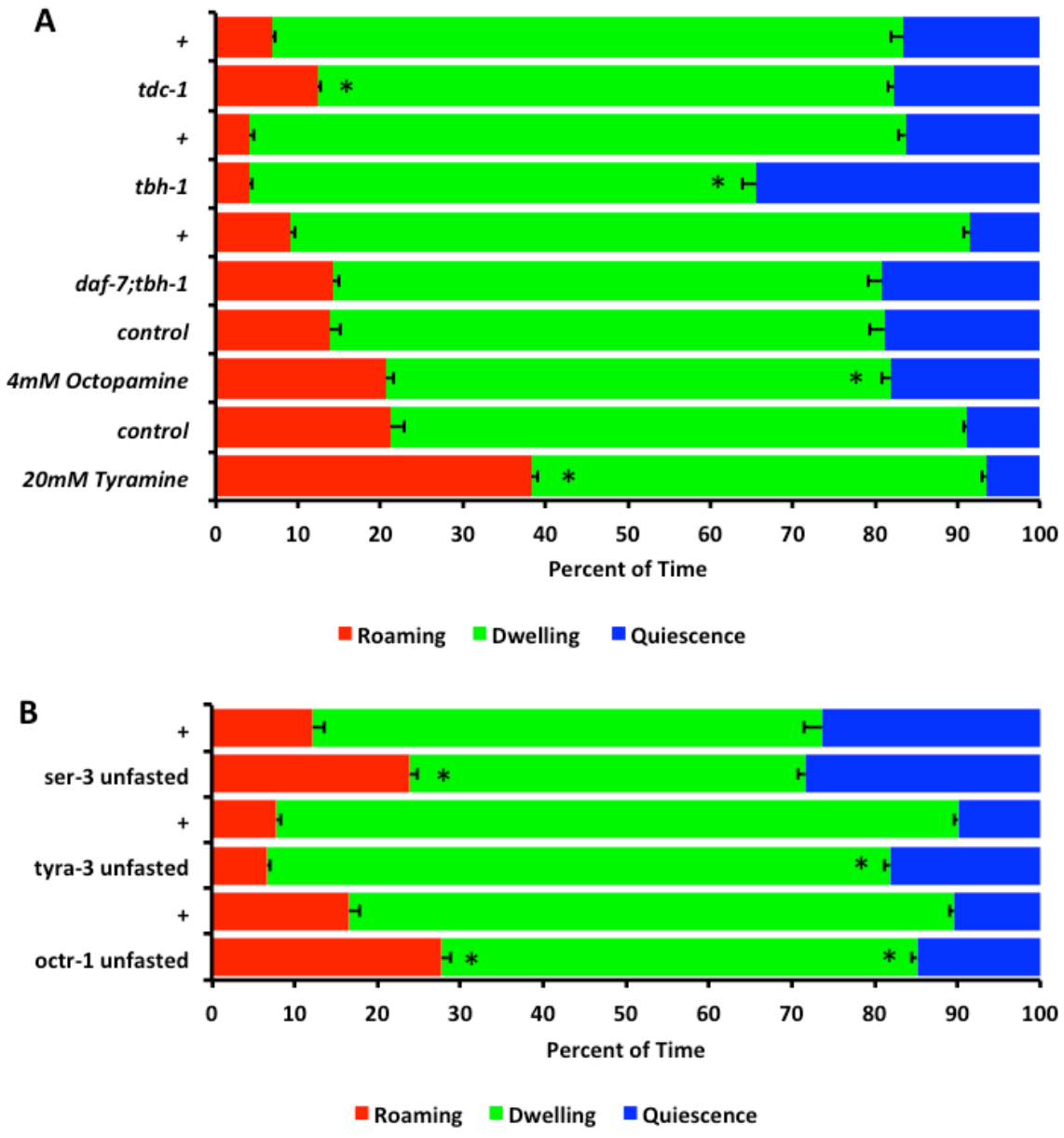
A
+
tdc-1
+
tbh-1
+
daf-7;tbh-1
control
4mM Octopamine
control
20mM Tyramine
0
10
20
30
40
50
60
70
80
90
100
Percent of Time
Roaming
Dwelling
Quiescence
B
+
ser-3 unfasted
+
tyra-3 unfasted
+
octr-1 unfasted
0
10
20
30
40
50
60
70
80
90
100
Percent of Time
Roaming
Dwelling
Quiescence

Figure 18. Octopamine and tyramine influence satiety behavior

A. Concurrent wild type (+)/vehicle, *tdc-1* mutants, *tbh-1* mutants, *daf-7;tbh-1* mutants, 4 mM octopamine-treated plates, and 20 mM tyramine-treated plates tested in the automated satiety quiescence assay. *tdc-1 n=27, + n=15; tbh-1 n=17, + n=9; daf-7;tbh-1 n=15, + n=8;* 4 mM octopamine-treated *n=23,* vehicle *n=13;* 20 mM tyramine-treated *n=29,* vehicle *n=15;* *= statistically significant

B. Concurrent wild type (+), *ser-3* mutants, *tyra-3* mutants, and *octr-1* mutants tested in the automated satiety quiescence assay. *ser-3 n=30, + n=15; tyra-3 n=21, + n=12; octr-1 n=21, + n=12* *= statistically significant

Figure 19

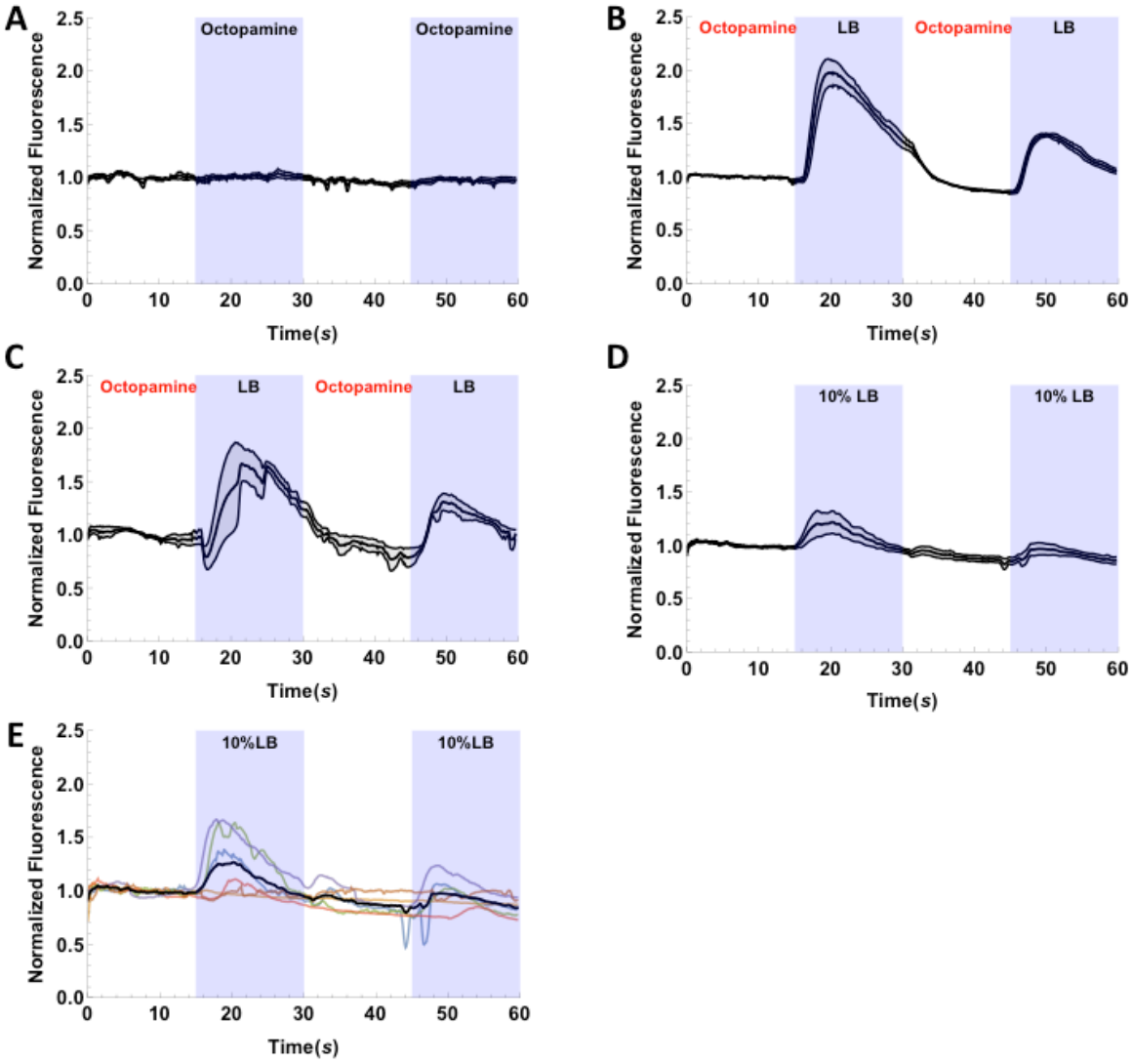
A
Octopamine
Octopamine
B
Octopamine
LB
Octopamine
LB
C
Octopamine
LB
Octopamine
LB
D
10% LB
10% LB
E
10%LB
10%LB
Normalized Fluorescence
Time(s)

Figure 19. Octopamine influences ASI activation after extended exposure

A. ASI activity to 4mM octopamine. *n=5*

B. ASI activation to LB after exposure to 4mM octopamine (4 min.). *n=5*

C. ASI activation to LB after exposure to 8mM octopamine (4 min.). *n=5*

D. ASI activation to LB after 2 hours on 4mM octopamine-treated plates average graph. *n=6*

E. ASI activation to LB after 2 hours on 4mM octopamine-treated plates individual traces. *n=6*

All graphs are normalized to the initial 15 second of the recording during which the worms' noses are washed with S buffer or octopamine (presence of which is indicated at the top of the graph). The dark central trace is the average and the lighter lines above and below are standard error of the mean. The blue segments indicate when the worms are receiving the stimulus.

with 10% LB compared to the 6 hours fasted condition. However, the activation to 10% LB looks the same as the well-fed response on average (Figure 19D). A couple of worms in this condition did not show any activation to 10% LB (Figure 19E), suggesting that octopamine could suppress ASI's activation. To more thoroughly test the role of octopamine, an over expression of either *tbh-1* in RIC or an octopamine receptor in ASI would give a cleaner, more accurate answer.

2.7 Nuclear hormone receptors: possible fat storage indicator

Nuclear hormone receptors (NHRs) are a group of transcription factors involved in development and metabolism that are regulated by lipophilic hormones (Antebi, 2006). The lab began testing NHRs based on the results of a microarray that was then confirmed using qPCR. There were several conditions in which worms were tested in the microarray: well-fed controls, 12 hours starved, 12 hours starved/1 hour refed, 12 hours starved/2 hours refed, ad 12 hours starved/3 hours refed. To identify genes whose expressions were changed by starvation and refeeding, each condition was compared to the well-fed controls. There were a total of 708 genes whose expression changed at these time points, 274 of which are development related and their expression was going to change independent of the worm's metabolic status. An additional 26 genes were up-regulated but they have no known functions/homologs. The rest of the 408 genes were divided into two groups, those genes up-regulated by starvation then down-regulated by refeeding and genes down-regulated by starvation then up-regulated by refeeding. Most of the genes in the second group are involved in stress responses and are not specific to the worm's

metabolic status. The first group, the genes down-regulated by starvation then up-regulated by refeeding, was further investigated to identify a signal of metabolic status to the rest of the worm. In this group of 284, NHRs were overrepresented from the worm's genome at 28 of the 284 genes or 9.6%, especially compared to other gene groups like GPCRs (worms have over 1000), which only accounted for 1% of the 284. Also this pattern of up-regulation during starvation and down-regulation during refeeding held true for all 28 NHRs that came up in the microarray.

Based on all of this, I tested each of the 28 NHRs in the automated satiety quiescence assay using individual RNAi of each gene. RNAi in *C. elegans* is accomplished by simply feeding the worms bacteria that carry the RNAi vector for each gene. The NHRs were tested in the well-fed condition because testing in the fasted condition produces a ceiling effect on satiety quiescence behavior. Testing in the well-fed condition allows the smaller differences between each genes' effect to be revealed more clearly. In addition, these genes were already identified to change expression during starvation and refeeding so testing in the fasted-refed condition would not provide new information and waste time. In conjunction with the satiety behavior, Dr. Moonjung Hyun completed Oil Red O staining to measure the fat storage in the RNAi conditions of each NHR. Based on statistically significant changes in satiety behavior and the fat storage, we broke up the NHRs into 4 groups.

The genes in group 1 are *nhr-170* and *nhr-206*. RNAi of these genes resulted in a decrease in satiety quiescence compared to the concurrent control (Figure 20A) and decreased fat storage. Without these genes, worms may have a defect in fat storage or

synthesis, which results in decreased satiety quiescence. The genes in group 2 are *nhr-21* and *nhr-64*. RNAi of these genes results in an increase in satiety quiescence compared to the concurrent control (Figure 20B) and an increase in fat storage. Group 2 genes work opposite of Group 1 genes, in their absence, fat storage/synthesis is increased and this increase in fat increases satiety behavior. The genes in group 3 are *nhr-8, nhr-50*, *nhr-99*, *nhr-120,* and *nhr-144*. RNAi of these genes increases satiety quiescence in comparison to the concurrent control (Figure 20C) and a decrease in fat storage. In the absence of these genes, worms may spend more time in quiescence and less time eating so there are fewer nutrients to store as fat. The genes in group 4 are *nhr-162* and *nhr-212*. RNAi of these genes resulted in decreased satiety quiescence in comparison to the concurrent control (Figure 20D) and an increase in fat storage. In the absence of these genes, worms may spend more time eating and less time in quiescence. The increased food intake provides more fat for storage. Group 3 and 4 genes may be involved in sensing the worm's metabolic status, our lab has seen similar results in satiety quiescence and fat storage when examining mutants defective in sensing the worm's metabolic status (Gallagher, Kim, et al., 2013).

The remaining 17 genes did not show a clear pattern in either assay (Figure 20E). Seven of these did not show a significant change in satiety quiescence or fat storage (*nhr-18, nhr-36, nhr-40, nhr-59, nhr-79* and *nhr-90*). These genes are negative controls, changes in the expression of these genes are related to metabolic changes but influence phenotypes related to starvation and refeeding were not measured here.

Figure 20

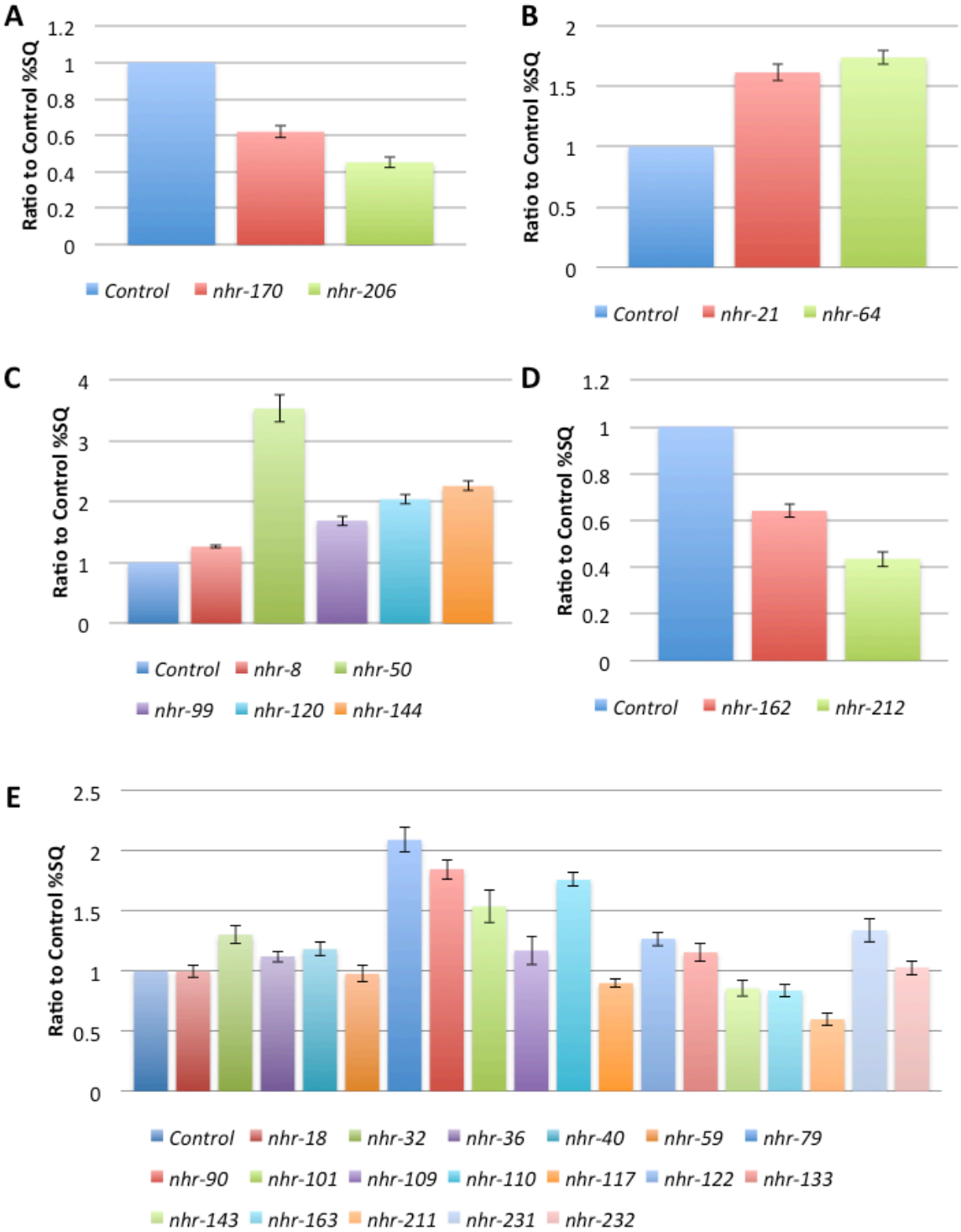
A
Ratio to Control %SQ
1.2
1
0.8
0.6
0.4
0.2
0
Control
nhr-170
nhr-206
B
Ratio to Control %SQ
2
1.5
1
0.5
0
Control
nhr-21
nhr-64
C
Ratio to Control %SQ
4
3
2
1
0
Control
nhr-8
nhr-50
nhr-99
nhr-120
nhr-144
D
Ratio to Control %SQ
1.2
1
0.8
0.6
0.4
0.2
0
Control
nhr-162
nhr-212
E
Ratio to Control %SQ
2.5
2
1.5
1
0.5
0
Control
nhr-18
nhr-32
nhr-36
nhr-40
nhr-59
nhr-79
nhr-90
nhr-101
nhr-109
nhr-110
nhr-117
nhr-122
nhr-133
nhr-143
nhr-163
nhr-211
nhr-231
nhr-232

Figure 20. Nuclear hormone receptors play a role in satiety quiescence

A. Automated satiety quiescence assay of concurrent control, *nhr-170 (n=17),* and *nhr-206 (n=16)* RNAi normalized to satiety quiescence level in concurrent controls.

B. Automated satiety quiescence assay of concurrent control, *nhr-21 (n=16),* and *nhr-64 (n=18)* RNAi normalized to satiety quiescence level in concurrent controls.

C. Automated satiety quiescence assay of concurrent control, *nhr-8 (n=17), nhr-50 (n=11), nhr-99 (n=16),* and *nhr-120 (n=12)* RNAi normalized to satiety quiescence level in concurrent controls.

D. Automated satiety quiescence assay of concurrent control, *nhr-162 (n=18),* and *nhr-212 (n=15)* RNAi normalized to satiety quiescence level in concurrent controls.

E. Automated satiety quiescence assay of concurrent control, *nhr-18 (n=18), nhr-32 (n=16), nhr-40 (n=12), nhr-59 (n=16), nhr-79 (n=17), nhr-90 (n=17), nhr101 (n=17), nhr-109 (n=18), nhr-110 (n=17), nhr-117 (n=17), nhr-122 (n=16), nhr-133 (n=17), nhr-143 (n=11), nhr-144 (n=17), nhr-211 (n=11), nhr-231 (n=16),* and *nhr-232 (n=16)* RNAi normalized to satiety quiescence level in concurrent controls.

2.8 Adenosine and its influence on satiety quiescence

The effects of caffeine are well known among the academic community as many of us use its ability to counteract drowsiness. Caffeine has this effect by blocking adenosine receptors in the brain; the adenosine is thought to build up in the brain over time when an individual is awake (Buolenger, Patel, & Marangos, 1982; Landolt, 2008). Our lab collaborated with Dr. Eric Jorgensen at the University of Utah in Salt Lake City to investigate the role of an adenosine receptor in *C. elegans,* which his post-doc, Dr. Hsiao-Fen Han, identified in her work. Dr. Han identified *ador-1* as an adenosine receptor in *C. elegans* and she also identified the function of *eat-1,* which is acting as an adenosine deaminase. Adenosine deaminase breaks down purines, which includes adenosine (Landolt, 2008). She originally determined these interactions via locomotion assays she did and by comparing sequence homology between the *C. elegans* and mammalian genes. I verified the role this system could play in sleep behavior by looking at well-fed worms.

Comparing to wild type, *eat-1* mutants show a very large amount of roaming ($p < 0.0001$, Figure 21A) while *ador-1* mutants show an increase in quiescence ($p < 0.0001$, Figure 21A). In *C. elegans* it appears that the adenosine receptor's activation actually prevents sleep. The worms with *eat-1* mutations would not be able to break down the adenosine so there would be higher levels and therefore greater activity at the ADOR-1 receptor. The ador-1 mutants showing increased quiescence, which is the equivalent of blocking the receptor and this supports the conclusion from the *eat-1* mutants. To further

support this conclusion, I tested an ADOR-1 overexpression line, if the previous evidence is correct, the data should resemble *eat-1* mutants. The ADOR-1 overexpression showed an even higher level of roaming when compared to *eat-1* mutants, concurrent wild type controls, and non-transgenic siblings that did not have the over expression of *ador-1* ($p < 0.0001$, Figure 21B). To confirm that it was the mutation in *ador-1* and *eat-1* and not some other background mutation in these worms, I tested the rescue of *ador-1* and *eat-1* under their own promoter (Figure 21C & D). The rescues were indistinguishable from the concurrent wild type controls.

Next, I tested the location of *eat-1* activity, to do this Dr. Han rescued *eat-1* under the *dpy-7* promoter. DPY-7 is a cuticle collagen, which is required for normal cuticle formation. The *dpy-7* promoter expresses the gene in the hypodermis of the worm (Johnstone, Shafi, & Barry, 1992). This rescue of *eat-1* in the hypodermis is a complete rescue of the roaming behavior seen in the *eat-1* mutants (Figure 22A). This suggests that EAT-1 functions in the hypodermis to breakdown the adenosine that would otherwise activate the ADOR-1 receptor. To verify that *eat-1* and *ador-1* are acting in the same pathway, I tested a double mutant of the two. The *ador-1* mutation rescues the roaming increase seen in the *eat-1* mutants while the increase in quiescence remains intact (Figure 22B). The persistence of the increase quiescence makes sense, while a lack of a receptor for *eat-1* mutants to influence rescues the roaming, the lack of *ador-1* will still cause the increase in quiescence.

Another rescue of *eat-1* I tested was a double mutant that paired *eat-1*with a mutation in *cha-1*. CHA-1 is a choline acetyltransferase that synthesizes acetylcholine and

Figure 21

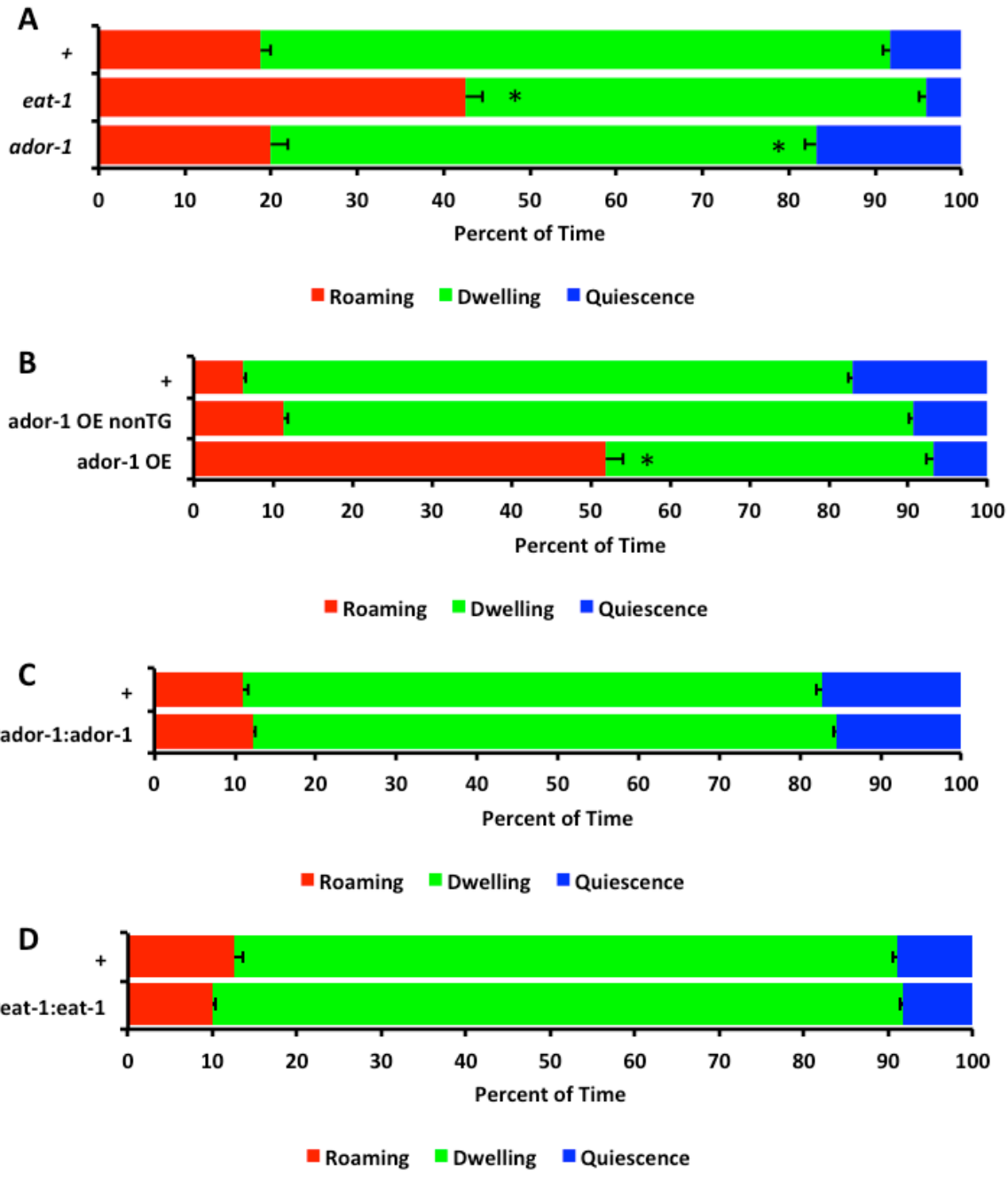
A
+
eat-1
ador-1
*
*
0 10 20 30 40 50 60 70 80 90 100
Percent of Time
Roaming Dwelling Quiescence
B
+
ador-1 OE nonTG
ador-1 OE
*
0 10 20 30 40 50 60 70 80 90 100
Percent of Time
Roaming Dwelling Quiescence
C
+
Pador-1:ador-1
0 10 20 30 40 50 60 70 80 90 100
Percent of Time
Roaming Dwelling Quiescence
D
+
Peat-1:eat-1
0 10 20 30 40 50 60 70 80 90 100
Percent of Time
Roaming Dwelling Quiescence

Figure 21. Adenosine and *eat-1* influence satiety quiescence part I

A. Concurrent wild type (+), *eat-1* mutants, and *ador-1* mutants tested in the automated satiety quiescence assay. *eat-1 n=12, ador-1 n=11, + n=10* ***=** statistically significant

B. Concurrent wild type (+), *ador-1* over-expression non-transgenic (OE nonTG), and *ador-1* over-expression trans-genic (OE TG) tested in the automated satiety quiescence assay. *ador-1* OE nonTG *n=19, ador-1* OE TG *n=16, + n=18* ***=** statistically significant

C. Concurrent wild type (+) and *Pador-1; ador-1* mutants tested in the automated satiety quiescence assay. *Pador-1; ador-1 n=37, + n=20*

D. Concurrent wild type (+) and *Peat-1; eat-1* mutants tested in the automated satiety quiescence assay. *Peat-1; eat-1 n=27, + n=15*

is expressed in neurons (J. B. Rand & Russell, 1984; J. Rand, 2007). It is also required for normal locomotion, growth, and viability (J. Rand, 2007). Previous work has shown that an incomplete loss of function *cha-1* mutation rescues the defects seen in *eat-1* mutants and it also rescues the satiety behavioral defects of *eat-1*.

In addition to the interaction between *eat-1* and *ador-1*, Dr. Han also identified a potential transporter for *eat-1*'s substrate, *ent-4*. ENT-4 is predicted to be a nucleoside transporter that acts in the membrane to transport nucleosides such as adenosine. The *ent-4* mutants show behavior that appears to be a mixture of *eat-1* and *ador-1*, there is a significant increase in roaming and an increase in quiescence (p <0.005, Figure 22D). If *ent-4* is the transporter, then a double mutation with *ador-1* should resemble double mutant of *ador-1* and *eat-1*. However, the double mutant shows approximately half of the roaming seen in concurrent wild type controls (p < 0.0001, Figure 22D). While *ent-1* seems to work in this pathway, it may be working on additional pathways that would explain the low levels of roaming compared to the concurrent wild type.

Figure 22

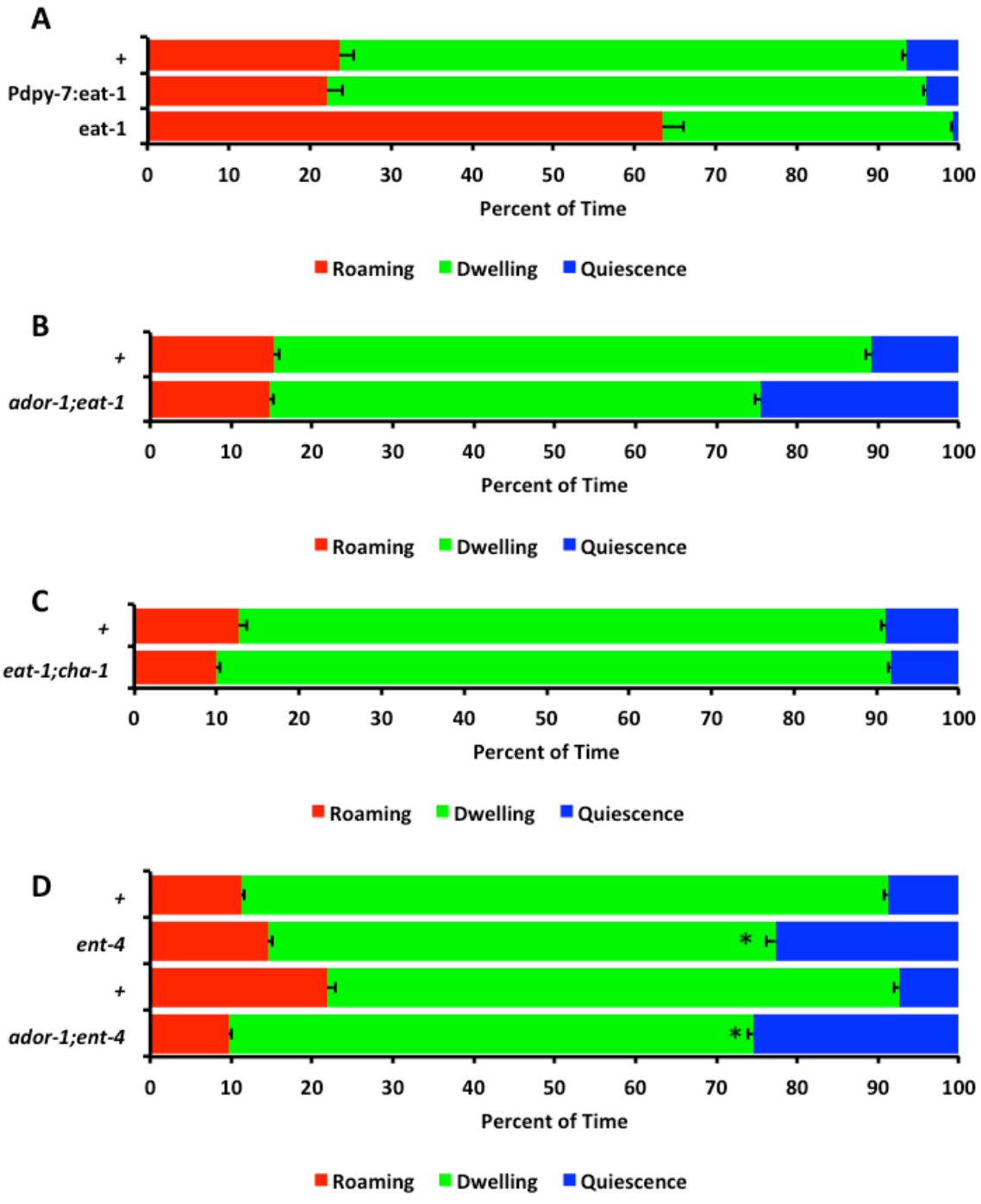
A
+
Pdpy-7:eat-1
eat-1
0 10 20 30 40 50 60 70 80 90 100
Percent of Time
Roaming Dwelling Quiescence
B
+
ador-1;eat-1
0 10 20 30 40 50 60 70 80 90 100
Percent of Time
Roaming Dwelling Quiescence
C
+
eat-1;cha-1
0 10 20 30 40 50 60 70 80 90 100
Percent of Time
Roaming Dwelling Quiescence
D
+
ent-4
*
+
ador-1;ent-4
*
0 10 20 30 40 50 60 70 80 90 100
Percent of Time
Roaming Dwelling Quiescence

Figure 22. Adenosine and *eat-1* influence satiety quiescence part II

A. Concurrent wild type (+), *Pdpy-7:eat-1* mutants, and *eat-1* mutants tested in the automated satiety quiescence assay. *Pdppy-7: eat-1 n=11, eat-1 n=11, + n=11*

B. Concurrent wild type (+), *ador-1;eat-1* mutants tested in the automated satiety quiescence assay. *ador-1*:eat-1 *n=28, + n=15*

C. Concurrent wild type (+), *eat-1;cha-1* mutants tested in the automated satiety quiescence assay. *eat-1;cha-1 n=27, + n=15*

D. Concurrent wild type (+), *ent-4* mutants, *ador-1;ent-4* mutants tested in the automated satiety quiescence assay. *ent-4 n=24; + n=12; ador-1*:*ent-4 n=29, + n=14* *= statistically significant

3. Discussion and future directions

ASI's activation to the nutrient-rich stimulus LB may be a response to amino acids. The sensation of amino acids is important to ensure consumption of amino acids; particularly amino acids worms cannot produce. The loss of the enhancement of casein by cysteine with the addition of DTT suggests ASI senses disulfide bonds or a small molecule containing a disulfide bond. The presence of cysteine alone is not sufficient to activate ASI, suggesting that it is an interaction of at least two difference amino acids. Cysteine is not an essential amino acid for *C. elegans*; it could be bonding with an essential amino acid (arginine, histidine, lysine, tryptophan, phenylalanine, methionine, threonine, leucine, isoleucine, and valine) (Braeckman, Houthoofd, & Vanfleteren, 2009). This list is shorter than the 17 amino acids I originally tested and did not see activation from ASI. Future work to identify the small molecule could begin with this list of 10 amino acids individually paired with cysteine.

An unorthodox possibility to pursue is to determine what makes ASI activating substances a yellow color. All of the nutrient rich stimuli that activate ASI are yellow except the 10% LB mixture, which is clear. The size of activation for 10% LB and the amino acid mixture are similar (Figure 5E & Figure 2E), perhaps higher concentrations of the correct amino acids could produce the yellow color I have observed in the other stimuli. The combination of amino acids that activated ASI did not appear yellow. The powder form of the amino acids are all clear to white, which does not give any indication of which, if any, may convey a yellow color. It is possible that some alternative component of the other stimuli is responsible for the color. Yeast extract was the darkest yellow of all

the stimuli and there is a multitude of components in yeast extract that could be responsible for this color. An in depth analysis of yeast extract compared to tryptone may reveal the common component that makes them both yellow and perhaps the common component that activate ASI.

The source of calcium during ASI's activation is another mystery that given more time, I would have pursued in more depth as well. The lack of *tax-4* did not stop the activation of ASI but a double mutant of *tax-4* and *tax-2* would give that cyclic nucleotide gated channel a firm shake as the calcium source. In addition, ASI also expresses *cng-3, cng-2,* and *cng-1* which are all three cyclic nucleotide gated channels. I have a triple mutant that lacks *tax-4, cng-1,* and *cng-3* but I did not get to test it because it would require injecting the GCaMP plasmid. I was unsuccessful at injecting another strain I was interested in testing and did not get to inject this triple mutant. A cross between the triple mutant and the integrated GCaMP line could remedy this but isolating a quadruple mutant is difficult and I was limited on time. In addition to the cyclic nucleotide gated calcium channels, the *itr-1* mutants would have shown if the calcium flux seen in ASI was driven from internal calcium stores. Crossing this worm with the integration line would have been much simpler than a triple mutant but time was a rate-limiting factor.

Identifying the source of calcium would be helpful but it would not reveal the receptor for this nutrient signal. The cyclic nucleotide gated channels are activated by an internal signal that is produced in response to the activation of a membrane-bound receptor (most likely). The simplest approach to find this receptor would be to mutagenize the integration line of GCaMP in ASI with EMS and screen for worms whose ASI neurons do

not activate to the nutrient-rich stimulus. This approach may give several mutations that are not receptors such as defects in the amphid (channel in the worm's nose through which ASI processes pass) or cyclic nucleotide gated channels. An alternative approach would be to use an RNAi of receptors pre-identified as potential candidates based on their expression patterns.

The change in ASI's activation to different concentrations of nutrients following 6 hours of starvation could be dug into even further. Testing 12 hour starved then 3 hour refed worms may reveal a difference in the tone of ASI similar to what is seen after a 6 hour starvation without refeeding. There is very likely a signal from the worm's fat storage that is changing the tone of ASI based on the worm's overall nutritional status (Figure 23). The signal and its receptor would be an incredibly exciting duo to identify. The work our lab did with NHRs identifies one possible link between the nervous system and the fat storage within worms. Many of those NHRs do not have known patterns of expression and several of those with known expression locations are in the pharynx, intestine, and head neurons. The depletion of fat could increase the expression of these NHRs to up regulate genes needed during starvation including possible neuropeptides that could convey the message of starvation to the necessary neurons and structures. NLP-24 is one possible neuropeptide involved in starvation; a former post-doc of the Avery lab, Dr. Mi Cheong Cheong, identified this neuropeptide (Cheong et al., 2015). Dr. Cheong found that *npr*-17 (receptor to *nlp*-24), modulates pharyngeal pumping, increases roaming behavior, and is expressed in ASI (Cheong et al., 2015). The results from the automated satiety assay support these conclusions (Figure 15A). Dr. Cheong's work also found that *nlp-24* shares

similar sequence to opioids in humans. NLP-24 contains the sequence YGGY on the N-terminus or internally, human opioids contain YGGF, while NPR-17 shares >20% sequence homology with the human nociception receptor, μ-opioid receptor, δ-opioid receptor, and the κ-opioid receptor (Cheong et al., 2015). Based on all of this evidence, Dr. Cheong tested and found that naloxone and morphine could interact with NPR-17 in an ASI-dependent manner, concluding that *nlp-24* and *npr-17* act as a pain relieving opioid system in *C. elegans* (Cheong et al., 2015). This system will come back up later in this section.

The previous work in our lab has demonstrated the importance of cGMP signaling in satiety behavior (Gallagher, Kim, et al., 2013). It was very disappointing that I could not detect changes in cGMP in ASI during its activation to LB, however changes in cGMP levels may be more long term and cannot be seen in a short term experiment such as this. Long term imaging of cGMP levels in ASI during fasting and refeeding may provide the answer. The answer could be in testing fasted and refed worms. There are also labs that can image the activity of neurons in worms using GCaMP and their behavior simultaneously. It would not be difficult to use this setup to test WincG2 because I was able to use in our GCaMP setup. A better understanding of when cGMP is important during satiety behavior could help in understanding the activation of ASI to nutrients.

Attempting to find a substance that activates ASH that is also easy to work with was a challenge. Glycerol is known to activate ASH but it was difficult to control the flow of glycerol across the worm's nose. After several attempts, I switched to NaCl which flows through the microfluidic device the same as the imaging buffer I use. While it would have

been interesting to determine the precise ingredient in food coloring that suppressed ASI, the company that manufactures the food coloring I used was not willing to tell me the full ingredient list. Even after explaining that I only wanted to know because of its use in my experiments that are completely unrelated to food product or additive development. It is possible that the color itself is bothersome to the worms. Initial experiments involving food coloring in calcium imaging used blue food coloring. Worms possess a receptor, LITE-1, which activates a light dispersal behavior to blue light. At least in calcium imaging, I do not think this is the explanation because the light source to image GCaMP is blue (470 nm). The data from the automated satiety assay did not reveal blue food coloring to induce more roaming or less quiescence than the concurrent control (Figure 7B).

The influence of NaCl in a dose dependent manner on ASI's activation to LB is interesting, suggesting that the suppression of ASI is not an all or none response. The magnitude to which NaCl activates ASH does not seem to be the determining factor, as 2M NaCl give the highest activation in my data but 4M NaCl results in the greatest suppression of ASI. One very likely explanation is that the line with ASH-specific GCaMP is carried as an extra-chromosomal array as such each worm can carry a different number of copies of the GCaMP transgene in ASH and therefore the expression of GCaMP varies between each worm. This makes comparing experiments between days challenging and daily controls help in making comparisons. However, 2M NaCl gave the greatest response in ASH of any NaCl concentration, potentially because the osmolarity of the solution begins to effect ASH's response to NaCl at 3M and 4M. The enhanced activation of ASI under starvation led me to test if ASI can overcome the NaCl suppression. The fact that it could not

suggests that the noxious signal is too strong, the starvation period is not long enough, and/or ASH is the true regulator feeding behaviors during starvation. This is possible because prior to the fasted calcium imaging experiments, no one in our lab had tested ASI activity during starvation. ASH could be regulating starvation related behaviors by acting on ASI, which would explain why it appeared as though ASI was the downstream neuron in this circuit. This is most apparent in the suppression of ASH's activation to NaCl following LB in the 6 hours fasted condition (Figure 9G & H). This experiment places ASH downstream of ASI during starvation while this same effect is not seen in the well-fed condition (Figure 7E & F). While the full role of ASH in starvation has not been full tested by others or me in our lab, there are indicators that ASH has a role. Along with the evidence I have already provided, the worms lack ASI and ASH produce far more dauers (arrested developmental stage induced by the worm's perception of extreme conditions such as starvation) than the individual mutations alone (observational evidence from Dr. Cheong and I). This suggests that ASI and ASH work together to regulate the worm's response to nutrition and starvation. To fully understand the food intake assay in which the worms are lacking ASI and ASH, I would need to way to quantify the fluorescence that eliminates the RFP marker associated with the ASH ablation. The construction of a strain using a GFP marker would alleviate this issue and allow the quantification of the food intake assay for the ASH ablation line. The ASI ablation line uses a GFP maker but it is only seen in the head of the worm, which would allow the use of a coelomocyte-expressed GFP marker in the ASH ablation line. I think quantification would be necessary to draw

firm conclusions because human beings can see patterns where one does not exist (for instance, shapes in clouds).

The relationship between ASI and ASH needed further evidence to clarify that the suppression was coming from ASH to ASI and not from another neuron pair that can also sense NaCl (for instance, ASE). The channel rhodopsin in ASH and the genetic ablation of ASH work nicely to confirm it (Figure 11A-D). I would have liked to identify the receptors and neurotransmitters responsible for this interaction. While others have published their findings regarding the suppression between ASI and ASH, they did not do so in a food-related manner (Guo et al., 2015). Guo and colleagues found that ASH suppresses ASI via a gap junction between ASH and RIC. RIC releases octopamine, which suppresses ASI via *ser-3*. They also concluded that ASI suppresses ASH by releasing an unknown neuropeptide to ADF then ADF releases serotonin to suppress ASH via *ser-5*(Guo et al., 2015). I explored these possibilities in the automated satiety assay and calcium imaging (Figures 17-19) and while some of the data supported their argument, other pieces did not fit in with it. For instance, the effects seen in the octopamine-producing enzyme mutants (*tdc-1* and *tbh-1*) show mixed results in the automated satiety assay and the calcium imaging does not show suppression on a time scale similar to the one in their paper (Guo et al., 2015). My methods were slightly different for testing these neurotransmitters and receptors, perhaps in future work crossing *tdc-1* and *tbh-1* mutants into the GCaMP-expressing backgrounds will provide a clearer picture than exposure to extra octopamine during or prior to calcium imaging. In addition to testing the enzyme mutants, I think testing the receptor mutants would help clear up the confusing results seen with tyramine.

It appears to strike a balance with octopamine and I think testing the mutants for each receptor in the well-fed and 6 hours fasted conditions could improve our understanding what is exactly going on. It is possible that during well-fed conditions, the Guo et al. circuit is controls feeding behaviors and during starvation my proposed circuit is the control for feeding behaviors.

RIC is frequently the neuron pair implicated in feeding and starvation in *C. elegans.* Previous work in our lab has shown that *daf-7* suppression of RIC specifically through expression of *daf-7*'s receptor subunits, *daf-1* and *daf-4*, is sufficient to rescue satiety behavior in a double mutant of *daf-1* and *daf-4* (Gallagher, Kim, et al., 2013). Testing calcium fluxes in RIC during starvation using GCaMP would help to confirm the role of RIC during starvation. In addition to monitoring RIC activity during starvation, I would also like to activate ASI and monitor activity in RIC. Exposing the worm's nose to LB for varying amounts of time then testing RIC activity may show the threshold of ASI activity needed to suppress RIC and octopamine production.

The role of serotonin in suppressing ASH is more straightforward and my results support this, however, the effects of serotonin on ASI were unexpected. This suppression of ASI by serotonin could be feedback from other neurons that respond to food. NSM is a pair of neurons located in the pharynx which release serotonin in response to bacteria's presence in the pharynx. Serotonin causes worms to pump their pharynx and increase their food intake. As previously discussed, this can explain my results (Figure 17A-D). If ASI induces the release of serotonin from ADF, this also could suppress ASI's activity in a feedback loop. Neurotransmitters in *C. elegans* do not act solely in the synapse in which

they are released; neurotransmitters can diffuse away and act elsewhere. This feedback mechanism could help to suppress ASI to prevent dispersal from bacteria and prevent premature entry into satiety quiescence. It is possible that ASI activation needs to be steady overtime and persist for a certain period of time to reach a threshold at which worms can overcome the serotonin suppression then enter satiety quiescence.

The major neurotransmitter released by ASH is glutamate. I tested glutamate inhibitory receptors and *eat-4* thinking that ASH's major neurotransmitter was responsible for ASI's suppression. The original experiment I wanted to try was the triple mutant of *avr-12, avr-15*, and *glc-1* in calcium imaging. However, I could not generate a stable transgenic line using microinjection of the ASI-GCaMP plasmid into this mutant background. I sent the plasmid and the strain to a company that produces transgenic lines as one of their main services and they could not generate a stable transgenic line either. This background is simply not compatible with the transgene I am attempting to express for some unknown reason. Future work to possibly test this triple mutant in calcium imaging could attempt to cross this strain with the integration line of ASI-GCaMP although isolating a quadruple mutant is challenging it is possible. Overall, it appears that glutamate is not the signal from ASH that influences ASI activation.

Revisiting the opioid system in *C. elegans, nlp-24* appears to modulate the interaction between ASI and ASH. Others have shown the importance of this signal under starvation conditions and that ASI is the site of action for the opioid signal (Cheong et al., 2015; G. Harris et al., 2010). I believe that the internal condition of starvation increases the release of *nlp-24* and perhaps other opioid related signals to alleviate the pain of starvation.

The worms do not release this under well-fed conditions so the lack of *nlp-24* in those conditions does not have any effect because they do not need it. However, once they are starved, the signal is needed to reduce the pain of starvation and without *nlp-24*, signals of pain from ASH are experienced more intensely than usual because ASI is already experiencing the pain of starvation. This is why every worm responds to LB following 2M NaCl in the well-fed condition but not all worms can respond in the fasted condition without the pain relief of *nlp-24*.

An alternative explanation for this opioid signal during starvation is that it enhances the hedonic (pleasurable) value of the food for *C. elegans* during starvation. It was previously shown that endogenous opioid signals are increased during starvation in rats and that administration of opioids increases feeding behavior (Bodnar, 2004; Vaswani & Tejwani, 1986). Exogenous administration of an opioid results in enhanced pleasure from pleasurable food items (measured by positive facial expression of rats) (Méndez-Díaz, Rueda-Orozco, Ruiz-Contreras, & Prospéro-García, 2012). Rats given a high sugar diet experienced withdrawal symptoms (similar to opiate withdrawal) when given naloxone (opioid receptor inverse agonist) (Spangler et al., 2004). NLP-24 was shown to increase pumping during starvation and expression of this gene is also increased starvation (Cheong et al., 2015). I cannot use any standard or known means to assess the worm's pleasure, if they are capable of such a sensation. Humans can answer a question and in other mammals facial expressions can serve as a proxy for language. However, satiety may be a close approximation to pleasure because it is the satisfaction of a drive. When the worms have the *nlp-24* gene, their satiety is at a normal level following starvation and

refeeding. *nlp-24* mutants show increased satiety behavior because their satisfaction is not enhanced by this opioid signal (Figure 15A). The mutants perception of feeding is less pleasurable so they feed less and spend more time in quiescence while the wild type worms that produce NLP-24 receive more enjoyment out of eating and spend more time on that following starvation.

The nervous system of *C. elegans* has been completely mapped out and available online. In looking at this connectivity, I identified an interneuron pair that appeared to be best placed to modulate the interaction between ASI and ASH, AIA, located in the nerve ring of the worm's head. AIA is ASI's major synaptic output and they also share a gap junction. All of ASI's other known connections place ASI as the pre-synaptic neuron; this gap junction is the only direct means by ASI could be modulated by another neuron. In addition, ASH and AIA both synapse onto each other. Of all the possible circuits to come up with using the connectivity data available, this was the simplest. The behavioral data seems to support the involvement of AIA in the ASI and ASH circuit. However, the calcium imaging is chaotic. Interneurons are difficult to image, the activation is frequently not seen in the cell body (as in sensory neurons such as ASI and ASH) but is seen in the processes. The processes are difficult to quantify because the slightest movement of the worm's nose can cause the process go out of focus or move too much for the analysis program to keep up. In addition to these challenges, interneurons give a "noisy" signal. They activate seemingly at random; it is the equivalent of watching the worm think. Imaging well-fed or 6 hour fasted worms did not give a clear role of AIA (Figure 12-13), however, maybe this is not the best way to test AIA's involvement. A genetic ablation and

channel rhodopsin expressed in AIA may provide the answer. The genetic ablation I tested in the automated satiety assay could not be used in calcium imaging because one of the markers for the ablation is GFP expressed throughout the body of the worm. Using a genetic ablation and channel rhodopsin, I could tease apart the effects of AIA activation or lack thereof on ASH and ASI under different feeding conditions and in response to different stimuli.

The identification of NHRs as important during starvation provides a potential link between the fat storage in gut granules found in intestinal cells and the neurons controlling feeding and starvation regulating neurons. Of the NHRs identified using the automated satiety assay and fat staining, NHR-8 and NHR-64 are the only ones that have been studied in depth by others. NHR-8 is involved in xenobiotic detoxification, fat metabolism, and cholesterol metabolism. All of these processes could contribute to the regulation of feeding behavior. NHR-64 antagonizes the Sterol regulatory element-binding protein (SREBP) pathway via a genetic interaction with POD-2 (a *C. elegans* acetyl-Co A carboxylase). SREBP is a major transcription factor that regulates the expression of fatty acid synthesis genes. POD-2 is predicted to catalyze the first step in *de* novo fatty acid biosynthesis. Worms lacking SREBP (*sbp-1*) arrest at the first larval stage (L1) and do not grow. RNAi of *sbp-1* and a reduced function mutant show decreased satiety quiescence. Without *pod-2*, worms show reduced satiety quiescence. In the absence of *nhr-64*, the activity of SBP-1 could be stronger and explain the increase in satiety and fat storage. NHRs could be acting similarly to leptin in invertebrates, conveying the status of fat storage to the rest of the worm. The tone of ASI activation could be influenced by this leptin-like signal and

influence feeding behaviors like satiety quiescence (Figure 23). The next step from this project is to identify the role of each NHR identified in the 4 groups previously mentioned. In addition, identifying the expression patterns of those that remain unknown. A GFP reporter transgene using each NHR's promoter should provide a starting point to identify the location of the genes expression. There is also a technique in which qPCR is completed on a single cell. This is a challenging technique but it could be used to validate the location of certain NHRs that may be detected in ambiguous neurons from the GFP reporter experiment.

The adenosine and *eat-1* project provides a unique look at adenosine and adenosine receptors in sleep-related behavior. The role of adenosine in sleep for humans is not fully understood. The establishment of *ador-1* working to regulate sleep in worms provides a means to further investigate and under the role it could play in humans and other mammals. The effects of caffeine on *C. elegans* sleep has not been published, only the protection against β-amyloid peptide toxicity (Dostal, Roberts, & Link, 2010). There several potential directions this project could take. Examining the role of *ador-1* and *eat-1* in other forms of quiescence in *C. elegans* such as lethargus (developmental sleep) and stress induced quiescence. Also, testing the effects of caffeine on satiety quiescence in a wild type background, an *ador-1* mutant background, and a rescue of *ador-1*. Several different rescue promoters could provide information on the site of action for *ador-1*, it is already known that *eat-1* acts in the hypodermis.

Overall, this collection of studies has shown that *C. elegans* make decisions about feeding behavior based on recent feeding history and current fat storage integrated with

potentially conflicting environment stimuli (for instance food mixed with a noxious stimulus, “bad” food). The behavioral decision is based on output from ASI and ASH whose interaction can be modulated by an opioid signal in *C. elegans*. RIM and RIC probably act to suppress ASI under hunger-inducing conditions and prevent entry into satiety quiescence although further experiments concerning these neurons would be help clarify their role in this circuit. It has already been established that ASI can suppress RIM and RIC via *daf-7* (Figure 24) (Gallagher, Kim, et al., 2013).

Work with model organisms rarely results in a direct translation of every aspect and detail to more complex organisms. This set of work is no exception; the signals and receptors mediating the behaviors seen in the worms will probably not be the exact same as those regulating the same behaviors in mammalians systems. However, the neuronal interactions as a whole almost certainly are the same; a neural network regulating feeding behavior that is modified based on external signals of dangerous stimuli or conditions. In addition, the signals may be not identical but they may be similar in nature, for instance a neuropeptide-related signal could regulate the same behavior between models.

Figure 23

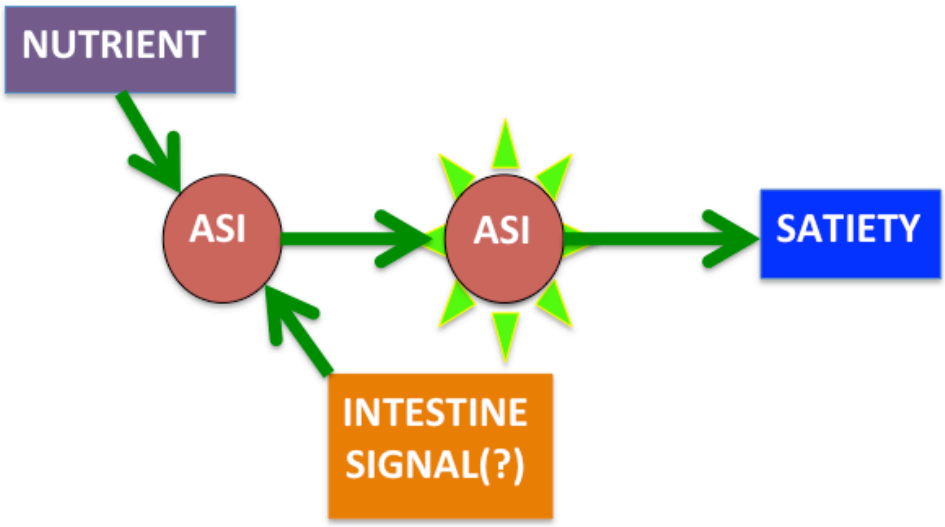

Figure 23. Model for fat storage signal to effect ASI activation and satiety

Bright green lines coming from behind ASI = activation.

Figure 24

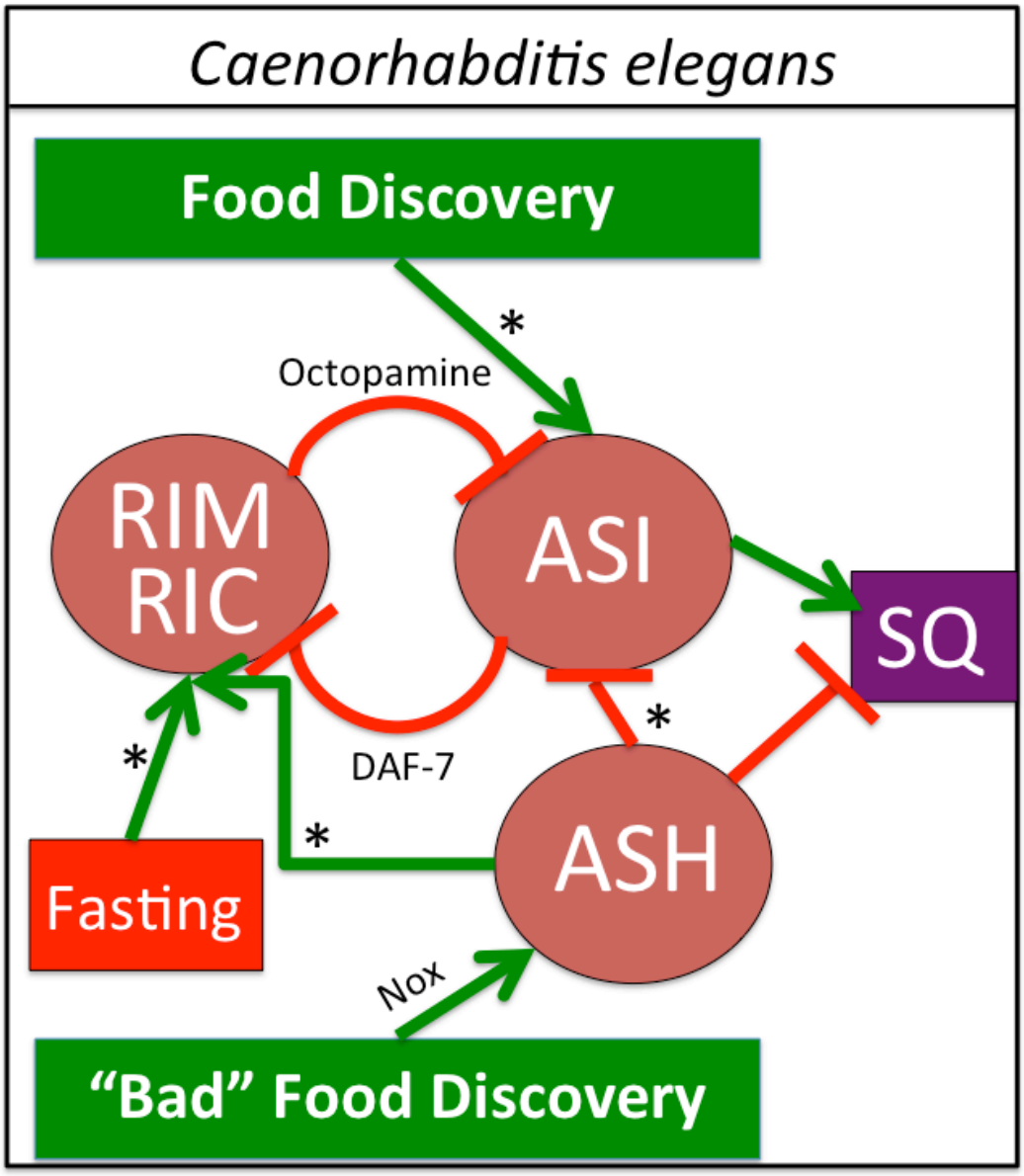
Caenorhabditis elegans
Food Discovery
*
Octopamine
RIM
RIC
ASI
SQ
*
*
DAF-7
*
ASH
Fasting
Nox
"Bad" Food Discovery

Figure 24. Model of *C. elegans* appetite control with conflicting cues.

Based on my current work and the other of previous lab members (Gallagher, Bjorness, et al., 2013; Gallagher, Kim, et al., 2013).

4. Materials and Methods

Strains and culture conditions

Worms were cultured and handled as described previously (Sulston & Hodgkin, 1988) with the following modifications: worms were routinely grown on NGMSR plates (L Avery, 1993). All worms were maintained at 20 ^{o}C on *E. coli* strain HB101 unless indicated otherwise. The wild-type strain was *C. elegans* variant Bristol, strain N2. The other strains used were JN1713 *peIs1713[sra-6p::mouse caspase1]*, CX10979 *kyEx2865[sra-6::GCaMP3, ofm-1::gfp]*, PY7505 *oyIs85[gpa-4p::TU813, gcy-27p::TU814, gcy-27p::eGFP, unc-122p::DsRed]*, YJ212 *uyIs[gpa-4p::gcamp2.2, unc-122::dsRed], YJ87 egl- 4(ks62) IV; uyEx87[gpa-4p::GCaMP2.2b unc-122::dsRed],* CX11073 *kyEx2916[To1A4::gcamp2.2b coel::gfp]* QD201 *Ex[gcy-28.dp::mec-4d(d), AIA-specific ins-1p::mRFP, myo3p::gfp]*, JZ21729 *pFGEx219[gpa-4p::WincG2*, *ofm-1::gfp],* MT15434 *tph-1 (mg280) II*, DA554 *eat-4 (ad537) III*, EG8828 *ador-1 (ox489) II; ent-4 (ok2161) IV*, EG8779 *ent-4 (ok2161) IV*, EG6396 *eat-1 (tg11) IV*, EG6962 *ador-1 (ox489) II; eat-1 (tg11) IV*, MT13113 *tdc-1 (n3419) II*, DA2264 *daf-7 (e1372) III; tbh-1 (n3247) X*, MT9455 *tbh-1 (n3247) X*, DA1774 *ser-3 (ad1774) I*, CX13079 *octr-1 (ok371) X*, CX11839 *tyra-3 (ok325) X*, YJ214 *eat-4 (ad537) III; uyIs[gpa-4p::gcamp2.2, unc-122::dsRed],* YJ215 *nlp-24 (tm2105) V; uyIs[gpa-4p::gcamp2.2, unc-122::dsRed],* YJ216 *uyIs[gpa-4p::gcamp2.2, unc-122::dsRed]; lite-1(ce314); ljIs114[Pgpa-13HFLPase*, *Psra-6HFTFHChR2H YFP],* YJ217 *oyis84 [gpa-4p::TU813*, *gcy-27p::TU814*, *gcy-27p::eGFP*,

unc-122p::DsRed]; *peis1713 [sra-6p::mCasp1+red marker],* DA1316 *avr-14 (ad1302) I, avr-15 (vu22) glc-1 (pk54) V,* DA2456 *nlp-24 (tm2105) V,* DA2457 *npr-17 (tm3210) III*

Automated Satiety Quiescence Assay

5 ml LB was inoculated with a single colony of *E. coli* strain HB101 expressing mCherry and incubated shaking overnight at 37 °C. The culture was removed from the incubator and allowed to sit at room temperature overnight. The sample was centrifuged at 4,000 RPM for 3 minutes. After decanting the supernatant, the pellet was resuspended in the small residual amount of broth and transferred to a microcentrifuge tube. 50 µl of this suspension was twice serially diluted 1:1 with M9 (for a final 4× dilution). 5 µL of this suspension was pipetted onto a 35 mm NGMSR plate and allowed to dry completely.

L4 worms were picked to a fresh NGMSR plate and given 8 hours to develop to young adult stage. Young adult worms (adults containing no eggs) were picked to individual 60 mm NGMSR plates without food and starved for 13 hours. A single starved worm was then transferred to an approximately 6 mm diameter spot of bacteria made by placing 5 µl bacterial culture on a plate, focused under the camera, and allowed to refeed for 3 hours. The light was then turned on and video capture was started at 1 frame/second for 1 hour.

For non-fasted assays, worms were prepared identically except that young adults were transferred to a 60 mm NGMSR plate with food for 13 hours and worms were given

30 minutes on the assay plate to recover from being transferred, followed by taking a 30 minute video at 1 frame/second.

All recordings for the automated satiety quiescence assay (TOBO) were recorded using Point Grey GRAS-14S5M-C digital cameras fitted with Computar MLM3X-MP macro zoom lenses. Images were recorded using Point Grey's freely available FlyCap2 software and worms were tracked using custom written program in MATLAB. A low pass filter was applied to each frame of the movie and the light/dark threshold was adjusted to find the outline of the worm. The center of mass was calculated at each time, reducing each recording to a series of (t, x, y) points, which were the basis for all subsequent analyses.

A complete description of the calculations and parameters of the HMM is available in the paper 'The Geometry of Locomotive Behavioral States in *C. elegans*' Gallagher et al. (2013) (Gallagher, Bjorness, et al., 2013).

Food Intake Assay

Food intake were measured as previously described (You et al., 2008). To measure food intake, mCherry-expressing *E. coli* strain HB101 was inoculated in LB and grown overnight at 37 °C, then left over night at room temperature. Plates were stored at room temperature for at least one night. Worms were picked as L4s approximately 24 hours before were plated. The bacteria were diluted and plated the same as for the locomotion analysis. Worms were plated and allowed to feed for 1 hour, worms were treated with 20 µl of 1 M sodium azide for their feeding status to be fixed. Worms were observed using a

Zeiss Axio A2 Imager with a 10× objective lens. Images were acquired using Zeiss Axiovision software and fluorescence was quantified using ImageJ.

Calcium & cGMP Imaging

All calcium-imaging experiments were performed on an Axio Observer.A1 with a 63× oil immersion DIC objective and a Hamamatsu C11440 digital camera. Analysis of the imaging data was performed with a custom written program in Mathematica, with one region of interest placed on the neuron of interest and a second placed nearby to measure background. The data are normalized to the initial 15 seconds of each file.

Worms were picked as L4s approximately 14-16 hours before testing would begin. In the starvation experiments, young adults were picked to empty NGM agar plates for 6 hours before calcium imaging. Young adult worms were picked and placed in a microfluidic device that restrains the worm with the tip of the head (where the AIA, ASI, and ASH are located) in a stream that can be rapidly switched (Chronis et al., 2007), "the olfactory chip") (Figure 25). Images were recorded at 10 frames/second for 60 seconds. Each worm was recorded for a 15 second baseline, followed by exposure to stimulus for 15 seconds, 15 seconds no stimulus, and a second 15 second exposure to stimulus. During the 15 seconds baseline and the 15 seconds without stimulus, worms typically received buffer across their noses. Integration line worms and ASH GCaMP worms exposed to a treatment during calcium imaging received that treatment for 4-5 minutes prior to the start of the

Figure 25

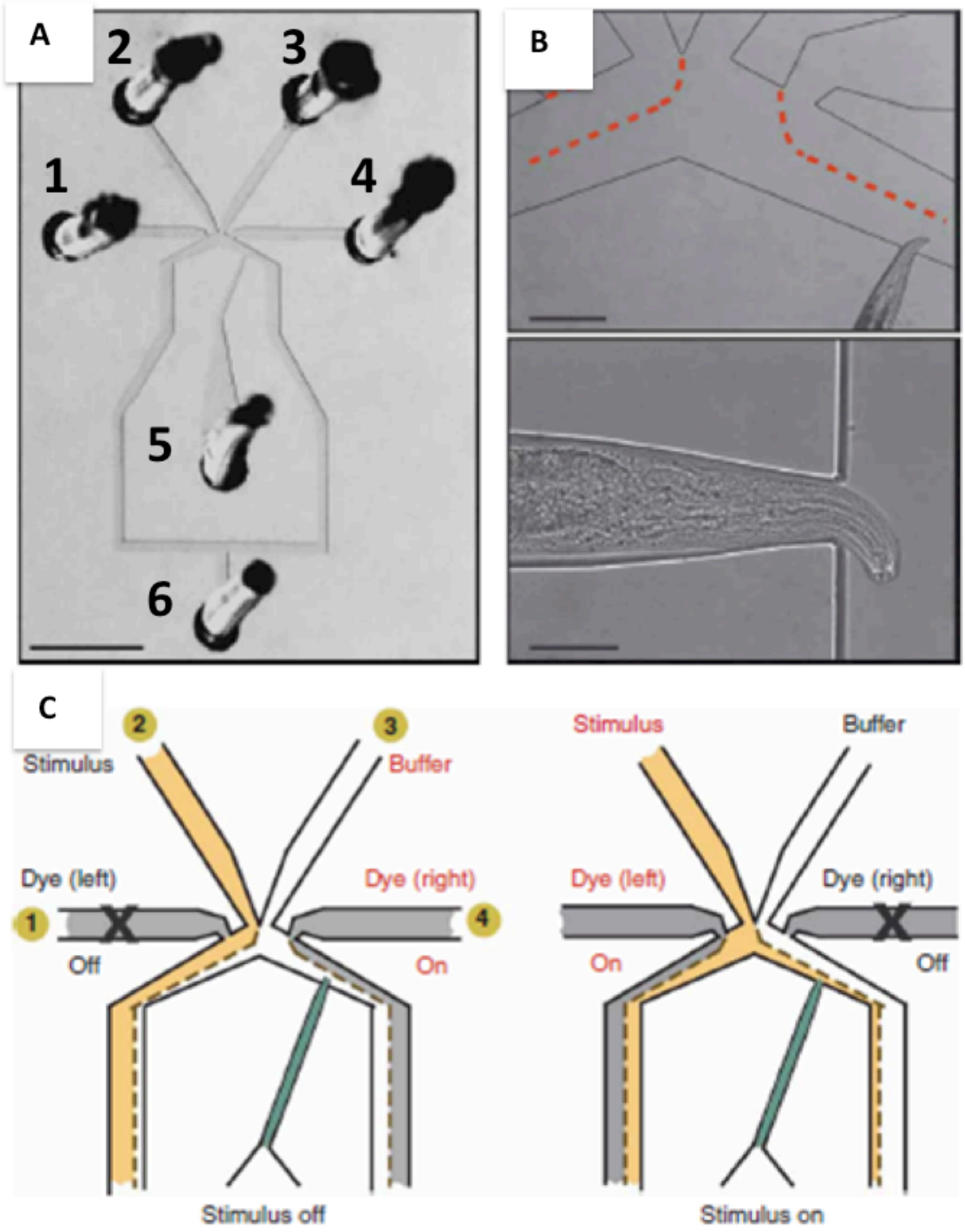
A
2
3
1
4
5
6
B
C
2
3
Stimulus
Buffer
Dye (left)
Dye (right)
1
4
Off
On
Stimulus off
Stimulus
Buffer
Dye (left)
Dye (right)
On
Off
Stimulus on

Figure 25. The olfactory chip layout and how it works

A. Overall pattern of the channels in the device. 1 and 4 are the switch channels, 2 is the stimulus channel, 3 is the continuous flow channel, 5 is the worm loading channel, and 6 is where the vacuum line is attached to the device.

B. This shows a close up of the worm and the dotted red lines show where the continuous flow is in the device when the stimulus is off (top half). The bottom half shows the head of the worm and demonstrates the ability to see the pharynx and other structures in the head.

C. The left portion shows which channels must be on when the stimulus flow is off; channel 4 is on while channel 1 is off, pushing the stimulus away from the worm's nose. The right portion shows which channels must be on when the stimulus flow is on; channel 1 is on while channel 4 is off, pushing the stimulus towards the worm's nose.

All three images are modified from (Chronis, Zimmer, & Bargmann, 2007).

imaging session and received the treatment during the baseline and 15 second period without stimulus. The worms constructed using the transgenic ASI GCaMP worms were exposed to NaCl for 1 minute prior to exposure to LB because that is sufficient to suppress their activation.

Fabrication of Microfluidic Devices for Calcium Imaging

Before doing anything else, put on a pair of snugly fitting nitrile gloves. The curing agent for PDMS is suspected to cause fertility damage and/or to the unborn. This risk seems to be more for ingestion or inhalation but the MSDS recommends washing it from skin as a precaution. Once PDMS is cured, it is considered biologically inactive. Using a 4' spring form pan, line it with aluminum foil and place a mold in the bottom as flat as possible. When lining the pan with foil, be sure the foil does not extend over the sides of the pan, this will interfere with covering the top of the pan with parafilm later. Next, get a plastic disposable cup and an individually wrapped plastic knife or spork (procured from Wendy's or Popeyes, respectively); rinse the cup with 70% ethanol then DI water and dry thoroughly. Determine where on the cup 90 mL would come to and pre-mark it to measure the silicon base added. Take the mold in the pan, the cup, the knife, the base, the curing agent, a piece of parafilm (sufficient in size to stretch and cover the pan), and a 10 mL glass serological pipette to a cell culture hood. Pour in 90 mL of the base and add 9 mL of the curing agent in the plastic cup using the glass serological pipette; stir with the plastic utensil until the mixture is very bubbly (approximate 1-2 minutes). Carefully pour the

mixture on top of the mold in the spring form pan then cover the pan with the parafilm. Bring the pan containing the mold and PDMS back to a bench and degas using the vacuum line for 1 hour. This may not be long be long enough to degas with some molds, brand new molds may need to be left over night to completely degas. To degas, make two punctures in the parafilm using pipette tips, one to place the vacuum line and the other to allow some air in (it is not creating a complete vacuum).

Once the degassing is complete, removed the parafilm and cover with half of a 15cm glass petri dish, then put an incubator setup at 55^{O}C and bake the PDMS for 1 hour and 40 minutes (if the PDMS was degassing overnight, this time can be reduce to ~1 hour). Take the mold out and allow it to cool long enough that it is safe to touch (~5 minutes). Once the mold is safe to handle, transport it back to the cell culture hood (leave the petri dish on to protect from debris) along with a plastic box, razor blades, and Scotch Magic Tape. Take the foil and cured PDMS out of the pan. Peel the foil off of the mold and remove the PDMS from the mold (be very careful in removing the PDMS from the mold, it can and will snap the mold in half).

Next, cover the chamber side of the PDMS with Scotch Magic Tape and cut out the individual microfluidic devices using the razor blades (be sure to leave the tape on). Once they are all cut out, place them in the plastic box (complete with lid) and transport to a bench to punch holes out. Using a large chunk of cured PDMS (leftover from previous pours), and 1 mm tissue punch, punch holes in the devices with the tape side up. Doing this tape side up allows you to see the chambers and where the connecting tubes should go. Once hole punching is complete on each device, replace the tape with a fresh piece of the

same tape to prevent contamination. Once all devices have been hole punched, it is time to bond the chips to the cover glasses.

Take all of the hole-punched chips to the plasma oxygen cleaner and take out the plastic trays. Place two chips (with tape removed, channel-side up) and two cover glasses on the plastic tray and place them in the plasma oxygen cleaner. Place the door on the chamber of the plasma oxygen cleaner, make sure the valve on the door is turned towards the oxygen port side but the oxygen port is closed. Turn on the vacuum for 3 minutes (the vacuum will hold the door on), then switch the RF up to high and run for an additional minute. After turning on the RF, open the oxygen port slightly until the purple glow inside the plasma oxygen cleaner is very bright purple. Once that minute has elapsed, turn off the RF, and the vacuum pump. Release the pressure on the door slowly using the valve on the door and remove the door. Pull out the plastic tray and quickly flip the chips chamber side down on the cover glasses. Cover the chip with tape once placed on the cover glass.

Generation of an Integration Line

To make the level of GCaMP expression uniform between worms, I used gamma irradiation to integrate the transgene into the worm's genome. The original strain with GCaMP in ASI was outcrossed twice then exposed to 30 grey of gamma irradiation for one hour at the L4 stage. After two days, the eggs and L1s of the irradiated worms were collected on another plate. From these worms, ~700 worms were singled that showed the RFP marker indicating they carried the gene of interest. Three days after this singling, the progeny of these worms were screened for ~70% transmission of the RFP marker. An

additional three days after this singling, the progeny of those singled worms were screened for 100% transmission of the RFP marker. Once a plate was identified to have 100% transmission of the RFP marker, the strain was maintained and outcrossed. There was only one line that reliably produced 100% of progeny carrying the RFP marker and this line was outcrossed 8x. The final fully outcrossed strain was named YJ212.

ChR2 Experiments

Worms were grown from hatching to adulthood on all-trans retinal plates (ATR) or ethanol plates. The concentration of ATR was 63 μm in 21.8 mM ethanol (

Statistics

All bar graphs denote mean ± SEM. Statistical tests were done using MatLab, Mathematica, Excel and Graphpad Prism tools. Calcium imaging data was bootstrapped 1000 times from the raw data using a custom script in Mathematica (provided by Dr. Leon Avery) to determine a mean and standard deviation for significance testing.

References

References

Adams, A. C., Clapham, J. C., Wynick, D., & Speakman, J. R. (2008). Feeding behaviour in galanin knockout mice supports a role of galanin in fat intake and preference. *Journal of Neuroendocrinology*, *20*(2), 199–206. doi:10.1111/j.1365-2826.2007.01638.x

Adan, R. A. H., Nijenhuis, W. A. J., & Kas, M. J. H. (2003). AgRP, physiological role of an inverse agonist. *International Congress Series*, *1249*, 195–206. doi:10.1016/S0531-5131(03)00605-8

Alkema, M. J., Hunter-Ensor, M., Ringstad, N., & Horvitz, H. R. (2005). Tyramine Functions Independently of Octopamine in the Caenorhabditis elegans Nervous System. *Neuron*, *46*(2), 247–260. doi:10.1016/j.neuron.2005.02.024

Antebi, A. (2006). *Nuclear Hormone Receptors in C. elegans*. (I. Greenwald, Ed.)*WormBook* (The C. ele.). doi:/10.1895/wormbook.1.64.1, http://www.wormbook.org

Avery, L. (1993). The genetics of feeding in Caenorhabditis elegans. *Genetics*, *133*(4), 897–917.

Avery, L., & You, Y.-J. (2012). C. elegans feeding. In *WormBook : the online review of C. elegans biology* (pp. 1–23). doi:10.1895/wormbook.1.150.1

Bacaj, T., Tevlin, M., Lu, Y., & Shaham, S. (2008). Glia are essential for sensory organ function in C. elegans. *Science (New York, N.Y.)*, *322*(5902), 744–747. doi:10.1126/science.1163074

Balthasar, N., Coppari, R., McMinn, J., Liu, S. M., Lee, C. E., Tang, V., … Lowell, B. B. (2004). Leptin receptor signaling in POMC neurons is required for normal body weight homeostasis. *Neuron*, *42*(6), 983–91. doi:10.1016/j.neuron.2004.06.004

Balthasar, N., Dalgaard, L. T., Lee, C. E., Yu, J., Funahashi, H., Williams, T., … Lowell, B. B. (2005). Divergence of melanocortin pathways in the control of food intake and energy expenditure. *Cell*, *123*(3), 493–505. doi:10.1016/j.cell.2005.08.035

Banks, W. a, DiPalma, C. R., & Farrell, C. L. (1999). Impaired transport of leptin across the blood-brain barrier in obesity. *Peptides*, *20*(11), 1341–5. Retrieved from http://www.ncbi.nlm.nih.gov/pubmed/10612449

Bargmann, C. I., Thomas, J. H., & Horvitz, H. R. (1990). Chemosensory Cell Function in the Behavior and Development of Caenorhabditis elegans. *Cold Spring Harbor Symposia on Quantitative Biology*, *55*, 529–538. doi:10.1101/SQB.1990.055.01.051

Bauer, F., Elbers, C. C., Adan, R. A., Loos, R. J., Onland-Moret, N. C., Grobbee, D. E., … van der Schouw, Y. T. (2009). Obesity genes identified in genome-wide association studies are associated with adiposity measures and potentially with nutrient-specific food preference. *The American Journal of Clinical Nutrition*, *90*(4), 951–9. doi:10.3945/ajcn.2009.27781

Bhatla, N. (2014). C. elegans Neural Network.

Bodnar, R. J. (2004). Endogenous opioids and feeding behavior: A 30-year historical perspective. *Peptides*, *25*(4), 697–725. doi:10.1016/j.peptides.2004.01.006

Braeckman, B. P., Houthoofd, K., & Vanfleteren, J. R. (2009). Intermediary metabolism. *WormBook*, 1–24. doi:10.1895/wormbook.1.146.1

Buolenger, J.-P., Patel, J., & Marangos, P. (1982). Effects of caffiene and theophylline on adenosine and benzodiazepine receptors in human brain. *Neuroscience Letters*, *30*(2), 161–166.

Chalfie, M., & White, J. (1988). The Nervous System. In *The Nematode Caenorhabditis elegans* (pp. 337–391).

Chatzigeorgiou, M., Bang, S., Hwang, S. W., & Schafer, W. R. (2013). tmc-1 encodes a sodium-sensitive channel required for salt chemosensation in C. elegans. *Nature*, *494*(7435), 95–9. doi:10.1038/nature11845

Chen, Y., Lin, Y.-C., Kuo, T.-W., & Knight, Z. A. (2015). Sensory Detection of Food Rapidly Modulates Arcuate Feeding Circuits. *Cell*, *160*(5), 829–841. doi:10.1016/j.cell.2015.01.033

Cheong, M. C., Artyukhin, A. B., You, Y.-J., & Avery, L. (2015). An opioid-like system regulating feeding behavior in *C. elegans*. *eLife*, *4*(April), 1–19. doi:10.7554/eLife.06683

Chronis, N., Zimmer, M., & Bargmann, C. (2007). Microfluidics for in vivo imaging of neuronal and behavioral activity in Caenorhabditis elegans. *Nature Methods*, *4*(9), 727–731. doi:10.1038/NMETH1075

Cowley, M. a, Smart, J. L., Rubinstein, M., Cerdán, M. G., Diano, S., Horvath, T. L., Cone, R., & Low, M. J. (2001). Leptin activates anorexigenic POMC neurons through a neural network in the arcuate nucleus. *Nature*, *411*(6836), 480–4. doi:10.1038/35078085

Culotti, J., & Russell, R. (1978). Osmotic Avoidance Defective Mutants of the Nematode

Caenorhabditis elegans. *Genetics*, 243–256. Retrieved from http://www.genetics.org/content/90/2/243.short

Cummings, D., & Overduin, J. (2007). Gastrointestinal regulation of food intake. *The Journal of Clinical Investigation*, *117*(1). doi:10.1172/JCI30227.Review

Dostal, V., Roberts, C. M., & Link, C. D. (2010). Genetic mechanisms of coffee extract protection in a Caenorhabditis elegans model of ??-amyloid peptide toxicity. *Genetics*, *186*(3), 857–866. doi:10.1534/genetics.110.120436

Elmquist, J., Elias, C., & Saper, C. (1999). Hypothalamic Control of Body Weight. *Neuron*. Retrieved from https://www.sciandmed.com/sm/journalviewer.aspx?issue=1042&article=577&action=1

Gallagher, T., Bjorness, T., Greene, R., You, Y. J., & Avery, L. (2013). The Geometry of Locomotive Behavioral States in C. elegans. *PLoS ONE*, *8*(3). doi:10.1371/journal.pone.0059865

Gallagher, T., Kim, J., Oldenbroek, M., Kerr, R., & You, Y.-J. (2013). ASI regulates satiety quiescence in C. elegans. *The Journal of Neuroscience : The Official Journal of the Society for Neuroscience*, *33*(23), 9716–24. doi:10.1523/JNEUROSCI.4493-12.2013

Garrett, B. (2009). *Brain & Behavior: An Introduction to Biological Psychology*. (V. Knight, D. Saoud, L. Grambling, & S. Quesenberry, Eds.) (Second.). SAGE.

Glicksman, C., Pournaras, D. J., Wright, M., Roberts, R., Mahon, D., Welbourn, R., Sherwood, R., Alaghband-Zadeh, J., & le Roux, C. (2010). Postprandial plasma bile

acid responses in normal weight and obese subjects. *Annals of Clinical Biochemistry*, *47*(Pt 5), 482–4. doi:10.1258/acb.2010.010040

Goldstein, E. (2010). *Sensation and Perception*. (J. Hague & J. Perkins, Eds.) (eight.). Belmont: Wadsworth.

Greer, E. R., Perez, C. L., Gilst, M. R. Van, Lee, B. H., & Ashrafi, K. (2008). Neural and Molecular Dissection of a C. elegans Sensory Circuit that Regulates Fat and Feeding. *Cell*, *8*(2), 118–131. doi:10.1016/j.cmet.2008.06.005.Neural

Grinberg, M., Schwarz, M., & Zaltsman, Y. (2005). Mitochondrial Carrier Homolog 2 Is a Target of tBID in Cells Signaled To Die by Tumor Necrosis Factor Alpha. *Molecular and Cellular Biology*, *25*(11). doi:10.1128/MCB.25.11.4579

Guo, M., Wu, T.-H., Song, Y.-X., Ge, M.-H., Su, C.-M., Niu, W.-P., Li, L.-L., Xu, Z.-J., Ge, C.-L., Al-Mhanawi, M., Wu, S.-P., & Wu, Z.-X. (2015). Reciprocal inhibition between sensory ASH and ASI neurons modulates nociception and avoidance in Caenorhabditis elegans. *Nature Communications*, *6*, 1–13. doi:10.1038/ncomms6655

Halaas, J., Gajiwala, K., Maffei, M., & Cohen, S. (1995). Weight-Reducing Effects of the Plasma Protein Encoded by the obese Gene. *Science*, *269*(5223), 543–546. Retrieved from http://www.sciencemag.org/content/269/5223/543.short

Harris, G., Mills, H., Wragg, R., Hapiak, V., Castelletto, M., Korchnak, A., & Komuniecki, R. W. (2010). The Monoaminergic Modulation of Sensory-Mediated Aversive Responses in Caenorhabditis elegans Requires Glutamatergic/Peptidergic Cotransmission. *Journal of Neuroscience*, *30*(23), 7889–7899. doi:10.1523/JNEUROSCI.0497-10.2010

Harris, R. B. (1999). Parabiosis between db/db and ob/ob or db/+ mice. *Endocrinology*, *140*(1), 138–45. doi:10.1210/endo.140.1.6449

He, W., Lam, T. K. T., Obici, S., & Rossetti, L. (2006). Molecular disruption of hypothalamic nutrient sensing induces obesity. *Nature Neuroscience*, *9*(2), 227–33. doi:10.1038/nn1626

Higham, a, Vaillant, C., Yegen, B., Thompson, D. G., & Dockray, G. J. (1997). Relation between cholecystokinin and antral innervation in the control of gastric emptying in the rat. *Gut*, *41*(1), 24–32. Retrieved from http://www.pubmedcentral.nih.gov/articlerender.fcgi?artid=1027223&tool=pmcentrez&rendertype=abstract

Hilliard, M. A., Apicella, A. J., Kerr, R., Suzuki, H., Bazzicalupo, P., & Schafer, W. R. (2005). In vivo imaging of C. elegans ASH neurons: cellular response and adaptation to chemical repellents. *The EMBO Journal*, *24*(1), 63–72. doi:10.1038/sj.emboj.7600493

Hilliard, M. A, Bergamasco, C., Arbucci, S., Plasterk, R. H. A, & Bazzicalupo, P. (2004). Worms taste bitter: ASH neurons, QUI-1, GPA-3 and ODR-3 mediate quinine avoidance in Caenorhabditis elegans. *The EMBO Journal*, *23*(5), 1101–11. doi:10.1038/sj.emboj.7600107

Johnson, L. R. (2011). *Regulation of gastrointestinal mucosal growth. Physiological reviews* (Vol. 68). Retrieved from http://www.ncbi.nlm.nih.gov/pubmed/21634069

Johnstone, I. L., Shafi, Y., & Barry, J. D. (1992). Molecular analysis of mutations in the Caenorhabditis elegans collagen gene dpy-7. *The EMBO Journal*, *11*(11), 3857–63.

Retrieved from http://www.pubmedcentral.nih.gov/articlerender.fcgi?artid=556895&tool=pmcentrez&rendertype=abstract

Katsuma, S., Hirasawa, A., & Tsujimoto, G. (2005). Bile acids promote glucagon-like peptide-1 secretion through TGR5 in a murine enteroendocrine cell line STC-1. *Biochemical and Biophysical Research Communications*, *329*(1), 386–90. doi:10.1016/j.bbrc.2005.01.139

Kerr, R. (2006). Imaging the Activity of Neurons and Muscles. *WormBook*. Retrieved from doi/10.1895/wormbook.1.113.1, http://www.wormbook.org.

Kerr, R. A. (2006). Imaging the activity of neurons and muscles. *WormBook : The Online Review of C. Elegans Biology*, 1–13. doi:10.1895/wormbook.1.113.1

Kohan, A. B., Yoder, S. M., & Tso, P. (2011). Using the lymphatics to study nutrient absorption and the secretion of gastrointestinal hormones. *Physiology & Behavior*, *105*(1), 82–8. doi:10.1016/j.physbeh.2011.04.056

Landolt, H. P. (2008). Sleep homeostasis: A role for adenosine in humans? *Biochemical Pharmacology*, *75*(11), 2070–2079. doi:10.1016/j.bcp.2008.02.024

Lee, R., Sawin, E. R., Chalfie, M., Horvitz, H. R., & Avery, L. (1999). EAT-4, a homolog of a mammalian sodium-dependent inorganic phosphate cotransporter, is necessary for glutamatergic neurotransmission in Caenorhabditis elegans. *Journal of Neuroscience*, *19*(1), 159–167. doi:10.1016/j.str.2010.08.012.Structure

Levi, J., Segal, L., Laurant, R., & Rayburn, J. (2013). Racial and Ethnic Disparities in Obesity. *Journal of Women's Health*, *15*(2), 103–134.

Li, C. (1998). Absence of Soluble Leptin Receptor in Plasma from dbPas/dbPas and Other db/db Mice. *Journal of Biological Chemistry*, *273*(16), 10078–10082. doi:10.1074/jbc.273.16.10078

Li, Z., Zhou, Y., Carter-Su, C., Myers, M. G., & Rui, L. (2007). SH2B1 enhances leptin signaling by both Janus kinase 2 Tyr813 phosphorylation-dependent and -independent mechanisms. *Molecular Endocrinology (Baltimore, Md.)*, *21*(9), 2270–81. doi:10.1210/me.2007-0111

Lin, S., & Huang, X. F. (1999). Altered hypothalamic c-Fos-like immunoreactivity in diet-induced obese mice. *Brain Research Bulletin*, *49*(3), 215–9. Retrieved from http://www.ncbi.nlm.nih.gov/pubmed/10435786

Lin, S., Storlien, L. H., & Huang, X. F. (2000). Leptin receptor, NPY, POMC mRNA expression in the diet-induced obese mouse brain. *Brain Research*, *875*(1-2), 89–95. Retrieved from http://www.ncbi.nlm.nih.gov/pubmed/10967302

Lints, R., & Hall, D. H. (2009). Reproductive system, egglaying apparatus. *WormAtlas*. doi:10.3908/wormatlas.1.24

Malik, S., McGlone, F., Bedrossian, D., & Dagher, A. (2008). Ghrelin modulates brain activity in areas that control appetitive behavior. *Cell Metabolism*, *7*(5), 400–9. doi:10.1016/j.cmet.2008.03.007

Meister, B. (2007). Neurotransmitters in key neurons of the hypothalamus that regulate feeding behavior and body weight. *Physiology & Behavior*, *92*(1-2), 263–71. doi:10.1016/j.physbeh.2007.05.021

Méndez-Díaz, M., Rueda-Orozco, P. E., Ruiz-Contreras, A. E., & Prospéro-García, O.

(2012). The endocannabinoid system modulates the valence of the emotion associated to food ingestion. *Addiction Biology*, *17*(4), 725–35. doi:10.1111/j.1369-1600.2010.00271.x

Mori, I., & Ohshima, Y. (1995). Neural regulation of thermotaxis in Caenorhabditis elegans. *Nature*. doi:10.1038/376344a0

Nagase, H., Nakajima, A., Sekihara, H., York, D. A, & Bray, G. A. (2002). Regulation of feeding behavior, gastric emptying, and sympathetic nerve activity to interscapular brown adipose tissue by galanin and enterostatin: the involvement of vagal-central nervous system interactions. *Journal of Gastroenterology*, *37 Suppl 1*, 118–27. Retrieved from http://www.ncbi.nlm.nih.gov/pubmed/12572879

Ogden, C. L., Carroll, M. D., Kit, B. K., & Flegal, K. M. (2012). *Prevalence of obesity in the United States, 2009-2010. NCHS data brief*. Retrieved from http://www.ncbi.nlm.nih.gov/pubmed/22617494

Pelleymounter, M. a, Cullen, M. J., Baker, M. B., Hecht, R., Winters, D., Boone, T., & Collins, F. (1995). Effects of the obese gene product on body weight regulation in ob/ob mice. *Science (New York, N.Y.)*, *269*(5223), 540–3. Retrieved from http://www.ncbi.nlm.nih.gov/pubmed/7624776

Qi, L., Kraft, P., Hunter, D. J., & Hu, F. B. (2008). The common obesity variant near MC4R gene is associated with higher intakes of total energy and dietary fat, weight change and diabetes risk in women. *Human Molecular Genetics*, *17*(22), 3502–8. doi:10.1093/hmg/ddn242

Rand, J. (2007). Acetylcholine. *WormBook*, 1–21. doi:10.1895/wormbook.1.131.1

Rand, J. B., & Russell, R. L. (1984). Choline acetyltransferase-deficient mutants of the nematode Caenorhabditis elegans. *Genetics*, *106*(2), 227–248.

Schäfer, M., Bräuer, A. U., Savaskan, N. E., Rathjen, F. G., & Brümmendorf, T. (2005). Neurotractin/kilon promotes neurite outgrowth and is expressed on reactive astrocytes after entorhinal cortex lesion. *Molecular and Cellular Neurosciences*, *29*(4), 580–90. doi:10.1016/j.mcn.2005.04.010

Schwartz, M., Woods, S., & Porte, D. (2000). Central Nervous System Control of Food Intake. *Nature*, *404*, 661–671. Retrieved from http://www.nature.com/nature/journal/v404/n6778/abs/404661a0.html

Shinkai, Y., Yamamoto, Y., Fujiwara, M., Tabata, T., Murayama, T., Hirotsu, T., Ikeda, D., Tsunozaki, M., Iino, Y., Bargmann, C., Katsurea, I., & Ishihara, T. (2011). Behavioral choice between conflicting alternatives is regulated by a receptor guanylyl cyclase, GCY-28, and a receptor tyrosine kinase, SCD-2, in AIA interneurons of Caenorhabditis elegans. *The Journal of Neuroscience : The Official Journal of the Society for Neuroscience*, *31*(8), 3007–3015. doi:10.1523/JNEUROSCI.4691-10.2011

Spangler, R., Wittkowski, K. M., Goddard, N. L., Avena, N. M., Hoebel, B. G., & Leibowitz, S. F. (2004). Opiate-like effects of sugar on gene expression in reward areas of the rat brain. *Brain Research. Molecular Brain Research*, *124*(2), 134–42. doi:10.1016/j.molbrainres.2004.02.013

Steinert, R. E., Peterli, R., Keller, S., Meyer-Gerspach, A. C., Drewe, J., Peters, T., & Beglinger, C. (2013). Bile acids and gut peptide secretion after bariatric surgery: a 1-year prospective randomized pilot trial. *Obesity (Silver Spring, Md.)*, *21*(12), E660–8.

doi:10.1002/oby.20522

Sulston, J., & Hodgkin, J. (1988). Methods. (Wood, W. B., ed). In *The Nematode Caenorhabditis elegans* (p. pp 587–606). Cold Spring Harbor, New York: Cold Spring Harbor Press.

Suo, S., Culotti, J. G., & Van Tol, H. H. M. (2009). Dopamine counteracts octopamine signalling in a neural circuit mediating food response in C. elegans. *The EMBO Journal*, *28*(16), 2437–2448. doi:10.1038/emboj.2009.194

Vaswani, K. K., & Tejwani, G. A. (1986). Food deprivation-induced changes in the level of opioid peptides in the pituitary and brain of rat. *Life Sciences*, *38*(2), 197–201. doi:10.1016/0024-3205(86)90012-3

Wang, Q., Liu, C., Uchida, A., Chuang, J.-C., Walker, A., Liu, T., Osborne-Lawrence, S., Mason, B., Mosher, C., Berglund, E., Elmquist, J., & Zigman, J. M. (2014). Arcuate AgRP neurons mediate orexigenic and glucoregulatory actions of ghrelin. *Molecular Metabolism*, *3*(1), 64–72. doi:10.1016/j.molmet.2013.10.001

You, Y., Kim, J., Raizen, D. M., & Avery, L. (2008). Insulin, cGMP, and TGF-beta signals regulate food intake and quiescence in C. elegans: a model for satiety. *Cell Metabolism*, *7*(3), 249–57. doi:10.1016/j.cmet.2008.01.005

VITA

Kristen Davis grew up in Arvonia, Virginia with her parents Debra and John M. Davis II. She has four younger sisters, Marsha, Jeannie, Hannah, and Scarlett Davis. She also has an older step-sister, Jennifer Davis and two step-parents, Sandra Davis and Carey Davis. Kristen graduated from Buckingham County High School and the Governor's School of Southside Virginia (Longwood site) with an advanced diploma in 2006. Kristen graduated from Longwood University with a Bachelors of Science in biology and psychology in 2011. She was in a post-baccalaureate PREP program under the supervision of Dr. Martha Ann Bell at Virginia Polytechnic Institute and State University from August 2011 to July 2012. Kristen enrolled in the Neuroscience PhD program at Virginia Commonwealth University in Fall 2012 and joined the lab of Dr. Young-Jai You in Fall 2013.